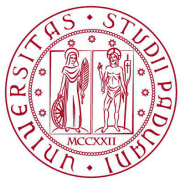

UNIVERSITÀ
DEGLI STUDI
DI PADOVA

UNIVERSITÀ DELGI STUDI DI PADOVA

-

DIPARTIMENTO DI FISICA ED ASTRONOMIA G. GALIEI

CORSO DI DOTTORATO DI RICERCA IN FISICA - CURRICULUM GENERALE - XXIX CICLO

SELECTED PROBLEMS IN QUANTUM MECHANICS: TOWARDS TOPOLOGICAL QUANTUM DEVICES AND HEAT ENGINES

Coordinatore: Ch.mo Prof. Gianguido Dall'Agata
Supervisore: Ch.mo Prof. Luca Dell'Anna

Dottorando: Antonio Alecce

Alla mia famiglia

Contents

List of Figures

List of Tables

Chapter 1

Introduction

The work presented in this thesis is related to some topics in theoretical quantum physics which are *quantum thermodynamics* and *topological order*. The first is a new research field where physicists are devoting a lot of efforts to build up a theory able to describe quite in general phenomena involving heat and energy exchanges in quantum systems. The second topic, instead, is related to unconventional phenomena like the quantum Hall effect or to new kinds of materials such as topological insulators or topological superconductors. The novelty of this topic lies on the fact that we need new paradigms with respect to the standard Landau description, resorting to concepts from topology in order to characterize such systems [1].

The importance of the quantum thermodynamics can be understood considering its classical counterpart and the concept of irreversibility. A definition of an irreversible quantum process, in fact, is a great task in modern physics. Moreover it could be of great impact for technological applications the possibility of producing work with heat engines using quantum processes in order to get high performances and efficiency. In classical mechanics the uniqueness of the solutions of the Hamilton equations of motion gives a deterministic character to the time evolution of the system, allowing for inverting the motion along the trajectory in phase space and recovering all the states occupied by the system in previous times. However from a practical point of view we cannot invert the arrow of time in the experiments since we cannot take trace of the motion of $N \sim 10^{23}$ particles, therefore we accept loosing information about all the details of the system, resorting to a statistical description for the time evolution of the whole system. Because of the great complexity it becomes very unlikely for a many body system to occupy the same state at a later time. From the point of view of classical statistics this fact is the origin of the irreversibility of time evolution.

In quantum mechanics also the dynamics of the wave function ψ_t (or in general

of the density operator ρ_t) can be generally reversed in time. A fundamental issue is therefore that of characterizing, from a theoretical point of view, irreversible quantum processes [2][3]. An example in quantum mechanics is provided by the thermalization of an open system which reaches the temperature of an external bath. In this evolution, dissipative processes spoil the quantum nature of the system letting the coherence of the quantum states to vanish (here the coherence is related to the phase between quantum states in superposition).

About this dissipative evolution, we present a series of our results. The first characterize the irreversibility of the dynamics of a quantum system under adiabatic conditions. We quantify such irreversibility by means of an entropy change. Such entropy remains unchanged if the process is "quantum reversible" and its growth is non zero (and always positive) otherwise. The second result, that we obtained, deals with the characterization of a quantum heat engine performing an Otto cycle. We depict the working of such cycle under dissipative branches. Then we give a proposal for an experimental optical implementations of it.

On the other hand, the possibility of getting quantum states which survive under dissipative phenomena, such as disorder or other perturbations, is of crucial importance for designing new technologies paving the way for quantum computation. Topological states actually exhibit such characteristic of being robust against some perturbations and their possible application is the basis for the so-called topological quantum computation [4]. This topological protection, that is the robustness of such states against dissipative sources, is the main reason why we moved on considering the simplest model exhibiting a topological phase, the Kitaev model [5]. It provides the link between two of the main research fields in quantum physics. Although physicists describe thermodynamics for systems in quantum regime, we have not a good understanding of what can happen when temperature influences topological states and, the implications of this aspect could be very important. We need to understand very well how thermodynamics works in quantum regime and what are the characteristics of topological orders in order to link these fields and to get a good new research in quantum physics.

The original model describes a topological 1D superconductor which has a Majorana zero mode (MZM) at each edge of the wire. We will consider generalizations of the Kitaev model with long range interactions, in the presence and in the absence of time reversal symmetry, obtaining several and very rich phase diagrams. In the presence of longer range interactions, instead, many Majorana modes can appear at the edges. In our investigation we recover preceding results but we also go deeper in depicting the topological phase under the standing or not of time reversal symmetry. We consider various ways to break such symmetry, that lead to different phase diagrams. Then we also give the set of Bogoliubov equations for the case of BTR regime, counting the general form for TR breaking parame-

ters. Finally we give the modes, including zero modes, when the lattice has a finite length. This last result generalizes a very particular case introduced in [5].

However, the problem of topological protection against dissipation has not been approached here, even if it remains the main motivation for the study of the two topics presented in this thesis, namely the quantum thermodynamics by dissipative processes and the topological order.
A possibility of characterizing the robustness of MZMs in dissipating environments, could be that of using devices like single particle transistors. What can be done is to substitute some components of the standard electron transistor with Kitaev chains in the topological phase. Then by studying the transport, we could get informations about the robustness of topological states as well as the thermodynamics.

For all these reasons, as building blocks, in this thesis we develop first the theory of quantum thermodynamic, addressing both fluctuation relations, for out of equilibrium quantum transformations, and quantum heat engines, then we will give a general overview of the Kitaev chain in the general case of long ranged interactions, and finally we will approach the phenomenon of *single electron tunneling* in electronic transistors (single electron transistors) as basis for future research. For that purpose, at the end of the thesis we give some notes about this last topic and its application as "heat-to-current" harvesting engines using quantum or metallic dots. This is important to understand possible different dynamics, with respect the usual configuration "metallic lead-dot island-metallic lead", when using Kitaev chains as leads or islands [6].

This theses is structured in order to discuss few aspects of the recent topics described above. In Chapter 2 we introduce the theoretical background for treating the evolution of close and open quantum systems. Then, in section 3.1, we will treat the equilibrium quantum thermodynamics, first looking at the single thermodynamic transformations and then considering quantum heat engines (QHE). In this chapter a general view of first and second principle of thermodynamics in quantum regime will be given. In section 3.3 we will approach the non-equilibrium quantum thermodynamics, providing the fluctuation relations and addressing the specific case of a quantum Otto cycle (QOC). In Chapter 4 we introduce the topological quantum order, explaining the main concepts in this field and afterwards, in Chapter 5, we will present the model of the Kitaev chain which shows Majorana zero modes. Chapter 6 is dedicated to the topological invariants, used to address the topological order for the systems we will consider. In Chapter 7 we study the Kitaev chain in the presence of long ranged interactions. We present several topological phase diagrams for generalizations of the Kitaev chain, getting many MZM per edge or massive edge modes (MEMs). Finally, in Chapter 8, we consider single electron tunneling devices, showing their main characteristics and their limits

in harvesting charge current from heat flow inside the circuit (Seebeck effect). In particular we show that Seebeck effect is absent for metallic dots. As already said, this last chapter is included in this thesis as a tool for future generalizations of such circuits with the insertion of topological components.

Chapter 2

Dynamics of Quantum Systems

In this chapter we describe the evolution of quantum systems according to their link with the surrounding physical world, the environment. At first we will consider closed systems where the dynamics of the states will be done in terms of unitary evolution operators, then we will deal with open systems although isolated, obtaining the evolution of a quantum state by means of the Markovian master equation with Limbland form. This latter gives an intuitive dynamics where we separate the contribution of the system Hamiltonian from the contribution of a dissipation term due to the interaction with a reservoir. The whole system, open system plus environment (see Figure 2.2), is closed but looking only to a part of it our quantum dynamics will be not merely unitary. We focus on these different treatments, closed and open system dynamics, in order to define quantum thermodynamic transformations, in analogy to the classical thermodynamic ones.

2.1 Closed Quantum System Dynamics

A closed system can be, in general, not isolated from an external control. Such situation is reflected in an explicit time dependence of the Hamiltonian by means of some parameters and it will lead to a formulation of the quantum system's dynamics in terms of Liouville-Von Neumann equation. This equation describes the evolution of a density state, in analogy to the classical statistical mechanics.
We begin considering a pure state. In quantum mechanics a pure state is described by a vector, ket $|\psi\rangle$, defined on a Hilbert space $\mathscr{H}$, which evolves according to Schrödinger equation (we use the convention $\hbar = 1$):

$$i\frac{d|\psi(t)\rangle}{dt} = H(t)|\psi(t)\rangle \tag{2.1}$$

where $H(t)$ is the Hamiltonian operator of the system. The ket $|\psi(t)\rangle$ in equation (2.1) can be represented also by an unitary evolution operator $U(t, t_0)$:

$$|\psi(t)\rangle = U(t, t_0)|\psi(t_0)\rangle \tag{2.2}$$

where $|\psi(t_0)\rangle$ is the system's state at time t_0 and the condition $U(t_0, t_0) = \mathbb{I}$ is assumed. From eqn (2.1) and (2.2) we get:

$$i\frac{dU(t, t_0)}{dt} = H(t)U(t, t_0) \tag{2.3}$$

which defines the operator of time evolution for a pure quantum state. The solution of Eq. (2.3) depends on the form of $H(t)$. In the simplest cases, if $[H(t_1), H(t_2)] = 0\,\forall t_1, t_2$ we get:

$$U(t, t_0) = exp\left\{-i\int_{t_0}^{t} dt' H(t')\right\}$$

On the other hand, if the addressed Hamiltonian does not commute with itself at different times, we obtain:

$$U(t, t_0) = \mathcal{T} exp\left\{-i\int_{t_0}^{t} dt' H(t')\right\} \tag{2.4}$$

where $\mathcal{T}$ stands for time ordering operator.
Generalizing to quantum mixtures, we describe our system by a density operator ρ defined as:

$$\rho = \sum_i w_i |\psi_i\rangle\langle\psi_i| \tag{2.5}$$

where $|\psi_i\rangle$ is a pure quantum state evolving as in (2.1) and w_i are classical weights with $\sum_i w_i = 1$. By the evolution law of $|\psi_i\rangle$ we can deduce:

$$\rho(t) = U(t, t_0)\rho(t_0)U^\dagger(t, t_0)$$

from which we write the Liouville-Von Neumann equation in Schrdinger picture:

$$i\frac{\rho(t)}{dt} = [H(t), \rho(t)] \tag{2.6}$$

It is possible to rewrite expression (2.6) as the analogue equation of motion for density states in classical statistical mechanics (the *Liouville* equation):

$$i\frac{\rho(t)}{dt} = \mathcal{L}(t)\rho(t) \tag{2.7}$$

In the above equation $\mathcal{L}$ is the Liouville super-operator acting on the space of density operators ρ (the term "super" comes from the fact that it acts on a space of operators giving another operator). Also here we can give a compact form for the solution of the Liouville equation in terms of time ordered product:

$$\rho(t) = \mathcal{T} exp\left\{-i\int_{t_0}^{t} dt' \mathcal{L}(t')\right\}\rho(t_0) \tag{2.8}$$

The equations above give a complete characterization of the quantum dynamics in Schrödinger picture. Now what we will present is a formalism, the interaction picture dynamics, useful to deal with systems which have an explicit time dependence of the form:

$$H(t) = H_0 + H_I(t)\,. \tag{2.9}$$

We now introduce two operators,

$$U_0(t,t_0) = exp\{-iH_0(t-t_0)\} \tag{2.10a}$$

$$U_I(t,t_0) = U_0^{\dagger}(t,t_0)U(t,t_0) \tag{2.10b}$$

and call A an operator representing an observable at time t_0. The time dependent expectation value of such an observable can be written as it follows

$$\begin{aligned}\langle A(t)\rangle &= Tr\{A(t)U(t,t_0)\rho(t_0)U^{\dagger}(t,t_0)\}\\ &= Tr\{U_0^{\dagger}(t,t_0)AU_0(t,t_0)U_I(t,t_0)\rho(t_0)U_I^{\dagger}(t,t_0)\}\\ &= Tr\{A_I(t)\rho_I(t)\}\end{aligned} \tag{2.11}$$

where we have introduced the interaction pictures operators

$$A_I(t) = U_0^{\dagger}(t,t_0)A(t)U_0(t,t_0) \tag{2.12}$$

and

$$\rho_I(t) = U_I(t,t_0)\rho(t_0)U_I^{\dagger}(t,t_0) \tag{2.13}$$

By Eqs. (2.12) and (2.13) we write the Von Neumann equation in the interaction picture

$$\frac{d\rho_I(t)}{dt} = -i[H_I(t),\rho_I(t)] \tag{2.14}$$

whose integral form is

$$\rho_I(t) = \rho(t_0) - i\int_{t_0}^{t} ds\,[H_I(s),\rho_I(s)]$$

which is the starting point for developing approximate solutions within perturbative approach.

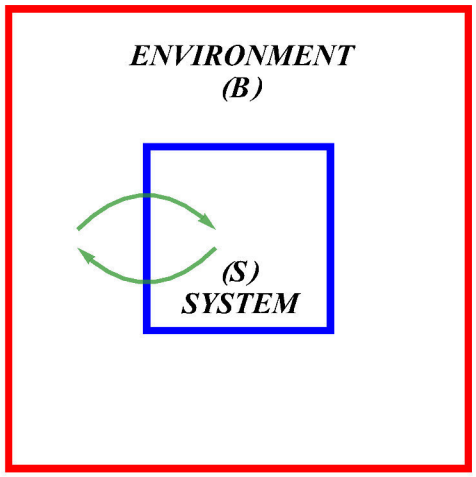

Figure 2.1: Pictorial representation of a system S in contact with an external environment B (generally a thermal bath). Both open system and environment are described by an Hamiltonian and a density operators ρ_S and ρ_B describing their respective states.

2.2 Open Quantum System Dynamics

What we now focus on is the dynamics of a system surrounded by another system, the environment (usually much bigger than the first one), and we assume there is some exchange of energy or particles between them. We refer to the first system as *open system* [7]. We will discuss this kind of dynamics in order to be able to deal with equilibrium and non equilibrium transformations in quantum thermodynamics in the further chapters. However here the open system will be assumed to be isolated. We will derive the master equation discussing the main approximations of the theory and its usefulness in quantum thermodynamics. We denote by S the open system which we want to analyze and by B the environment. Their Hamiltonians is respectively H_S and H_B defined on the Hilbert spaces $\mathcal{H}_S$ and $\mathcal{H}_B$, the state of the whole system $S + B$ is described by ρ_{S+B} defined on $\mathcal{H} = \mathcal{H}_S \otimes \mathcal{H}_B$ and the Hamiltonian is of the form

$$H(t) = H_S \otimes I_B + I_S \otimes H_B + H_I(t)$$

As we can see in the above equation, the interaction term is time depending while the Hamiltonians H_S and H_B are not. The environment B is a *reservoir*, namely it is a system with an infinite number of degrees of freedom such that the frequencies, which characterize it, form a continuum, and we call *bath* a reservoir which is in a

thermal equilibrium state. The starting point in order to obtain the dynamics of an open system, is that of considering the density operator of the whole system $\rho(t)$ in the interaction picture, written in its integral form

$$\rho(t) = \rho(0) - i \int_0^t ds \, [H_I(s), \rho(s)] \; . \tag{2.15}$$

Using the von Neumann equation and tracing out the degrees of freedom of B we get

$$\frac{d\rho_S(t)}{dt} = \int_0^t ds Tr_B \left\{ [H_I(t), [H_I(s), \rho(s)]] \right\} \tag{2.16}$$

where we have assumed that $Tr_B \left\{ [H_I(t), \rho(0)] \right\} = 0$.
Now a series of approximations will follow. The first important assumption that we will do is the so called *Born approximation*. We assume a weak coupling term $H_I(t)$ so that the influence of the system on the reservoir is negligible and we can write:

$$\rho(t) \approx \rho_S(t) \otimes \rho_B \quad \forall \, t \tag{2.17}$$

Generally the evolution of the whole system, counting an interacting term, would reflect on the two subsystems, changing their reduced states and the whole state would be generally entangled for $t > 0$. Here we assume that the reservoir is so big that it has a very large number of degrees of freedom, and that its state remains unchanged in time, given the weak interacting term with the system. The reservoir will always take the same state ρ_B and the state of the whole system is assumed to be separable as in Eq. (2.17). Thus Eq. (2.16) becomes

$$\frac{d\rho_S(t)}{dt} = \int_0^t ds Tr_B \left\{ [H_I(t), [H_I(s), \rho_S(s) \otimes \rho_B]] \right\} \tag{2.18}$$

Then we perform the *Markov approximation*, i.e. we assume that the evolution of $\rho_S(t)$ at time t does not depend on its state at time $s < t$, thus we obtain:

$$\frac{d\rho_S(t)}{dt} = \int_0^t ds Tr_B \left\{ [H_I(t), [H_I(s), \rho_S(t) \otimes \rho_B]] \right\} \tag{2.19}$$

The only change in Eq. (2.19) with respect to Eq. (2.18) is $\rho_S(s) \to \rho_S(t)$ in the integral. Although the latter equation is local in time it is not yet Markovian since its evolution depends on the way we prepare the state at time $t = 0$. To achieve such Markovianity we proceed as follows. At first we note that the commutator in the above equation involves time correlation functions for the reservoir. We consider the case that such functions decay very rapidly in a time τ_B, compared to the characteristic time in which the system appreciably varies, which we label τ_R.

It follows that the time t, at which we consider the state $\rho_S(t)$, is greater that the characteristic time τ_B in which the integrand in Eq. (2.19) goes to zero and this implies that we can let the upper limit of the integral go to infinity. Then changing the integration variable s by $s \to t - s$ we can rewrite the last expression as:

$$\frac{d\rho_S(t)}{dt} = \int_0^\infty ds Tr_B \left\{[H_I(t), [H_I(t-s), \rho_S(t) \otimes \rho_B]]\right\} \tag{2.20}$$

To gain a Markovian master equation we have to perform the last approximation, i.e. the *rotating wave approximation*. Before developing it we need to rewrite eq. (2.20) in a different form. We focus on the interacting term $H_I(t)$. Its most generic form in Schrdinger picture is:

$$H_I = \sum_\alpha A_\alpha \otimes B_\alpha \tag{2.21}$$

Where A_α and B_α are hermitian operators respectively acting on $\mathcal{H}_S$ and $\mathcal{H}_B$. Assuming that the spectrum of H_S is discrete, we have a complete set of projector operators $\{\prod(\epsilon)\}$ where each one of them projects into the eigenspace associated to the eigenvalue ϵ of H_S. We define:

$$A_\alpha(\omega) = \sum_{\epsilon' - \epsilon = \omega} \prod(\epsilon) A_\alpha \prod(\epsilon') \tag{2.22}$$

Using eqn. (2.22) together with the completeness relation of the projectors set, we get:

$$\sum_\omega A_\alpha(\omega) = \sum_\omega A_\alpha^\dagger(\omega) = A_\alpha \tag{2.23}$$

Another consequence of equation (2.22) is that:

$$[H_S, A_\alpha(\omega)] = -\omega A_\alpha(\omega) \tag{2.24a}$$

$$[H_S, A_\alpha^\dagger(\omega)] = \omega A_\alpha^\dagger(\omega) \tag{2.24b}$$

From eqns. (2.24) we have that the interaction picture representation of the operators $A_\alpha(\omega)$ and $A_\alpha^\dagger(\omega)$ is given by:

$$e^{iH_S t} A_\alpha(\omega) e^{-iH_S t} = e^{-i\omega t} A_\alpha(\omega) \tag{2.25a}$$

$$e^{iH_S t} A_\alpha^\dagger(\omega) e^{-iH_S t} = e^{i\omega t} A_\alpha^\dagger(\omega) \tag{2.25b}$$

It follows that about H_I we have:

$$\sum_{\alpha,\omega} A_\alpha(\omega) \otimes B_\alpha = \sum_{\alpha,\omega} A_\alpha^\dagger(\omega) \otimes B_\alpha^\dagger \tag{2.26}$$

Thus, considering the interaction picture operator of the interacting Hamiltonian term, we get:

$$H_I(t) = \sum_{\alpha,\omega} e^{-i\omega t} A_\alpha(\omega) \otimes B_\alpha(t) \tag{2.27}$$

$$= \sum_{\alpha,\omega} e^{i\omega t} A_\alpha^\dagger(\omega) \otimes B_\alpha^\dagger(t) \tag{2.28}$$

with $B_\alpha(t) = e^{iH_B t} B_\alpha e^{-iH_B t}$.
It is important to note that the statement $Tr_B\{[H_I(t), \rho(0)]\} = 0$, that has been assumed before, becomes $\langle B_\alpha(t)\rangle = Tr_B\{B_\alpha(t)\rho_B\} = 0$ which tells that the the reservoir average of $B_\alpha(t)$ vanishes. Combining eqn (2.26) and (2.20) we obtain:

$$\begin{aligned}\frac{d\rho_S(t)}{dt} = \int_0^\infty ds\, Tr_B\Big\{ & H_I(t-s)\rho_S(t)\rho_B H_I(t) \\ & - H_I(t)H_I(t-s)\rho_S(t)\rho_B\Big\} + h.c. \\ = \sum_{\omega,\omega'}\sum_{\alpha,\beta} & e^{i(\omega'-\omega)t}\Gamma_{\alpha,\beta}(\omega)\Big(A_\beta(\omega)\rho_S(t)A_\alpha^\dagger(\omega') - \\ & A_\alpha^\dagger(\omega')A_\beta(\omega)\rho_S(t) + h.c.\Big)\end{aligned} \tag{2.29}$$

where

$$\Gamma_{\alpha,\beta}(\omega) = \int_0^\infty ds\, e^{i\omega t}\left\langle B_\alpha^\dagger(t)B_\beta(t-s)\rho_B\right\rangle \tag{2.30}$$

The writing eqn. (2.29) is the form, for the evolution of $\rho_S(t)$, that we were looking for. Eqn. (2.30) is the Fourier transform of reservoir correlation functions. The last consideration about this result is that for stationary reservoir states, $[H_B, \rho_B] = 0$, the reserve correlation functions ore homogeneous in time so:

$$\left\langle B_\alpha^\dagger(t)B_\beta(t-s)\rho_B\right\rangle = \left\langle B_\alpha^\dagger(s)B_\beta(0)\rho_B\right\rangle$$

which implies that $\Gamma_{\alpha,\beta}(\omega)$ does not depend on time. We now return on the rotating wave approximation. The time scale for the evolution of the system is proportional to the difference of the frequencies involved into the dynamics of the system $\tau_S \propto |\omega - \omega'|$ with $\omega \neq \omega'$. Because of $\tau_S > \tau_R$, we may neglect the terms with $\omega' \neq \omega$ in eqn (2.29) since they oscillate very fastly in the time τ_R for whose the system appreciably varies. Thus we get:

$$\begin{aligned}\frac{d\rho_S(t)}{dt} = \sum_{\omega}\sum_{\alpha,\beta}\Gamma_{\alpha,\beta}(\omega)\Big(& A_\beta(\omega)\rho_S(t)A_\alpha^\dagger(\omega') \\ & - A_\alpha^\dagger(\omega')A_\beta(\omega)\rho_S(t) + h.c.\Big)\end{aligned} \tag{2.31}$$

Now we rewrite $\Gamma_{\alpha,\beta}(\omega)$ as follow:

$$\Gamma_{\alpha,\beta}(\omega) = \frac{1}{2}\left(\gamma_{\alpha,\beta}(\omega) + iS_{\alpha,\beta}(\omega)\right)$$

with $\gamma_{\alpha,\beta}(\omega)$ and $S_{\alpha,\beta}(\omega))$ being respectively positive and hermitian:

$$S_{\alpha,\beta}(\omega) = \frac{1}{2i}\left(\Gamma_{\alpha,\beta}(\omega) - \Gamma^*_{\alpha,\beta}(\omega)\right) \tag{2.32a}$$

$$\gamma_{\alpha,\beta}(\omega) = \left(\Gamma_{\alpha,\beta}(\omega) + \Gamma^*_{\alpha,\beta}(\omega)\right) = \int_{-\infty}^{\infty} ds\, e^{i\omega s}\left\langle B^\dagger_\alpha(s)B_\beta(0)\right\rangle \tag{2.32b}$$

By means of equations (2.32) we define the dissipator of the master equation as:

$$\mathcal{D}\left(\rho_S\right) = \sum_{\omega}\sum_{\alpha,\beta}\gamma_{\alpha,\beta}\left(A_\beta\rho_S A\alpha^\dagger(\omega) - \frac{1}{2}\left\{A_\alpha(\omega)^\dagger A_\beta(\omega), \rho_S\right\}\right) \tag{2.33}$$

and the hermitian operator:

$$H_{LS} = \sum_{\omega}\sum_{\alpha,\beta} S_{\alpha,\beta}A_\alpha(\omega)^\dagger A_\beta(\omega) \tag{2.34}$$

which commutes with the system's Hamiltonian, $[H_S, H_{LS}] = 0$. By means of eqn (2.33) and (2.34) we can write the *interaction picture master equation*:

$$\frac{d\rho_S(t)}{dt} = -i\left[H_{LS}, \rho_S(t)\right] + \mathcal{D}\left(\rho_S(t)\right) \tag{2.35}$$

Such form can be brought into the one of the well note *Limbland equation* by diagonalizing the matrices $\gamma_{\alpha,\beta}$ with the help of appropriate unitary transformations. Limbland equation is fundamental in the field of open system physics since it gives the dynamics of a generic open system in terms of generator of dynamical group. Now we briefly formulate the main concepts of this evolution formalism about an open system in order to better understand the main meaning of what we done via Markovian master equation. In the scenario we considered, the system at time $t = t_0$(we suppose $t_0 = 0$) is of the form $\rho(t) = \rho_S(t)\otimes\rho_B$ and now we assert the that the state $\rho_S(t)$ at some time $t > 0$ can be written in the form:

$$\rho_S(t) = V(t)\rho_S(0) \equiv Tr_B\left\{U(t,0)\left(\rho_S(0)\otimes\rho_B\right)U^\dagger(t,0)\right\} \tag{2.36}$$

If we look at ρ_B and t as fixed, the above relation defines a map from $\mathcal{S}(\mathcal{H}_S)$, the space of density operators of the reduced system, into itself:

$$V(t)\ :\ \mathcal{S}(\mathcal{H}_S) \to \mathcal{S}(\mathcal{H}_S)$$

This is called *dynamical map*. By means of dynamical map, in fact, we avoid to consider the whole Hilbert space $\mathcal{H}$ and we act only on $\mathcal{H}_S$, as shown in the following diagram:

$$\begin{array}{ccc} \rho(0) = \rho_S(0) \otimes \rho_B & \xrightarrow{\text{Whole System's Evolution}} & \rho(t) = U(t,0)\rho(0)U^\dagger(t,0) \\ \Big\downarrow Tr_B & & \Big\downarrow Tr_B \\ \rho_S(0) & \xrightarrow[\text{Dynamical Map}]{} & \rho_S(t) = V(t)\rho_S(0) \end{array}$$

It is possible to show that $V(t)$ is a convex-linear, completely positive and trace-preserving operator.

What we now do is to allow t to vary and thus we get a family of one parameter $\{V(t)|t \geq 0\}$ dynamical maps where we assume $V(0)$ to be the identity map.
Now because of the assumption of Markovian evolution of S we can get the semi-group property for $V(t)$:

$$V(t_1)V(t_2) = V(t_1 + t_2) \quad \forall\, t_1, t_2 \geq 0 \tag{2.37}$$

The set of $V(t)$ is therefore a quantum dynamical semigroup, i.e. a one-parameter family of dynamical maps underlying property (2.37). We can give the expression of $V(t)$ in terms of generator $\mathcal{L}$ of the quantum dynamical semigroup:

$$V(t) = exp\{\mathcal{L}t\} \tag{2.38}$$

which yields to the first order differential equation:

$$\frac{d\rho_S(t)}{dt} = \mathcal{L}\rho_S(t) \tag{2.39}$$

which is the generic Markovian master equation. It can be shown that the action of $\mathcal{L}$ on ρ_S can be expressed as the contribution of two terms; a standard unitary evolution term and a dissipator which provides the irreversibility for the whole process [7]:

$$\mathcal{L}\rho_S = -i[H, \rho_S] + \sum_{k=1}^{N^2-1} \gamma_k \left(A_k \rho_S A_k^\dagger - \frac{1}{2}\{\rho_S, A_k^\dagger A_k\} \right) \tag{2.40}$$

Eqn(2.40) is the most general form that the generator $\mathcal{L}$, acting on a state ρ_s, can have. The commutator represents the unitary part of the evolution. The hermitian operator H is generally different from the system Hamiltonian as in the case of eqn. (2.35). Parameters $\{\gamma_k\}$ count the correlation functions of the environment

and they play the role of the relaxation rates for the modes of the open system. Finally the operators $\{A_k\}$, called Limbland operators, are linear combinations of the generators of the Liouville space of ρ (of dimensions N^2), excluding the identity operator that is counted in the choice of such basis of generators ($A_{N^2-1} = \mathbb{I}$). As consequence of this, the expression (2.39) is called Limbland equation. What we obtained in (2.20) is therefore the action of quantum dynamical semigroup generator $\mathcal{L}$ on the system's density operator. It is important to stress the aspect of irreversible dynamics generated by the quantum dynamical semigroup generator. In contrast to the closed system, that counts a unitary dynamics alone, here, for an open system, the dissipator $\mathcal{D}(\rho_{\mathcal{S}})$ gives rise to a non null entropy production rate, σ, for the whole system $S + B$.
Let us consider two states ρ and ρ_0 of $\mathcal{S}(\mathcal{H}_S)$ and the change in the quantum relative entropy induced by the same dynamical map $V(t)$ acting on both of them. We remember that the relative entropy between two density operators ρ and σ is defined as:

$$S(\rho_1||\rho_2) = Tr(\rho \ln(\rho)) - Tr(\rho \ln(\sigma)) \tag{2.41}$$

Since the properties of relative entropy we can get:

$$\begin{aligned} S(V(t)\rho||V(t)\rho_0) &= S(Tr\{U(t,0)\rho \otimes \rho_B U(t,0)^\dagger\}||Tr\{U(t,0)\rho_0 \otimes \rho_B U(t,0)^\dagger\}) \\ &\leq S(U(t,0)\rho \otimes \rho_B U(t,0)^\dagger||U(t,0)\rho_0 \otimes \rho_B U(t,0)^\dagger) \\ &= S(\rho \otimes \rho_B||\rho_0 \otimes \rho_B) \\ &= S(\rho||\rho_0) \end{aligned} \tag{2.42}$$

If ρ_0 is a stationary state (not necessary an equilibrium state) then $\mathcal{L}\rho_0 = \rho_0$ thus:

$$S(V(t)\rho||V(t)\rho_0) = S(V(t)\rho||\rho_0) \leq S(\rho||\rho_0) \tag{2.43}$$

That is the dynamical map reduces the relative entropy of the generic system state ρ with respect to a stationary state ρ_0. Assuming the expressions (2.38) and (2.43) we can define, as entropy production rate, the negative derivate of the above relative entropy that will be positively defined:

$$\sigma(\rho(t)) = -\frac{d}{dt} S(\rho(t)||\rho_0) \geq 0 \tag{2.44}$$

where $\rho(t) = V(t)\rho(0)$. In this expression we can explicit the contribution of the generator $\mathcal{L}$ as:

$$\sigma(\rho) = -kTr\{(\mathcal{L}\rho)\ln(\rho)\} + kTr\{(\mathcal{L}\rho)\ln(\rho_0)\} \geq 0 \tag{2.45}$$

where k represents the Boltzmann constant. It can be proved that the entropy production rate $\sigma(\rho)$ is a linear, convex and non-negative functional defined on the state space of the open system. It is significant to underline that the entropy production rate for the whole system (that now is a closed system) is given by means of the relative entropy. Eqn. (2.45) can be also achieved by nonequilibrium arguments but here we will not report such discussion because it is not a central topic for our work.

Chapter 3

Quantum Thermodynamics

The development of classical thermodynamic theory and thus the building of big heat engines, adopted in the industrial production precesses, led a great transformation of society known as *second industrial revolution*. This was one of the most important changing in the history of the world in making modern society. Heat was used to produce work! It means that we can take a disordered form of energy, the heat, and convert a part of it into ordered energy, mechanical work. In the last years physicists tried to build a thermodynamic theory in the quantum regime so to take advance from the richness of processes of quantum mechanics. A new branch of physics, known as *Quantum Thermodynamics*, is developing. In this chapter we will give the idea of "thermodynamics" behind the quantum mechanical processes. Then we will use the new thermodynamic language", just introduced, in order to describe phenomena as irreversibility, linked to the finiteness in time of quantum evolutions, and to propose a finite power *quantum heat engine*. In the following we will describe the main thermodynamic transformations, characterizing the quantum regime, following their equivalent processes in classical thermodynamics. At first we will introduce the first and the second principle of the thermodynamics and then we will define the particular thermodynamic transformations as adiabatic, isochoric and isothermal ones. As we are interested in the quantum regime, then the physical variables will be given as functionals of the density operator ρ and by the spectrum of the system Hamiltonian $H(t)$. As in the classical case, the concept of adiabatic, isochoric and isothermal will be respectively linked to closed systems, "null work" transformations and open system evolutions where the working substance has the same temperature during the whole branch. The physics involved in such steps can be very different according to the way in which such evolutions are driven. For instance a quasistatic transformation gives rise to thermodynamic outputs (in terms of performed work for instance) that are quite different from the

ones of a finite time branch. In the following we will distinguish between these two regimes that have been very well studied for the case of an adiabatic quantum transformation.

3.1 The Laws of Thermodynamics in Quantum Regime

For defining our transformations we start from the first principle of thermodynamics. Here we make two assumptions: first we assume that the initial and final states of the process are equilibrium states (generally answering to the Gibbs-Boltzmann distribution), second, in the case of an external driving, the system underlies to quasistatic evolutions. Otherwise, when no driving is acted, the dynamics can be thought as a generic process pushing the initial state into an equilibrium one as in the case of a thermalization.

In the case of an external driving this latter is assumed to be quasistatic and thus the quantum adiabatic theorem stands [9]. According to such theorem the population of each level (where these latter modify in time) do not change. Thus, given a state ρ_t, we can write its average energy as $U_t = Tr\{\rho_t H_t\} = \sum_n P_n E_n$ where both ρ_t and H_t are written in Schrödinger picture, and E_n and P_n are respectively the n-th level's energy and population. In case of equilibrium state such average energy coincides with the internal energy that is just an equilibrium variable. The infinitesimal change of U, which now coincides with the *internal energy* of the system, has therefore the form:

$$dU = \sum_n (P_n dE_n + E_n dP_n) \tag{3.1}$$

The first principle of thermodynamics reads $dU = dW + dQ$, where dU is the infinitesimal change in average energy of the state, dW is the work made on the system and dQ is the heat exchanged by the latter with some environment.
Under the assumptions we made (equilibrium initial and final states and quasistatic transformation for non isolated systems), it is natural to identify the two terms in (3.1) with dW and dQ, thus we get [10]:

$$\begin{cases} dW = \sum_n P_n dE_n \\ dQ = \sum_n E_n dP_n \end{cases} \tag{3.2}$$

Set of equations (3.2) allows for defining thermodynamic transformations such as isochoric, adiabatic and isothermal branches. Generally, for non quasistatic processes, dU will not coincide with the internal energy. In this scenario, a although the form of dQ is always as in eqn. (3.2), $dQ = \sum_n E_n dP_n$, it is not the case for

dW. We will deeply approach this problem in section 3.3.1. Further characterizations will be given by the second law of thermodynamics. For this aim we need to distinguish between the case of open and closed system. At first we approach the case of an open system. We look for a good definition of entropy for both the system and the environment that is assumed to be a thermal bath. It can be shown [11], that, for a process involving open systems, the thermodynamic entropy change of the latter, obtained via Clausius relation $\int \delta Q_{res\to syst}/T$, equals the Shannon entropy $S = -\int \rho ln\,(\rho)$ (the integration is performed over all the phase space) only if canonical equilibrium is achieved between the system and its reservoir. Here ρ is a classical density function but in the quantum regime such ρ is an operator, as defined in eqn. (2.5). In such case we would deal with von Neumann entropy $S_{inf} = -Tr(\rho \ln(\rho))$. However a link between heat and entropy (Shannon or von Neumann entropy according to the classical or quantum nature of the system) holds also for nonequilibrium transformations. In fact if we consider to go from ρ_i to ρ_f (neither is assumed to be an equilibrium state) then the following disequality holds [12]:

$$\int \delta Q^{res\to syst}/T \leq -Tr\left\{\rho ln\left(\rho_f\right)\right\} + Tr\left\{\rho ln\left(\rho_i\right)\right\} = \Delta S_{inf} \tag{3.3}$$

You can recognize in (3.3) the Clausius disequality, showing that the von Neumann entropy (or the Shannon entropy for a classical system) plays the role of the system's entropy for general transformations, equilibrium and non equilibrium ones. Now we focus on the reservoir. Its state is always assumed to answer the canonical distribution with the same initial temperature during the whole process (isochoric or isothermal transformation), i.e. reservoir does not evolve. So every kind of thermodynamic branch will be reversible since ρ_B (the density operator of the reservoir) goes through equilibrium states, that, in this case, always equal the initial one. It follows that the entropy change for the reservoir is given by:

$$S_{res} = \int \frac{\delta Q^{S\to R}}{T} = -\int \frac{\delta Q^{R\to S}}{T} \tag{3.4}$$

Counting the contribution of both the open system and the reservoir, we can define the growing of entropy of the whole system $S+B$ that here we address as universe:

$$\Delta S_{uni} = S_{res} + \Delta S_{inf} \geq 0 \tag{3.5}$$

Eqn. (3.5) is the second law of thermodynamics for open systems. The positivity of the total entropy ΔS_{uni} follows from (3.3). ΔS_{uni} is null for reversible transformations otherwise the entropy of the universe ($S + B$) will always increases. We underline that here we tell about *thermodynamics reversibility* which is quite

different from the quantum mechanical reversibility. This latter always holds since for each unitary evolution U, acting on the whole system, there exists the inverse transformation $U^{-1} = U^{\dagger}$ that in principle can drive back the system to the initial state. The concept of irreversibility appears when, dealing with the open system dynamics, we trace over the degrees of freedom of the reservoir and, by various approximations, we treat the environment as constant in time.
The case of non isolated closed quantum systems will be treated in section 3.3.1. Indeed situation drastically changes for such systems. Von Neumann entropy is conserved for unitary transformations and, since for a closed system the dynamics is driven by some unitary operator U, then S_{inf} is not a good choice for the entropy function. Situation is analogue in the case of classical mechanics since the Shannon entropy of the density function ρ remains constant in time by the Liouville's theorem.

3.2 Quantum thermodynamic Transformations: An Introduction

In the following we will introduce the main thermodynamic transformations as isochoric, adiabatic and isothermal branches. The adiabatic and the isothermal transformations will be assumed to be reversible, that is the working substance density operator goes through equilibrium states during the branch. In this case we tell about equilibrium thermodynamics. Then in section 3.3.1 we will generalize the case of the adiabatic driving. For the aims of this thesis the generalization to nonequilibrium of the reversible isothermal branch is not approached.

3.2.1 Quantum isochoric Transformation

For quantum isochoric transformation we mean a quantum process in which no work is done on the system: $dW = 0$. It follows that the only form of energy present in this transformation is heat:

$$dQ = \sum_n E_n dP_n \tag{3.6}$$

If we think about a thermal reservoir as environment, a standard isochoric transformation can be a thermalization process in which the energy levels of the system remain unchanged but, at the same time, heat transferring between system and bath allows for populations change, $dP_n \neq 0$. Under general assumptions, following the quantum formalism introduced in the preceding chapter, the isochoric transformation is described by the master equation formalism. According to the system

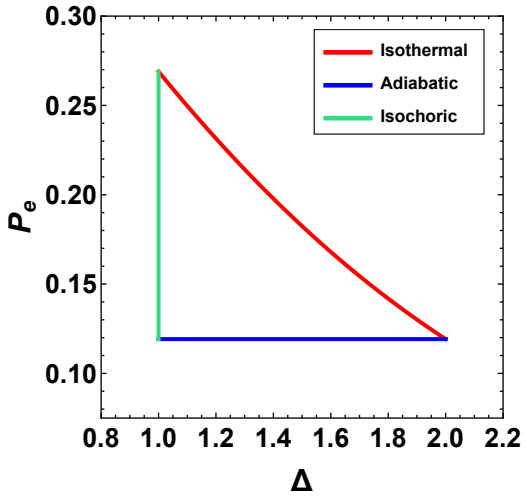

Figure 3.1: $\Delta - P$ plane for thermodynamic transformations with a qubit as working substance. In green the isochoric branch, in red the isothermal one and in blue a quantum adiabatic transformation.

and the environment we deal with, we apply the Limbland equation formalism so to achieve an open system dynamic that drives the working substance state. The final state can be hopefully an equilibrium state as it is the case under the physical assumptions we make hereafter.

Let us assume to have an initial state prepared in thermal equilibrium with a reservoir, such a bosonic thermal bath,, at temperature T_1 and then to uncouple it and to let it interact with another resevoir at temperature $T_2 \neq T_1$. Addressing the case of a qubit, we can write the state of the system, diagonal in the eigenbasis $\mathcal{B} = \{|e\rangle, |g\rangle\}$ of H_S, as $\rho = P_e(\Delta)|e\rangle\langle e| + P_g(\Delta)|g\rangle\langle g|$. Δ is just the energy spacing between the excited and the ground state so that $H_s = \Delta|e\rangle\langle e|$ ($E_g = 0$). Indeed, according to the optical master equation formalism, for our case, the final system state of the evolution will be a thermal state at the same temperature of the reservoir. This happen whatever is the initial state ρ of the system. In the $\Delta - P$ plane (see Figure 3.1) the isochoric branch is depicted by a straight -line at fixed Δ form some $P_e^{(i)}(\Delta)$ to another $P_e^{(f)}(\Delta)$. The intermadiate states of the branch are not equilibrium states. Indeed the P_n's change thus we have not the steady state condition (more in particular the equilibrium condition) or, form another point of view, there are non null currents (looking at the master equation) between the states thus, there is not equilibrium. This latter assertion is equivalent to say that there is

some heat flow between system and bath. The heat absorbed by the system from the reservoir will be $Q = \sum_n \int E_n dP_n = \Delta(P_e^{(t_f)}(\Delta) - P_e^{(t_i)}(\Delta))$. Since, during the evolution, the thermal reservoir and the working substance are not in thermal equilibrium then this process is not reversible. This irreversible behaviour can be directly noted by the positivity of ΔS_{uni} for this case.
We assumed initial equilibrium state and perfect thermalization at the end of the process but, the above discussion can be applied to whatever initial and final states as well as to generic evolution at constant H_S.

3.2.2 Quantum adiabatic transformation

A second important thermodynamic process is the adiabatic transformation. In contrast with the isochoric branch (and following the classical thermodynamics) we define a quantum adiabatic transformation as a branch in which no heat is exchanged with any environment. Considering only quasistatic driving (although the system is closed it is not isolated) and starting the evolution with an equilibrium state we can invoke the adiabatic theorem to underline that the populations of the system will not change during the branch. According to (3.1) we now have:

$$dW = \sum_n P_n dE_n \tag{3.7}$$

Population are left unchanged and only the energies E_n will change according to the external driving, $dP_n = 0 \rightarrow dQ = 0$. This is a quantum adiabatic transformation. On the other hand a classical adiabatic transformation does not necessarily require that the occupation probabilities are invariant. It follows that classical adiabatic processes form a set that includes the quantum adiabatic ones.
An important variable characterizing quantum adiabatic process is the effective temperature. To introduce it let us consider any two level system (TLS) whose Hamiltonian eigenstates ($|e\rangle_t$ and $|g\rangle_t$) have energies $E_e(t)$ and $E_g(t)$ (energy spacing $\Delta(t)$). For whatever steady state, not necessary an equilibrium state, we can imagine that it is in a "virtual" thermal equilibrium with some effective reservoir and its state is characterized by the following parameter (the effective temperature):

$$T_{eff} = \frac{\Delta(t)}{k_B} \left[ln \left(\frac{P_g}{P_e} \right) \right]^{-1} \tag{3.8}$$

where P_e and P_g are left unchanged ($dP_n = 0$) and we externally change $\Delta(t)$ which has, therefore, a given value which we assume to know. By this way we can always consider the system in equilibrium with some reservoir at different effective temperature and thus the branch is thermodynamically reversible. A good

entropy state function has to be null for such transformation and non null otherwise. Although such temperature can be always defined for a qubit, this is not the case for a quantum system with at least three levels. In such cases we require that for each energy spacing of the system we can define, via (3.8) an unique effective temperature. As an example if we considering three states $|1\rangle$, $|2\rangle$ and $|3\rangle$ we require that:

$$\frac{\Delta(t)}{k_B}\left[\ln\left(\frac{P_1}{P_2}\right)\right]^{-1} = \frac{\Delta(t)}{k_B}\left[\ln\left(\frac{P_2}{P_3}\right)\right]^{-1}$$

If at the end of such transformation we want to link the system to a thermal bath (as for instance in the case of a Carnot cycle) then the reversibility requirement for the whole cycle (isothermal transformation are thermodynamically reversible, $\Delta S_{uni}^{isoth} = 0$) counts also that the final effective temperature is the same as the temperature of the bath [13]. Then it can be shown that the two requirements, done for having a reversible adiabatic process (unique T_{eff} for each energy spacing and $T_{eff} = T_{bath}$), are equivalent to

- All the energy gaps are changed by the same ratio during the quantum adiabatic process: $E_n(t) - E_m(t) = \lambda\left(E_n(0) - E_m(0)\right)$

- The coefficient λ in the above equation is equal to the rapport between the initial end final (effective) temperature that the equilibrium state sees: $\lambda = T_f/T_i$

Now we name expansion a quantum adiabatic process in which the working substance (the system) does work ($dW > 0$) and compression the opposite process, $dW < 0$ (see Figure 3.1).

3.2.3 Quantum isothermal transformation

In quantum isothermal processes the working substance is kept in contact with a heat bath, the open system is always in equilibrium with it at fixed temperature T and, simultaneously, we drive the system's Hamiltonian by a protocol that depends on time. To get equilibrium conditions, during this transformation, both the energy gaps and the occupation probabilities change simultaneously. Thus now the first law of thermodynamics counts both terms, work and heat. This scenario can be achieved by assuming that the driving is quasistatic. Let us consider the example of a two-level system.

The time depending system Hamiltonian has two eigenstates $|e\rangle_t$ and $|g\rangle_t$ and an energy spacing $\Delta(t) = E_e(t) - E_g(t)$ that are time depending. Also the levels population change in time but in such quasistatic limit, the two occupation probabilities, P_e and P_g, must satisfy both the Boltzmann distribution and the normalization condition:

$$r(t) = \frac{P_e(t)}{P_g(t)} = e^{-\beta\Delta(t)} \quad \text{and} \quad P_g(t) + P_e(t) = 1 \tag{3.9}$$

where again $\beta = 1/k_B T$.
Since in a sufficiently slow process, at every instant the system is in thermodynamic equilibrium with the heat bath, such transformation is reversible, $\Delta S_{uni} = 0$. This implies that the heat exchanged with the reservoir can be written as:

$$dQ = \sum_n E_n dP_n = TdS \tag{3.10}$$

where with dS we address the differential of von Neumann entropy of the state. Also here we end the treatment of the thermodynamic transformation by defining as expansion a branch in which the system performs work on the environment, $dW > 0$, and compression the opposite process for whose $dW < 0$ (see again Figure 3.1 for a graphic representation of the isothermal transformation).

3.2.4 Quantum Otto Cycle, Harvesting Work from Quantum Systems

The building up of a quantum heat engines represents one of the most interesting challenge in the field of quantum thermodynamics. Because of this aim, a great interest has been given to theoretical characterization of quantum cycles as Otto [14], Carnot [15], Stirling [16] and Szilard cycle [17] as well as theoretical proposals of heat engines [18] and recently some experimental result has been obtained [19]. Here we briefly introduce an example of thermodynamic cycle in quantum regime: the quantum Otto cycle. Such cycle is made up by four steps and we assume again that the initial state of the cycle is a canonical equilibrium state at temperature T_c. Such cycle is made in series by (look at Figure 3.2):

- One adiabatic compression where the system Hamiltonian changes as $H_1 = H(\lambda(0)) \to H_2 = H(\lambda(\tau))$ according to the driving protocol $\lambda(t)$
- One isochoric transformation, in our case a thermalization process with a bath at temperature T_h
- One adiabatic expansion where the Hamiltonian goes from $H_3 = H_2 = H(\tau)$ to $H_4 = H_1 = H(\lambda(0))$ following the path $\lambda(\tau - t)$ (the backward protocol)

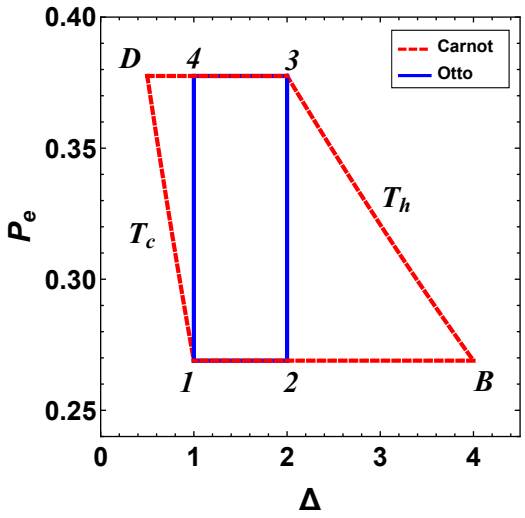

Figure 3.2: Quantum Otto cycle with blue lines and quantum Carnot cycle with red dashed lines. For both the cycles the reservoirs temperatures are $T_c = 1$ and $T_h = 4$ ($\beta = \hbar = 1$), then both of them start in the point "1" in the plane, corresponding to an equilibrium state. The Otto cycle is depicted by the branches $1 \to 2 \to 3 \to 4 \to 1$ and the working of Carnot engine by the steps $1 \to B \to 3 \to D \to 1$. The quantum adiabatic branches are larger in the Carnot cycle and, for this latter, the two isochoric transformations of the Otto cycle are replaced by two isothermal branches.

- Final thermalization process which gets the final state of the working substance equal to the initial one; an equilibrium state at temperature T_c

The example, by which we introduce this cycle, takes in consideration a TLS. Both the adiabatic compression and expansion are assumed to be performed quasistatically, thus they are quantum adiabatic processes and this, for a qubit, coincides with the reversibility of these branches. In the first step we start with a thermal equilibrium state at temperature T_c, $\rho_1 = \exp(-\beta_c H_1)/Z(\beta_c)$ where $Z(\beta_c)$ is the partition function. Then the system is not anymore in contact with the bath, we deal with a closed system although it is not isolated. Thus we quasistatically change the energy spacing until we reach the final value $\Delta_2 = E_e^{(2)} - E_g^{(2)}$ with $\Delta_2 > \Delta_1 = E_e^{(1)} - E_g^{(1)}$. Since the transformation is quantum adiabatic we get $dP_n = 0$. The final state of the qubit can be written by using an effective tempera-

ture:

$$\beta_2 = \frac{\Delta_2}{k_B}\left[ln\left(\frac{P_g^{(1)}}{P_e^{(1)}}\right)\right]^{-1}$$

thus the state of the system at position 2 in the $\Delta - P_e$ plane is:

$$\rho_2 = \frac{e^{-\beta_2 H_2}}{Z(\beta_2)}$$

Here the work done on the system, obtained by the fist principle, is:

$$W_1 = (E_e^{(2)} - E_e^{(1)})P_e^1 - (E_g^{(2)} - E_g^{(1)})P_g^1$$

After this branch we put the qubit in contact with a bath at temperature T_h higher than T_c, $T_h > T_c$. This assumption is crucial for the right working of the heat engine. It ensures that the system can produce positive net work at the end of the cycle. At the end of the branch we will have an equilibrium state at inverse temperature β_h since complete thermalizations are assumed. In this branch we only have heat exchange and it is quantified by:

$$Q_{in} = E_e^{(2)}(P_e^{(3)} - P_e^{(2)}) + E_g^{(2)}(P_g^{(3)} - P_g^{(2)}) \tag{3.11}$$

For the next step we split system and reservoir and perform a quantum adiabatic expansion such that the system's Hamiltonian is driven back to the initial one, i.e. $\Delta_4 = \Delta_1$. Here the effective temperature and the system state are $\beta_4 = (\Delta_2/k_B)(\ln(P_g^{(3)}P_e^{(3)}))^{-1}$ and $\rho_4 = \exp(-\beta_4 H_1)/Z(\beta_4)$. The work done on the system is

$$W_3 = (E_e^{(1)} - E_e^{(3)})P_e(3) - (E_g^{(1)} - E_g^{(3)})P_g(3)$$

To conclude the cycle we perform another thermalization process with a bath at temperature T_c that is the initial temperature characterizing the thermal state ρ_1. Thus we will get $\rho_4 \to \rho_1$. In this last step the heat exchanged is

$$Q_{out} = E_e^{(1)}(P_e^{(1)} - P_e^{(4)}) + E_g^{(1)}(P_g^{(1)} - P_g^{(4)}) \tag{3.12}$$

Q_{in} and Q_{out} are respectively the heat absorbed from the hot reservoir and absorbed from the cold reservoir. Using the first principle we have for the whole cycle:

$$\begin{aligned}\Delta U &= \Delta U_1 + \Delta U_2 + \Delta U_3 + \Delta U_4 \\ &= W_{1\to 2} + Q_{in} + W_{3\to 4} + Q_{out} \\ &= 0 \to W_{tot} = -(W_{1\to 2} + W_{3\to 4}) = Q_{in} + Q_{out}\end{aligned} \tag{3.13}$$

Where W_{tot} is the net work produced in the whole cycle. Since this expression we can obtain, as in classical Otto cycle, the following form for the efficiency η of the cycle:

$$\eta = \frac{W_{tot}}{Q_{in}} = 1 - \frac{|Q_{out}|}{Q_{in}} \tag{3.14}$$

The expression for the efficiency of Otto cycle is the same as in classical thermodynamics. It is very important to report that, as for the Otto cycle, we can build up a quantum Carnot cycle. In this case assuming that the cycle is reversible (isothermal and quantum adiabatic processes can be reversible but thermalization cannot) the efficiency for such cycle is $\eta_C = 1 - T_c/T_h$. We can see that the efficiency of Otto cycle is smaller than the one of Carnot cycle. the irreversibility of the isochoric transformation is linked to dissipation processes which reduce the efficiency of the cycle respect to the maximum available value that is the Carnot efficiency.

3.3 Nonequilibrium Thermodynamics

What we approach in this section is the generalization of quantum thermodynamic transformations for closed systems when a finite time protocols is assumed to drive the dynamics. Indeed, when going to quasistatic transformations to finite time ones, the definition of "work" is a central problem. Thus, for simplifying the problem, we consider isolated systems so to avoid unwanted phenomena as dissipation due to the interaction with reservoirs. The assumption of initial equilibrium states always will hold. For focusing on the most general case where each kind of initial state is considered then look at [20]. We will continuously look at classical statistical mechanics approach to the problem (or sometime at stochastic thermodynamics), to see how applying these arguments to the case of quantum thermodynamics. We will obtain the main work definitions in classical as well as in quantum regime and we will characterize them by fluctuation relations. In this way we aim to underline and clarify fundamental concepts about irreversibility and dissipation for nonequilibrium transformations. As last step we will use one of the obtained relations, the inner friction work, to describe the working of a quantum Otto cycle undergoing to finite time dynamics in its adiabatic branches.

3.3.1 Fluctuation Relations

Here we first introduce the various definitions of work in classical nonequilibrium statistical mechanics, such as *inclusive* and *exclusive* work and underline their physical meanings. Then we will obtain the Crooks fluctuation theorem and the Jarzynski equality. This will be recovered also for the quantum regime. Then, for

this latter case, we will characterize the entropy production in a nonequilibrium (irreversible) transformation in terms of quantum relative entropy. Two different characterizations will be given, respectively corresponding to two different definitions of nonequilibrium work: the irreversible work and the inner friction work.

Classical Fluctuation Relations

As first step we recover the classical nonequilibrium fluctuation relations so to have a guideline for better explaining the meaning of the quantum fluctuation relations we will obtain. The main fact is that matter, at microscopic level, is in a continuous state of agitation so many physical variables randomly fluctuate. Among these variable we are interested in describing heat and work. What we will do is to track fluctuation relations that characterize these variables. We will always assume thermodynamic equilibrium initial states (according to canonical ansamble) but then, we need another property of the systems: *microreversibility*. We will introduce it soon. In general our system (here at the level of classical theory) is described by an Hamiltonian such:

$$H(\mathbf{z}, \lambda_t) = H_0(\mathbf{z}) - \lambda_t Q(\mathbf{z}) \tag{3.15}$$

In the above equation λ_t is our protocol that contributes at driving the perturbation of the system, $Q(\mathbf{z})$ is an observable depending on $\mathbf{z} = (\mathbf{q}, \mathbf{p})$, the state vector in the phase space, and H_0 is the unperturbed Hamiltonian. We refer to λ_t and to $Q(\mathbf{z})$ as force and conjugate coordinate. Then we will assume that the perturbation driven by λ_t starts at $t = 0$ and finishes at $t = \tau$. According to the Hamilton equations of motion and given an initial point in the phase space $\mathbf{z}_0 = (\mathbf{q}_0, \mathbf{p}_0)$, the generic point $\mathbf{z}_t$ for $t \in [o, \tau]$ will be given by:

$$\mathbf{z}_t = \varphi_{t,0}(\mathbf{z}_0, \lambda) \tag{3.16}$$

The function on the right side of (3.16) is called flow. In enunciating the microreversibility principle we restrict to time reversal Hamiltonians (but the discussion can be also generalized to non time reversal ones) and to conjugate coordinates with parity $\epsilon_Q = \pm 1$ under the same time reversal transformation. It can be showed [22] that, defined the reverse protocol $\tilde{\lambda}_t = \lambda_{\tau - t}$, the following equality, the microreversibility principle, holds:

$$\varphi_{t,0}(\mathbf{z}_0, \lambda) = \epsilon \varphi_{\tau - t, 0}(\epsilon \mathbf{z}_\tau, \epsilon_Q \tilde{\lambda}) \tag{3.17}$$

It states that in order to recover backward the trajectory $\mathbf{z}_t$ one has to invert the sign of momenta ($\epsilon \mathbf{z} = (\mathbf{q}, -\mathbf{p})$) and perform the protocol $\epsilon_Q \tilde{\lambda}$ (see Figure 3.3(a)). It is important to underline that (3.17) stands for nonautonomous systems.

Thus we have well defined both the initial states of the driving and the guide principle for the trajectories $\mathbf{z}_t$. Now we introduce two different definitions for the work done on the system during such evolution: inclusive and exclusive work. Remember that the initial state of the system is given by the (canonical) equilibrium distribution $\rho_{th} = \exp\{-\beta H\}/Z(\beta)$ at inverse temperature β. Thus the initial state in the phase space $\mathbf{z}_0$ is a random value sampled from this distribution; it is a random variable. We now define a new variable, the exclusive work, as function of this initial random variable:

$$W_0(\mathbf{z}_0;\lambda) = \int_0^\tau d\,t\lambda_t \dot{Q}_t(\varphi_{t,0}(\mathbf{z}_0;\lambda)) \tag{3.18}$$

Because this definition, the same exclusive work is a random quantity. Jarzynski showed in [23] that through the Hamilton equations of motion one can obtain:

$$W(\mathbf{z}_0;\lambda) = H_0(\varphi_{\tau,0}(\mathbf{z}_0;\lambda)) - H_0(\mathbf{z}_0) \tag{3.19}$$

This equality allows to interpret the exclusive work as the energy injected into the system during the action of the force protocol λ_t from $t = 0$ to $t = \tau$. From eqn. (3.18) and using microreversibility (3.17) we can get the so called Bochkov-Kuzovlev equality:

$$\left\langle e^{\beta W_0} \right\rangle_\lambda = 1 \tag{3.20}$$

The subscript λ means that the process, leading to the work W_0 made on the system, is the forward process driven by λ_t which transforms the unperturbed Hamiltonian from $H_0(\mathbf{z}_0)$ to $H_0(\varphi_{\tau,0}(\mathbf{z}_0;\lambda))$ and, the average $\langle\cdot\rangle$ is performed on the initial equilibrium state. By (3.20) we know that the average on the equilibrium initial state of the exponential of the random variable "exclusive work" is independent of the details of the system as well as the particular protocol (path) λ_t. Applying the Jensen disequality to eqn. (3.20) we finally get:

$$\langle W_0 \rangle \geq 0 \tag{3.21}$$

Which means that if the system is driven out of equilibrium by the force λ than, in average, it can only absorb energy. We now explicitly write down the work distribution $p(W_0';\lambda)$ whose integration, on the domain of all possible W_0', gives the exclusive work (3.18). That is:

$$\langle W_0 \rangle = \int dW_0'\, P_0(W_0';\lambda) W_0'$$

Such pdf $P(W_0';\lambda)$ reads:

$$P_0(W_0';\lambda) = \int d\,\mathbf{z}_0 \rho_0(\mathbf{z}_0)\delta\left[W_0 - H_0(\mathbf{z}_\tau) + H_0(\mathbf{z}_0)\right] \tag{3.22}$$

Applying microreversibility arguments to the above equation we get the fluctuation relation:

$$\frac{P_0(W_0;\lambda)}{P_0(-W_0;\epsilon_Q\tilde{\lambda})} = e^{\beta W_0} \tag{3.23}$$

that is the Bochkov-Kuzovlev fluctuation relation.
It expresses the second law of thermodynamics. Indeed if we assume $W_0 > 0$ then eqn. (3.23) asserts that the probability that the work in injected into the system is $e^{\beta W_0}$ times greater than the probability that the same amount of work is released by the system in the reversed protocol. By eqn. (3.23)we can assert that processes in which energy is consumed are exponentially more probable than the ones in which the same amount of energy is released.

Another approach to define of "work" is to consider the whole Hamiltonian eqn. (3.15), so that:

$$W(\mathbf{z}_0;\lambda) = H(\mathbf{z}_\tau,\lambda_\tau) - H(\mathbf{z}_0,\lambda_0) \tag{3.24}$$

Such variable is called *inclusive work* since it counts also the perturbation part of the system's Hamiltonian. The inclusive work can be expressed as:

$$W(\mathbf{z}_0,\lambda) = \int_0^\tau \dot{\lambda}_t \frac{\partial H(\mathbf{z}_t,\lambda_t)}{\partial \lambda_t} \tag{3.25}$$

Now we address, by the same guideline of the exclusive work, a forward and a backward protocol and we will look at the average of the exponential of the work $W(\mathbf{z}_0;\lambda)$, in order to relate it to equilibrium variables. Jarzynski equation will be obtained. As we have assumed until now, our protocol starts with an initial equilibrium state at inverse temperature β. Then we will perform the protocol λ_t, driving the system out of equilibrium and, we will stop at time τ. The backward protocol is performed considering as initial state the thermal state of the system as it saw the same initial temperature but now with the system's Hamiltonian $H(\mathbf{z}_\tau,\lambda_\tau)$. such state is:

$$\rho_{th,B} = \frac{e^{-\beta H(\mathbf{z}_\tau,\lambda_\tau)}}{Z(\beta,\lambda_\tau)}$$

By applying microreversibility, it can be derived the Jarzynski equation [24]:

$$\left\langle e^{-\beta W} \right\rangle_\lambda = e^{-\beta \Delta F} \tag{3.26}$$

Where the right side of the above equation counts the difference between the free energies of the state at the beginning of forward and backward protocol:

$$\Delta F = -\beta \ln \left[\frac{Z(\beta,\lambda_\tau)}{Z(\beta,\lambda_0)} \right]$$

Now applying the Jensen disequality to eqn. (3.26) we get:

$$\langle W \rangle_\lambda \geq \Delta F \tag{3.27}$$

Also in this case, as for the exclusive work, we consider the expression for the inclusive work pdf:

$$P(W;\lambda) = \int d\,\mathbf{z}_0 \rho_0(\mathbf{z}_0) \delta\left[W - H(\mathbf{z}_\tau) + H(\mathbf{z}_0)\right] \tag{3.28}$$

and by the microreversibility principle we obtain a fluctuation relation for such inclusive work.

$$\frac{P(W;\lambda)}{P(-W;\tilde{\lambda})} = e^{\beta(W-\Delta F)} \tag{3.29}$$

Eqn. (3.29) is known as Crooks fluctuation theorem. Such theorem stands also if we considered Q to be odd under time reversal, but in this case $\tilde{\lambda}$ would have been replaced by $-\tilde{\lambda}$.

Quantum Fluctuation Relations

What we will do know is to obtain the quantum analogue of the preceding fluctuation theorems valid in the regime of classical statistical mechanics. The first point to exploit out is about the physical interpretation of work in quantum mechanics. We remark that here we assume closed quantum systems. The measure postulate of the theory plays a central role in the quantum formulation of the fluctuation relations since it counts the collapse of the quantum state on a specific eigenstate of the measured observable. The problem was explicitly approached in [21]. At first we have to replace the classical Hamiltonian and density state by their relative quantum operators that is $H(\mathbf{z}, \lambda_t)$ is replaced by the Hamiltonian operator $\hat{H}(\lambda_t)$, acting on the system Hilbert space $\mathcal{H}$ and, the probability density in the phase space $\rho(\mathbf{z}, \lambda(t))$ will be replaced by the density operator $\hat{\rho}(\lambda_t)$, evolving under the assumption of closed quantum system. Hereafter we will omit the hat in writing the preceding operators. The state system is initialized, according to the quantum statistical canonical ansamble, to a thermal state at inverse temperature β. This reads:

$$\rho(\lambda_0) = \frac{e^{-\beta H(\lambda_0)}}{Z(\lambda_0)}$$

where $Z(\lambda_0) = Tr\left(e^{-\beta H(\lambda_0)}\right)$.
Now we define the constrain of microreversibility for nonautonomous quantum systems. The concept is very closed to the classical one and can be expressed by:

$$U_{t,\tau}(\lambda) = \Theta^\dagger U_{\tau-t,0}(\tilde{\lambda})\Theta \tag{3.30}$$

Where Θ is the time reversal operator whose aim is to flip the momenta of the system [29]. We claim that (3.30) stands for time reversal Hamiltonian i.e.

$$H(\lambda_t)\Theta = \Theta H(\lambda_t) \tag{3.31}$$

In system with external magnetic field also the latter have to be flipped. Now also in quantum regime we have the initial equilibrium distribution condition and the microreversibility principle thus, we can approach the problem of work definition. In analogy to (3.18) and (3.25) we could think to write down the quantum version of

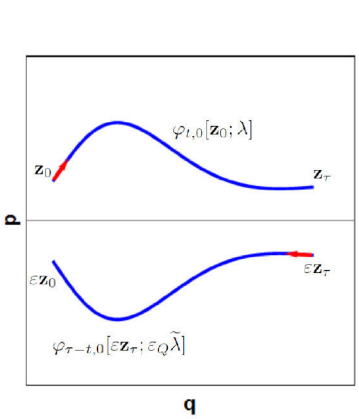

(a) Classical Microreversibility

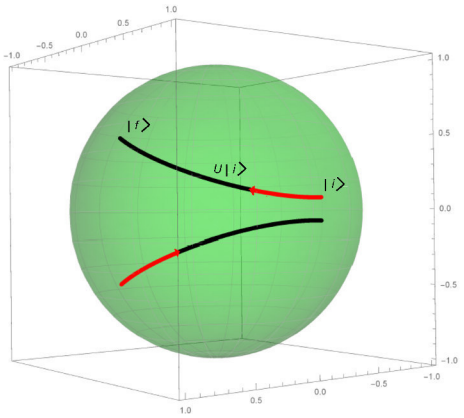

(b) Quantum Microreversibility

Figure 3.3: Illustration of Classical and quantum microreversibility principles. In the classical case we have trajectories in the phase space and the dynamics is driven by the fluxes in such space. Moving to the quantum case the trajectories are replaced by the state, a pure state $|\psi_t\rangle$, that lies on the surface of the Bloch sphere. At last the fluxes are replaced by the unitary time evolution operators U.

exclusive and inclusive work as $\mathcal{W}_0 = \int_0^\tau \lambda_t Q^H$ and $\mathcal{W} = H(\lambda_t) - H(\lambda_0)$ but we cannot obtain the same fluctuation relations as in (3.20) and (3.26) (see respectively [26] and [27]). We have to find a good definition of work, such definition will take into account the so called TEMA protocol. We proceed by measuring the value of energy of the system at the beginning of the protocol, at $t = 0$. In doing this we project the state in one of the Hamiltonian eigenstates $|E_n\rangle_0$, then we act the protocol λ_t which generally drives the system in a generic superposition of states $\{|E_n\rangle_t\}$ (eigenstates of $H(\lambda_t)$) until $t = \tau$ when we measure again the energy of the system projecting again the its state in some of the $H(\lambda_\tau)$'s eigenstates $|E_m\rangle_\tau$. The same though can be done for measurements of the unperturbed Hamiltonian H_0 in the whole expression for $H(\lambda_t)$. Addressing this $H(\lambda_t)$, by TEMA protocol

we will have two values of the energy, $E_n^{\lambda_0}$ and $E_m^{\lambda_\tau}$. The measured quantum inclusive work is then:

$$w = E_m^{\lambda_\tau} - E_n^{\lambda_0} \tag{3.32}$$

Due to the randomness of the measured energy, (3.32) is a random variable following an appropriate pdf. Indeed according to the definition of work $W = Tr(\rho_\tau H((\lambda_\tau))) - Tr(\rho(\lambda_0)H(\lambda_0))$ we could define an observable "work" $\hat{W}_t = H_H(\lambda_t) - H(\lambda_0)$, where $H_H(\lambda_t) = U^\dagger H(\lambda_t)U$ is the Heisenberg representation of the system Hamiltonian $H(\lambda_t)$ (here in Schrdinger pictrue) and thus we could get $W = Tr(\rho(\lambda_0)\hat{W}_t)$. Such operator is not a good physical observable. In fact we cannot measure $\hat{W}_t$. Then if we focus of the other momenta of $\hat{W}_t$ above, we see that the they are not finite. $\hat{W}_t$ is not an observable. What we want to underline is that we cannot get the result for the work measurement by sampling only one time any operator but in two different instants. What we can do is to measure energy values by some experimental apparatus. Another important aspect about work in quantum mechanics is that we cannot express the inclusive quantum work in the form of a integral of power (see [31] for a detailed analysis of the difference between a work obtained according to TEMA protocol and the one obtained by the power approach). W in eqn. (3.32) will be distributed according to some pdf. We can write down such work pdf by some considerations about the whole TEMA protocol. As we already said, the initial state is given by the thermal equilibrium canonical distribution at inverse temperature β according to the Hamiltonian $H(\lambda_0)$. The instantaneous eigenvalues (and eigenstates of the Hamiltonian) are given by:

$$H(\lambda_t)|\psi_{n,\gamma}^{\lambda_t}\rangle = E_n^{\lambda_t}|\psi_{n,\gamma}^{\lambda_t}\rangle \tag{3.33}$$

In the above equation n specifies the energy eigenvalues and γ considers eventual degeneration for g_n-fold degeneracy. Thus at time $t = 0$ we measure the energy of the state and we get some output $E_n^{\lambda_0}$ with probability:

$$p_n^0 = g_n \frac{e^{-\beta E_n^{\lambda_0}}}{Z(\lambda_0)} \tag{3.34}$$

projecting the whole state into:

$$\rho_n = \frac{\Pi_n^{\lambda_0}\rho(\lambda_0)\Pi_n^{\lambda_0}}{p_n^0} \tag{3.35}$$

where $\Pi_n^{\lambda_0} = \sum_\gamma |\psi_{n,\gamma}^{\lambda_0}\rangle\langle\psi_{n,\gamma}^{\lambda_0}|$ is the projector in the g_n-fold degenerate $H(\lambda_0)$'s eigenspace. We again remark that our system is thermally isolated from any kind of environment. This is a very strong requirement, it is difficult to achieve in quantum regime. After such assumption the evolution is given by:

$$\rho_n(t) = U_{t,0}(\lambda)\rho_n U_{t,0}^\dagger(\lambda) \tag{3.36}$$

Such evolution will stand until $t = \tau$ when we will operate the second measurement of $H(\lambda_t)$ giving a generic output $E_m^{\lambda_\tau}$ with probability:

$$p_{m|n}(\lambda) = Tr\left(\Pi_m^{\lambda_\tau}\rho_n(\tau)\right) \tag{3.37}$$

Finally we write the work pdf as:

$$P(w;\lambda) = \sum_{m,n}\delta\left(w - \left(E_m^{\lambda_\tau} - E_n^{\lambda_0}\right)\right)p_{m|n}(\lambda)p_n^0 \tag{3.38}$$

Integrating the quantum inclusive work (3.32) over (3.38) we will obtain the average work we was looking for.

It is important to note the the average work $\langle W\rangle$, obtained via work pdf, coincides with the difference of average energies $Tr(\rho(\lambda_0)\hat{W}_t)$ (see appendix A.2). The important difference between them is that the momenta:

$$P^n = \int dw\, w^n P(W) \tag{3.39a}$$

$$\tilde{P}^n = Tr(\hat{W}_\tau^n\rho(\lambda_0)) \tag{3.39b}$$

are finite in the case of expression (3.39a) and not for (3.39b). This point again underlines the physical meaningfulness of the definition of work as average of a stochastic variable on a pdf.

We now consider the Fourier transform of the work pdf, the characteristic function, which is shown to be given by a time-ordered correlation function of the exponentiated Hamiltonian [21, 30] for both nondegenerate end degenerate Hamiltonian cases:

$$\begin{aligned} G(u;\lambda) = \left\langle e^{iuw}\right\rangle &= \int dw\, P(w)e^{iuw} \\ &= \left\langle e^{iuH_\tau^H(\lambda_\tau)}e^{-iuH(\lambda_0)}\right\rangle \\ &= Tr\left(\frac{e^{iuH_\tau^H(\lambda_\tau)}e^{-(iu+\beta)H(\lambda_0)}}{Z(\lambda_0)}\right) \end{aligned} \tag{3.40}$$

In the above equation we used the superscript H to denote the Heisenberg picture of the operators and the average is performed on the canonical initial distribution. For a sudden quench (3.40) becomes:

$$Tr\left(e^{iuH_\tau(\lambda_\tau)}e^{-iuH(\lambda_0)}\frac{e^{-\beta H(\lambda_0)}}{Z(\lambda_0)}\right) \tag{3.41}$$

What we do now is to rewrite the eqn. (3.40) in order to have a formula closed to (3.25). Making use of the time ordering operator, from (3.40) we can get:

$$\begin{aligned} G(u;\lambda) &= Tr\left(\mathcal{T}e^{iu\left(H_\tau^H(\lambda_\tau)-H(\lambda_0)\right)}\,\frac{e^{-\beta H(\lambda_0)}}{Z(\lambda_0)}\right) \\ &= Tr\left(\mathcal{T}\,\exp\left\{iu\int_0^\tau dt\,\dot{\lambda}_t\frac{H_t^H(\lambda_t)}{\lambda_t}\right\}\right) \end{aligned} \tag{3.42}$$

Using the quantum microreversibility we have [3]:

$$Z(\lambda_0)G(u;\lambda) = Z(\lambda_\tau)G(-u+i\beta;\tilde{\lambda}) \tag{3.43}$$

Using the definition of free energy $F = -(1/\beta)\ln\left(e^{-\beta H}\right)$ we obtain the quantum Crooks-Tasaky fluctuation relation (3.45):

$$\begin{aligned} P(w,\lambda) &= \frac{1}{2\pi}\int du\,e^{-iwu}G(u;\lambda) \\ &= \frac{1}{2\pi}\int du\,e^{-iwu}\frac{Z(\lambda_\tau)}{Z(\lambda_0)}G(-u+i\beta;\tilde{\lambda}) \\ &= e^{-\beta\Delta F}\frac{1}{2\pi}\int du\,e^{-iwu}G(-u+i\beta;\tilde{\lambda}) \\ &= e^{-\beta\Delta F}\frac{e^{\beta w}}{2\pi}\int d\nu\,e^{iw\nu}G(\nu;\tilde{\lambda}) \\ &= e^{\beta(w-\Delta F)}P(-w,\tilde{\lambda}) \end{aligned} \tag{3.44}$$

that is:

$$\frac{P(w,\lambda)}{P(-w,\tilde{\lambda})} = e^{\beta(w-\Delta F)} \tag{3.45}$$

From the quantum Crooks-Tasaky fluctuation relation we can arrive to the quantum version of the Jarzynski equality:

$$\begin{aligned} \left\langle e^{-\beta w}\right\rangle_\lambda &= G(u,\lambda)\Big|_{u=-i\beta} \\ &= G(-u+i\beta)\Big|_{u=i\beta}\,e^{-\beta\Delta F} \\ &= e^{-\beta\Delta F} \end{aligned} \tag{3.46}$$

In the above equation, in going to the second to the third step we made use of (3.43). Thus the Jarzynski equality in quantum mechanics (as in classical mechanics) reads:

$$\left\langle e^{-\beta w}\right\rangle_\lambda = e^{-\beta\Delta F} \tag{3.47}$$

From (3.47) and applying the Jensen disequality we can get:

$$\langle w \rangle \geq \Delta F \tag{3.48}$$

As in the classical case we link the work done on the system, in a generic nonequilibrium process on a closed system, to the one obtained considering a isothermal branch from $\rho_i^{th} = \rho(\lambda_0) = \exp\{-\beta H(\lambda_0)\}/Z(\beta, H(\lambda_0))$ to $\rho_B = \rho(\lambda(\tau))^{th} = \exp\{-\beta H(\lambda_\tau)\}/Z(\beta, H(\lambda_\tau))$. Free energy is an equilibrium variable and ΔF is just the work done on the system in an isothermal transformation. It is highlighting to link this work, obtained form out of equilibrium dynamics, with the second law of thermodynamics, so to relate the irreversibility of the process, i.e. the increasing of some kind of entropy for the system, to the amount of work done on the working substance To this aim we define the *irreversible work as*:

$$\langle w \rangle_{irr} = \langle w \rangle - \Delta F \tag{3.49}$$

Following [32] and considering that we are dealing with a closed system, thus $\delta Q = 0$ we can write down an expression for the irreversible entropy that is:

$$\Delta S_{irr} = \beta \langle w \rangle_{irr} \tag{3.50}$$

Again in [32] it is shown that the irreversible entropy (3.50), that can be obtained by thermodynamic considerations, can be related to the quantum relative entropy between $\rho_\tau = U(\lambda_\tau)\rho_i^{th}U(\lambda_\tau)^\dagger$ and ρ_B:

$$\Delta S_{irr} = D(\rho_\tau || \rho_\beta(\lambda_\tau)) \tag{3.51}$$

so that the Clausius disequality can be generalized counting the Bures length between the two states put in the relative entropy above:

$$\Delta S_{irr} \geq \frac{8}{\pi^2}\mathcal{L}(\rho(\lambda_\tau)||\rho_\beta(\lambda_\tau)) \tag{3.52}$$

for the upper equation we recall that:

$$\mathcal{L}(\rho_1, \rho_2) = \arccos\left(\sqrt{F(\rho_1, \rho_2)}\right) \qquad \text{with}$$
$$F(\rho_1, \rho_2) = \left(Tr\left(\sqrt{\sqrt{\rho_1}\rho_2\sqrt{\rho_1}}\right)\right)^2 \tag{3.53}$$

Very intuitively (3.52) states that entropy production is larger when a system is driven farther away from equilibrium. We underline that relative entropy is not merely a metric so even if in some way its value is as great as the two operators ρ_τ

and$\rho_\beta(\lambda_\tau)$ are different one from each other, it does not formally give a distance between them. Eqn. (3.52) has been used to study the amount of irreversibility in various systems as simple harmonic oscillators [33] or spin chain [34] and ultracold gases [35]. Finally we can again characterize the irreversible work by its relation with the state ρ_B by [36]:

$$\langle w_{irr} \rangle = T_B(S_B - S_i) - \left\langle Q^{th}_{\tau \to B} \right\rangle \tag{3.54}$$

As last argument of the field of fluctuation relations we want to introduce and analyze the so called *inner friction work* [37]. As we already said in the last section, the concept of inner friction was preceding introduced in [28]. It stands that if the driving of the Hamiltonian, of a closed and non isolated quantum system, is performed in a finite time than the upper levels population of its state will be generally increased; it seems like a certain amount of heat is absorbed by the system. We repeat that we are dealing with closed quantum systems, thus for each evolution operator U there exists U^{-1}, the quantum mechanical reversibility always stands. From this point of view the name "inner friction" for a closed quantum system could be misleading, but here, at thermodynamic level, adopting the concept of thermodynamic reversibility as in [13], we describe the physics by thermodynamics concepts that will help us in characterizing such dynamics; the concept of friction in an adiabatic branch (a thermodynamic transformation) is one of them. What we do is to compare the difference of average energy of a system in a finite time evolution, $\langle H \rangle_{i \to \tau} = \langle w \rangle = Tr\left(H(\lambda_\tau)\rho_\tau\right) - Tr\left(\rho^{th}_i H(\lambda_0)\right)$, with the work of the reversible quantum adiabatic processes defined in 3.2, that coincides with the internal energies difference $\langle w_{i \to A} \rangle = \sum_n P_n \Delta E_n$. These two variables are generally different if the system's Hamiltonian does not commute with itself at different times, $[H(\lambda_{t_1}), H(\lambda_{t_2})] \neq 0$ for $t_1 \neq t_2$ and, as we assumed, the evolution is performed on a finite time, thus adiabatic theorem does not apply. The state gained by the reversible protocol is $\rho_A = \exp\left[-\beta_A H(\lambda_\tau)\right] / Z(\beta_A; H(\lambda_\tau))$ where β_A is the effective temperature defined as in (3.8) (hereafter we assume that it is possible to define an effective temperature for the transformation). Thus we now study the difference:

$$\langle w_{fric} \rangle = Tr\big(H(\lambda_\tau)\rho_\tau\big) - Tr\left(\rho^{th}_i H(\lambda_0)\right) - \langle w_{i \to A} \rangle \tag{3.55}$$

As in the case of irreversible work (3.49), we will show that eqn. (3.55), the inner friction work, can be expressed through the quantum relative entropy between the state ρ_τ and ρ_A. In this sense we can link such inner friction work to the generation of entropy in the process. The passages of this demonstration are showed in

appendix A.3 and the final result reads:

$$\langle w_{fric} \rangle = \frac{1}{\beta_A} D(\rho_\tau || \rho_A) \tag{3.56}$$

Inner friction work is then always greater then zero since Klein's inequality, that is the relative entropy is positive defined. We can add new information to this new kind of work getting a lower geometric bound expressed in terms of Bures length:

$$\beta_A \langle w_{fric} \rangle \geq \frac{8}{\pi^2} \mathcal{L}^2(\rho_\tau, \rho_A) \tag{3.57}$$

in the above equation, $\mathcal{L}$ is defined as in (3.53). The inner friction work is then related to the heat absorbed in a thermalization from the state ρ_τ to ρ_A:

$$- \langle w_{fric} \rangle = \left\langle Q^{th}_{\tau \to A} \right\rangle \tag{3.58}$$

In writing the above equation we have brought the result of eqn. (3.54) to the case where $\rho_B \to \rho_A$ so that $S_A - S_i = 0$. Note that if we address the Von Neumann entropy change $S(\rho_\tau) - S(\rho_i)$, instead of $D(\rho_\tau || \rho_i)$ linked to $\langle w_{fric} \rangle$, it would be null. To clarify why this difference is null we can note that there exists a path in the space of operator ρ_t that goes from ρ_τ to ρ_0 by $U^\dagger(\lambda_t)$ and from ρ_0 to ρ_A with the same protocol λ_t but now performing the transformation in an infinite time. The time evolution operator driving this last dynamics is however unitary. Then ρ_τ and ρ_A can be linked by a whole unitary transformation and consequently they have the same Von Neumann entropy. We want to say that the results in eqns. (3.54) and (3.58) can be obtained by standard thermodynamic considerations for nonequilibrium transformations. Again eqn. (3.58) relates the increasing of entropy due to the irreversibility of the adiabatic transformation in the quantum system to the heat dissipated by a reservoir at inverse temperature β_A which allows the system to thermalize from ρ_τ to ρ_A. It is thus interesting to compare the two definitions of irreversible and inner friction work. At first we compare the two average heat that appears in eqns. (3.54) and (3.58):

$$\left\langle Q^{th}_{\tau \to A} \right\rangle - \left\langle Q^{th}_{\tau \to B} \right\rangle = \mathcal{U}_A - \mathcal{U}_B \tag{3.59}$$

We used the notation $\mathcal{U}$ to indicate the internal energy, $\mathcal{U} = Tr(\rho_{eq} H)$ where ρ_{eq} is an equilibrium state. Internal energy is linked to the entropy (the von Neumann entropy) and the free energy of a state by $\mathcal{U} = TS - F$, thus we can get:

$$\langle w_{fric} \rangle - \langle w_{irr} \rangle = (\mathcal{U}_A - \mathcal{U}_B) - T_i (S_A - S_B) \tag{3.60}$$

That can be read as:

$$\langle w_{irr}\rangle + F_B + T_B S_B = \langle w_{fric}\rangle + F_A + T_A S_A \tag{3.61}$$

The link between irreversible and inner friction work can be also characterized by expressing the equations (3.60) and (3.61) in terms of relative entropies:

$$\begin{aligned} T_B D(\rho_\tau||\rho_B) - T_A D(\rho_\tau||\rho_A) &= T_B D(\rho_A||\rho_B) \\ &= -T_A D(\rho_B||\rho_A) + (S_A - S_B)(T_A - T_B) \end{aligned} \tag{3.62}$$

The first term above is directly equal to the difference of the irreversible and inner friction work, the second and the third terms can be obtained by some algebraic passage.
We can go deeper, in characterizing the entropy production, $D(\rho_\tau||\rho_A)$, by giving its pdf according to TEMA protocol. Given the two outcomes of energy measurement $E_m^{\lambda_t}$ and $E_n^{\lambda_0}$, we can built the stochastic variable entropy by:

$$s = \beta_A E_m^{\lambda_t} - \beta_i E_n^{\lambda_0} \tag{3.63}$$

Such variable will by distributed according to the pdf:

$$P(s, \lambda_t) = \sum_{n,m} P_n^0 P_{m|n} \delta\left(s - \beta_A E_m^{\lambda_t} - \beta_i E_n^{\lambda_0}\right) \tag{3.64}$$

The average value, $\langle s\rangle$, of s at time t is given by integrating the latter with the entropy pdf eqn. (3.64) over all the possible outputs s (later eqn. (3.65a)) but the same result can be obtained by the following eqn. (3.65b) (see appendix A.4):

$$\langle s\rangle = \int ds\, sP(s;\lambda_t) \tag{3.65a}$$

$$\langle s\rangle = \beta_A Tr(\rho_\tau H(\lambda_\tau)) - \beta_i \mathcal{U}_i \tag{3.65b}$$

Now by following the same reasoning used for obtaining the Jarzynski equation in quantum regime, we cen get a fluctuation theorem for the entropy variable s:

$$\begin{aligned} \left\langle e^{-s}\right\rangle &= \sum_s \sum_{n,m} P_n^0 P_{m|n} \delta\left(s - \beta_A E_m^{\lambda_t} - \beta_i E_n^{\lambda_0}\right) e^{-s} \\ &= \sum_{n,m} P_n^0 P_{m|n} \delta\left(s - \beta_A E_m^{\lambda_t} - \beta_i E_n^{\lambda_0}\right) e^{-(\beta_A E_m^{\lambda_t} - \beta_i E_n^{\lambda_0})} \\ &= \frac{Z_A}{Z_i} \\ &= e^{-(\beta_A F_A - \beta_i F_i)} \end{aligned} \tag{3.66}$$

However a more general solution has been obtained in [38]. Using the Jansen inequality we can obtain:

$$\langle s \rangle \geq \beta_A F_A - \beta_i F_i \tag{3.67}$$

It is natural to define the entropy production, according to the above equation, as:

$$\langle \Sigma \rangle = \langle s \rangle - (\beta_A F_A - \beta_i F_i) \tag{3.68}$$

It can be shown that the latter variable is equal to the quantum relative entropy $D(\rho_\tau || \rho_A)$ (see A.4). So we have:

$$\langle \Sigma \rangle = D(\rho_\tau || \rho_A) = \beta_A \langle w_{fric} \rangle \tag{3.69}$$

Thus also considering the statistic of the entropy production, in an irreversible process, we obtain that inner friction apppears. The average excess of entropy coincides with the inner friction work time the inverse effective temperature β_A. We end this part about inner friction work by showing that (in an analogous way as done in [24]) the cumulants C_n of the distribution of the variable s are related to the combination of free energies $-(\beta_A F_A - \beta_i F_i)$ (see appendix A.5) as :

$$-(\beta_A F_A - \beta_i F_i) = \sum_{n=1} \frac{(-1)^n}{n!} C_n \tag{3.70}$$

where $C_2 = \left\langle s^2 \right\rangle - \langle s \rangle^2$ is the variance, $C_3 = \left\langle s^3 \right\rangle - 3 \left\langle s^2 \right\rangle \langle s \rangle + 2 \langle s \rangle^3$ is the skewness and so on for the other terms. This implies that the inner friction can be expressed as combination of cumulants of order greater then two.

3.3.2 Finite Time Otto Cycle and Disorder Effects

To apply the thermodynamics described before to the field of heat engines is a natural requirement. It helps to test the thermodynamic rules and, on the other hand contributes to create possible applications. Thus in this section we will use the nonequilibrium thermodynamics to study a particular QHE, a QOC working at finite power. Since the power is non null it means that each branch of the cycle is performed on a finite time, thus, we describe a system which works in a more realistic way than the one in section 3.2.4. The choice of the Otto cycle is not casual. In fact, if in studying Otto cycle we focus on its applications as heat engine, getting advance from the quantumness of the system, on the other hand it is a useful test ground for studying the concept of inner friction work, linked to the irreversibility of the adiabatic branches. Indeed QOC, as its classical correspondent, is made by two isochoric and two adiabatic transformations. Considering the isochoric branches as thermalizations, we can perfectly reproduce the initial

canonical equilibrium condition for the state at the end of such processes and we can then perform the finite time drivings, which will push the system out of equilibrium. So many works have approached the same problem of irreversibility in quantum regime using Otto cycle. As important reference we cite [28] [39][40] and[42], where the concept of inner friction, together with other dissipative elements such noise, have been taken into account. The system that we will define is the one considered in [41]. In Particular we consider the quantum friction effects coming from finite time dynamics on a disordered system used as working substance; we will consider an ensemble of noniteracting qubits as components of the whole system in a setting where the parameters are not homogeneous. The same scenario can be implemented in two different ways as shown in Figure 3.4. It can be modelled by different oriented spins with tilting angles $\theta_i \quad i = 1, 2, \ldots$ with respect to the direction of a uniform external field **B**. Such different orientation will be then described by the pdf $G(\theta)$ (see Figure 3.4(a)). Alternatively, all sample dipoles could be perfectly aligned in an ordered configuration as frozen, but now we allow for an inhomogeneous external field in space as in Figure 3.4(b). The field orientation across the sample is then given, in this case, by the function $G(\theta)$ describing the distribution of the spin's orientations in the preceding example. We

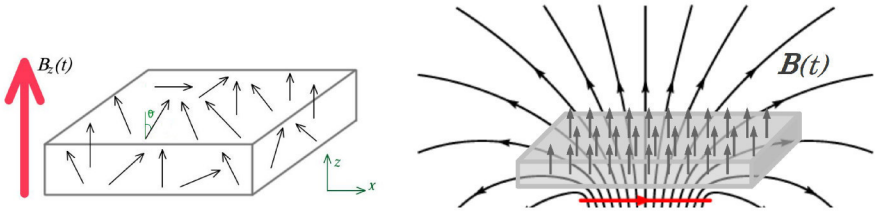

(a) Disordered Sample (b) Inhomogeneous Field

Figure 3.4: Content taken by [41]. The scenarios depicted above are equivalent. They reproduce the same dynamics and thermodynamic outputs as work, power and efficiency on the Otto cycle.

consider for each qubit in the system, when it is in the non isolated configuration, an Hamiltonian such as:

$$H(\lambda(t)) = \frac{\omega_0}{2}\sigma_z + \lambda(t)(\cos(\theta)\sigma_z + \sin(\theta)\sigma_x) \tag{3.71}$$

The adiabatic transformation, is given by the unitary finite time branch generated by the Hamiltonian (3.71). In this Hamiltonian we have a linear driving protocol at fixed rate:

$$\lambda(t) = \alpha\frac{\omega_0}{2}t \tag{3.72}$$

generated by an external field which we assume to be misaligned by an angle θ respect to the static field ω_0 (we take in mind the case in Figure 3.4(a)). As we can note eqn. (3.71) is such that $[H(t_1), H(t_2)] \neq 0$ for $t_1 \neq t_2$ if $\theta \neq 0$. Therefore the angle θ is the parameter which will allow for the appearing of inner friction in the branch. Then, in the case of many qubits (as in the system we want to describe) we will consider different values of θ for each of them. Such angle will be the inhomogeneous parameter we addressed before and such inhomogeneity is a kind of disorder of the system. By a quantum mechanical point of view it affects the energy spacing of the single qubit as well as the eigenstates of $H(\lambda(t))$ and their populations. The parameter α in eqn. (3.72) regulates the adiabaticity of the transformation, in the limit $\alpha << \omega_0$ we approximatively have quantum adiabatic dynamics. We repeat that we assume that at the initial time, $t = 0$, the qubit is in a thermal state at inverse temperature β. Thus the interesting case we will explore will be characterized by $\theta \neq 0$ and $\alpha \sim \omega_0$ (the cases $\alpha << \omega_0$ and $\alpha >> \omega_0$ are trivial, since the first one corresponds to the reversible quantum adiabatic case and in the second one the evolution operator is closed to the identity [9]). To see how inner friction affects the efficiency and the power of the heat engine, we will operate in two steps. At first we will analyze these effects on a cycle for a single qubit and then we will mediate over the disorder (we will assume a distribution $G(\theta)$ for the misalignments) characterizing the disordered sample. Before approaching the QOC we want to analyze the effects of a finite time adiabatic transformation on a single qubit whose unitary dynamics is generated by Hamiltonian (3.71) under the assumption that its initial state is given by canonical equilibrium distribution $\rho_0 = \exp[-\beta H(\lambda_0)]/Z(\beta; H(\lambda_0))$. In particular we study the effects of a unitary transformation counting two steps. At first $\lambda_t^{(F)}$ changes from λ_0 up to λ_{t_f} in a scaled time $\alpha_F t_F$, that is $\lambda_t^{(F)} = \frac{\omega_0}{2}\alpha_F t$. We call such $\lambda_t^{(F)}$ forward protocol. Then at time t_F we will perform a second unitary transformation, the backward process, in which the system Hamiltonian is obtained inserting in (3.71) the backward protocol $\lambda_t^{(B)} = \lambda_{t_F}^{(F)} - \alpha_B \omega_0 t/2$. Finally the backward process will end at the condition $\lambda_{t_B}^{(B)} = \lambda_{t_F}^{(F)}$ so that $H(\lambda_{t_B}^B) = H(\lambda_{t_F}^F)$. The time evolution operator for the forward process is $U_F(0, \tau_F) = \mathcal{T} \exp\{-i \int_0^{t_F} dt' \, H(\lambda_{t'}^F)\}$ and for the backward process we have $U_B(0, \tau_B) = \mathcal{T} \exp\{-i \int_0^{t_B} dt' \, H(\lambda_{t'}^B)\}$. The whole forward-backward protocol is schematize in the following diagram:

$$\begin{array}{ccc} \rho_0 & \xrightarrow{U_F(0,t_F)} & \rho_1 \\ \rho_2 & \xleftarrow[U_B(0,t_B)]{} & \rho_1 \end{array} \tag{3.73}$$

The state ρ_2, can differ from ρ_0 due to the inner friction effects. By this fact we try to give an idea about what means "irreversibility" (thermodynamic irreversibility). For reversible processes we obtain $\rho_0 = \rho_2$.

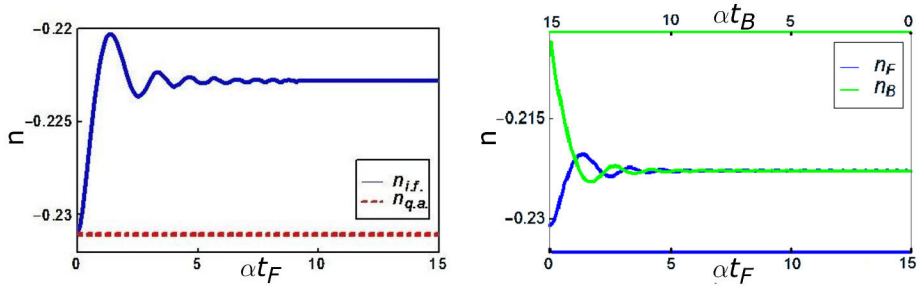

(a) Polarization Growth

(b) Thermodinamical Irreversibility

Figure 3.5: Content taken by [41]. At left we see the increasing of the polarization for a finite time adiabatic branch respect to the quasistatic case in a qubit dynamics driven by eqn. (3.71). At right we show that, although the protocol in driven forward and backward to its initial value, then the thermodynamic irreversibility, linked to the finiteness in time of the driving, pushes the state far away from the initial one.

In order to better describe the above protocol we look at the time-dependent polarization, defined as $n(t) = Tr[\rho(t)H(t)]/\omega(t)$, where in this expression the frequency $\omega(t)$ indicates the energy level spacing, at time t, for both the forward and backward protocols. This variable gives a measure of the capability of the state system to "follow" the external field. If we think at the system as a spin and at the field as a magnetic field then the time dependent polarization gives an idea of how much these are aligned. It gets its minimum value if they are parallel and grows up otherwise.
In the forward protocol the trajectory $n(t)$ at any $\alpha_F t$ is shown in Figure 3.5(a), where we can see that that finite time evolution introduces deviations of the polarization with respect to the quantum adiabatic case. Moreover, as it is shown in Figure 3.5(b), by applying also the backward protocol, the system does not get back to its initial state, but reaches a different polarization (green line) at the end of the protocol. This already gives a quantitative indication that finite time driving leads to an irreversible behaviour. Now we can also characterize the irreversibility of the process by the inner friction work defined in last section 3.3.1. According to eqn. (3.56) we have $-\beta_0 Q(\rho_f \to \rho_{th}^{rev}) = \beta_{eff} W_{fric} = D(\rho_f || \rho_{th}^{rev})$ where $Q(\rho_f \to \rho_{rev}^{th})$ is the heat that the system takes to thermalize from ρ_2 to ρ_{rev}^{th} at the inverse effective temperature β_{eff}. The variable $D(\rho_f || \rho_{rev}^{th})$ for the time evolu-

tion given by the system Hamiltonian eqn. (3.71) is reported in Figure 3.3.2, where we note that, when both transformations are very slow (quantum adiabatic case) or very fast (diabatic or sudden case) at the end of the protocol the system is found to be in (or very close to) its initial state. For finite time branches, however, the final state deviates from the initial one. Again the thermodynamic interpretation of this difference is the appearing of inner friction related to the irreversibility of the branch forward-backward.

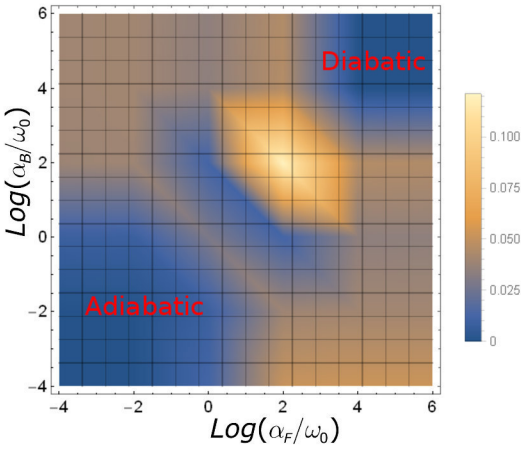

Figure 3.6: Content taken by [41]. The quantum relative entropy between the state at the end of the backward step and the one gained by quasistatic transformation $\rho_{rev}^{th} = \rho_0$ (they are the same state although they are expressed by different parameters). Inner friction is very close to zero both for $\alpha_{F,B} \to 0$ and $\alpha_{F,B} \to \infty$. The state parameters are $\beta_i = \omega_0$ ($\hbar = k_B = 1$), $\theta = \pi/5$ and $\alpha_F t_F = \alpha_B t_B = 15$.

Now that we have identified the irreversible dynamics given by the Hamiltonian (3.71) we can characterize the various branches of the cycle. For the adiabatic branches we will consider the case where them ($1 \to 2$ and $3 \to 4$) are equally long, namely, $t_F = t_B = \tau_{ad}$, and have the same rate of change for the field, $\alpha_F = \alpha_B$. These latter are connected by two isochoric transformations, namely thermalization processes. We will assume that perfect thermalization is achieved very quickly with respect to the characteristic time of the isochoric branch and that this latter is smaller than τ_{ad}:

$$\tau_{therm} << \tau_{iso} << \tau_{ad} \tag{3.74}$$

The pedices indicate respectively the thermalization, isochoric and adiabatic processes.

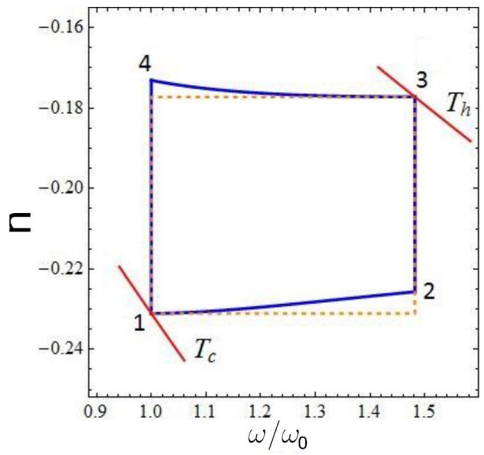

Figure 3.7: Content taken by [41]. QOCs for a single qubit in the $\omega - n$ plane. The orange dashed line corresponds to the QOC having reversible quantum adiabatic branches, we can see that the polarization does not change during such transformations. On the other hand the blue lines represent a QOC with finite time adiabatic processes. The unitary evolution is driven by Hamiltonian (3.71) with $\theta = \pi/5$, $\alpha\tau_{ad} = \omega_0\tau_{ad} = 0.5513$,$\beta_c = \omega_0^{-1}$ and $\beta_h = /\beta_c/2$.

With these assumptions, the quantum Otto cycle appears as the one in Figure 3.7. The thermodynamic variable of the cycle are the extracted work, the power and the heat exchanged with the reservoirs in contact with the system, respectively W_{ex}, $\mathcal{P}$ and Q. According to the result in appendix A.2 we can indicate as work done on an adiabatic branch the variable:

$$W = Tr(\rho_f H(\lambda_{\tau_{ad}})) - Tr(H(\lambda_0)\rho_0)$$

Where the pedices refer to the states and Hamiltonians at the beginning and at the and of the adiabatic branch. Then the heat exchanged during an isochoric transformations, given in the set of eqns. (3.2), can be explicitly brought into the following form (for a two levels system):

$$Q_{iso} = E_e\left(p_e^{(f)} - p_e^{(i)}\right) + E_g\left(p_g^{(f)} - p_g^{(i)}\right) = \omega\left(p_g^{(i)} - p_g^{(f)}\right) \tag{3.75}$$

The apexes indicate the initial and final states of the branch and, again, $\omega = E_e - E_g$ is the energy spacing. By this way, considering that the total change of average energy on a whole cycle vanishes, we have:

$$\Delta U_{tot} = W_{1\to 2} + Q_h + W_{3\to 4} + Q_c = 0 \tag{3.76}$$

where $Q_{h,c}$ represent the heat exchanged with the thermal bath at inverse temperature $\beta_{h,c}$. Thus we give the following expression for the extractable work:

$$\begin{aligned} W_{ex}(\tau_{ad}, \theta, \beta_h/\beta_c) &= Q_h + Q_c \\ &= \left(\omega_2 \left(p_0^{(2)} - p_0^{(3)}\right) + \omega_1 \left(p_0^{(4)} - p_0^{(1)}\right)\right) \end{aligned} \tag{3.77}$$

For a QOC it can be shown [28] that according to the definition of heat engine, i.e. an engine for which we have $W_{ex} > 0$, it holds:

$$\omega_1(n_1 - n_4) < \omega_2(n_2 - n_3) \tag{3.78}$$

Other figures of merit as power and efficiency are respectively defined, respect to (3.77), as:

$$P(\tau_{ad}, \theta, \beta_h/\beta_c) = \frac{W_{ex}}{2\tau_{ad}+\tau_{iso}} \tag{3.79}$$

$$\eta(\tau_{ad}, \theta, \beta_h/\beta_c) = \frac{W_{ex}}{Q_h} = 1 + \frac{Q_c}{Q_h} \tag{3.80}$$

It is important to note that for such cycle the assumption that its efficiency is not greater than the Carnot efficiency, $\eta_C = 1 - T_c/T_h$, reduces to $\beta_h/\beta_c > \omega_1/\omega_2$ and that for a quantum adiabatic branches this latter condition is equivalent to the requirement of positive net work (extractable work) for the cycle. The above variables refer to a single qubit with generic misalignment θ, now we define the analogue variables, but considering the whole sample, thus according to the generic distribution of the misalignment angle $G(\theta)$. We have:

$$\overline{W}_{ex}(\tau_{ad}, \beta_h/\beta_c, \sigma) = \int_0^\pi G_\sigma(\theta) W_{ex}(\tau_{ad}, \theta, \beta_h/\beta_c) d\theta \tag{3.81}$$

$$\overline{\mathcal{P}}(\tau_{ad}, \beta_h/\beta_c, \sigma) = \int_0^\pi G_\sigma(\theta) \mathcal{P}(\tau_{ad}, \theta, \beta_h/\beta_c) d\theta \tag{3.82}$$

$$\overline{\eta}(\tau_{ad}, \beta_h/\beta_c, \sigma) = \int_0^\pi G_\sigma(\theta) \eta(\tau_{ad}, \theta, \beta_h/\beta_c) d\theta. \tag{3.83}$$

As we said before we present the results dividing them in two groups. At first we consider a generic angle θ, this refers to the case where the working substance is a single qubit, then we will average over some $G(\theta)$ distribution (average on the disorder) so to consider the whole simple. For the case of a single qubit working substance in Figure 3.8 we report W_{ex}, $\mathcal{P}$ and η as functions of the total time of the cycle $t_{tot} \sim 2\tau_{ad}$, fixing the rapport between the temperatures of cold and hot reservoir at $\beta_h/\beta_c = 0.5$. We can see in Figure 3.8(a) that the extractable work becomes negative if the τ_{tot} exceeds a maximum value, $\tau_M(\theta)$, which is a function of the misalignment θ and the temperature rapport β_h/β_c. This means that if the cycle lasts too long then we are actually doing work on the system, that is we have not anymore a heat engine. Moreover there exists a critical value of θ such that

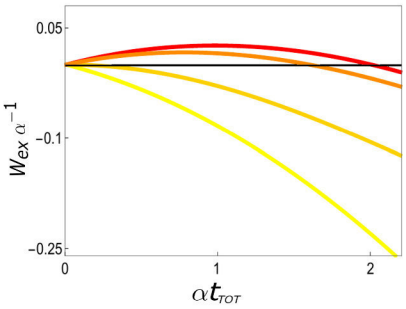

(a) Extractable work (W_{ex}) vs. αt_{tot} for different values of θ

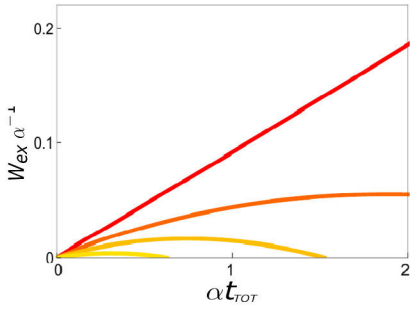

(b) Extractable work (W_{ex}) vs. αt_{tot} for various β_h/β_c

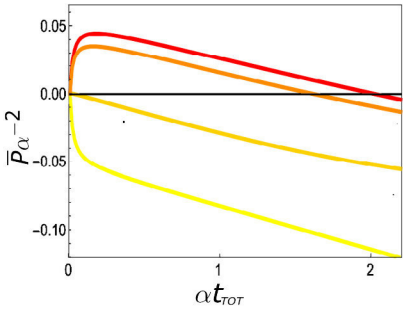

(c) Power ($\mathcal{P}$) vs. αt_{tot} for various of θ

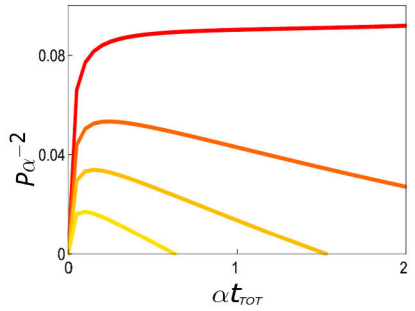

(d) Power ($\mathcal{P}$) vs. αt_{tot} for various of β_h/β_c

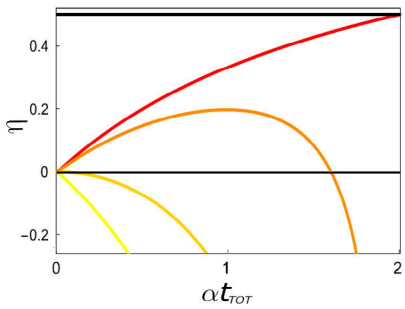

(e) Efficiency (η) vs. αt_{tot} for various θ

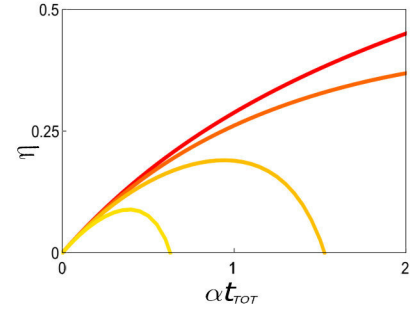

(f) Efficiency (η) vs. αt_{tot} for various β_h/β_c

Figure 3.8: Content taken by [41]. Extractable work W_{ex}, power $\mathcal{P}$ and efficiency η as functions of the total time of the cycle αt_{tot}. In Figure 3.8(a), 3.8(c) and 3.8(e) we fix the temperature ratio at $\beta_h/\beta_c = 0.5$ and vary the misalignment angle θ. We start from $\theta = 0$ for the highest (red) plot and then we consider $\theta = \pi/5, \pi/2$ and finally $\theta = \pi$ for the lowest (yellow) curve. On the other hand, in Figure 3.8(b), 3.8(d) and 3.8(f) we fix the misalignment to $\theta = \pi/5$ and vary β_h/β_c. Again, going from the top (red plot) down to the yellow curve, the temperatures rapports takes the values $\beta_h/\beta_c = 0.01, 0.31, 0.51, 0.71$.

the extractable work W_{ex} is negative for any value of τ_{tot}. In the regime where the extractable work is negative our one-qubit-engine works as a refrigerator, which uses external work to cool the cold reservoir. For sudden quench we observe that, although the transformation is reversible ($U(0,0) = \mathbb{I}$), the extractable work is null. An analogous behaviour is shown by power and efficiency in Figure 3.8(c) and 3.8(e).

We want to underline the aspect that finite time transformations are however fundamental in order to have non null power heat engines and thus inner friction effects are expected for real quantum heat engine. However, different ways to minimize such effect are proposed in [43] under the generic names 'shortcuts to adiabaticity' and in [44] with the name of "quantum lubrification". In the first case the control sequences λ_t is designed such that the irreversibility at the end of the adiabatic branch is minimized and for the case of "quantum lubrification" an additional noise is considered so to minimize the coherences in the final state of the system at the end of unitary evolution. Such tricks have not been tested for this Otto cycle, however better performance of the engine would be expected.

Returning to our QOC, it is natural to ask what is the working of the cycle as function of the temperature thus in Figure 3.8(b) 3.8(d) and 3.8(f), we look at the dependence of W_{ex}, $\mathcal{P}$, and η on the total time of the cycle for a fixed misalignment angle $\theta = \pi/5$ and for different values of the ratio β_h/β_c. We can see that as the latter ratio increases then the extractable work increases too (Figure 3.8(b)). This is something which is expected; nevertheless, we can clearly see that the finiteness in the time of the cycle introduces again negative works for cycle time greater than a certain value, $t_{tot} > \tau_M(\beta_h/\beta_c)$. This behaviour is due to the inner friction effects. The lost of performances for the cycle, due to the inner friction can be explicitly found. Indeed Inner friction work is explicitly shown in Figure 3.9, where the sum of the friction produced in the two adiabatic strokes is shown as a function of the total cycle time for various misalignment angles θ and $\beta_h/\beta_c = 0.5$. As we can see, the case $\theta = 0$ is very special, as no friction is generated for whatever rate of variation for the protocol λ_t. In this case indeed the system Hamiltonian commutes with itself at different time and, since for a qubit we can always define an effective temperature for quantum adiabatic processes, then the transformation is reversible. On the other hand, $\langle W_{fric} \rangle$ increases with the angle θ and decreases with the decreasing of the driving rate α.

We now consider the whole sample, and the effects of disorder on it, assuming that θ is a Gaussian random variable with mean value $\theta = 0$ and variance σ^2. Thus it will be σ that will give rise to dissipative effects. In Figure 3.10(a) 3.10(c) and 3.10(e) we show the behaviour of extractable work, power, and efficiency for different values of the variance at given temperature ratio $\beta_h/\beta_c = 0.5$. We can see that, the best performance is always obtained with sharper distributions. Thus, if

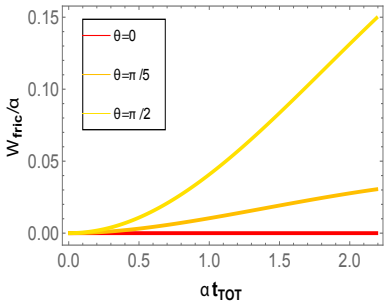

Figure 3.9: Content taken by [41]. Inner friction accumulated in the cycle as a function of the total time t_{tot} for different misalignments θ, at $\beta_h/\beta_c = 0.5$.

the disorder of the system grows, σ grows up, then the capability of the working substance of providing work as well as doing it in a more efficient way and the power of the conversion of heat into work decrease. Again we mention the fact that there exists a maximum total time τ_M for which the QOC is not a heat engine anymore. We also notice that even a small disorder has the effect in reducing the efficiency for long enough times, as already happened for the case of a single qubit system. Figure 3.10(b) 3.10(d) and 3.10(f) we plotted the behaviour of the same thermodynamic variables for different values of the ratio of temperatures between hot and cold reservoirs, β_h/β_c, at a given variance $\sigma^2 = 0.1$. Again, all of the quantities increase as β_h/β_c goes to zero, that is as the hot reservoir temperature is greater and greater than the cold reservoir temperature. However, it has to be mentioned that some care should be paid when comparing the values of the efficiency at different operating times. Indeed the ideal cycle with infinitely slow adiabatic branches, corresponding to the absence of misalignment, is characterized by the efficiency $\eta_{ideal} = 1 - \omega_1/\omega_2$ and ω_2 is a function of the time. The dependence of η_{ideal} on ω_2 implies that the efficiency η of the finite time cycle should be compared with a different η_{ideal} at each t_{tot} so to understand how the increasing of dissipation will affect the efficiency of the cycle. We show this comparison in Figure 3.11. As last figure of merit we introduce the efficiency at maximum power. Since the efficiency takes its maximum value for reversible transformations, that means infinitely long cycle, and this implies zero power for the heat engine working for such cycles, a useful figure of merit for characterizing the utility of the cycle is just the efficiency at maximum power. We look for the t_{tot} such that the power has its maximum value and at this time we consider the efficiency of the engine. This relation is considered in Figure 3.12. In studying this figure of merit we focused only on the efficiencies and powers for the whole sample, the averaged ones, for both cases of dependence by the variance at fixed temperature rapport β_h/β_c

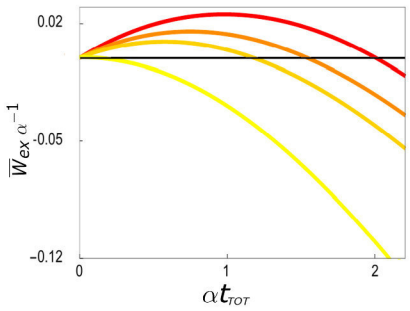

(a) Average extractable work ($\overline{W}_{ex}$) vs. αt_{tot} for various σ

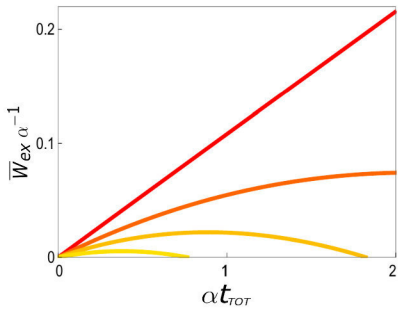

(b) Average extractable work ($\overline{W}_{ex}$) vs. αt_{tot} for various β_h/β_c

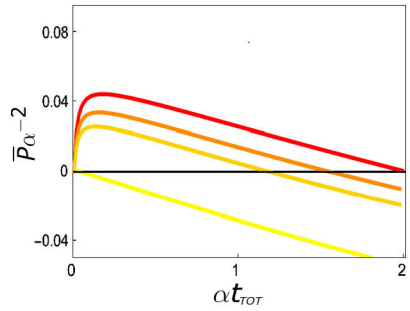

(c) Averaged power ($\overline{\mathcal{P}}$) vs. αt_{tot} for various σ

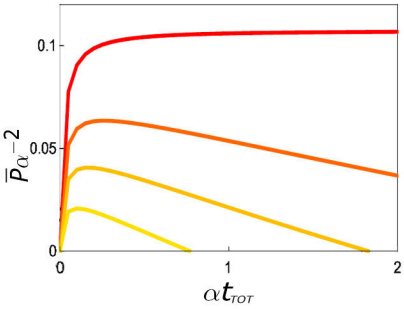

(d) Averaged power ($\overline{\mathcal{P}}$) vs. αt_{tot} for various β_h/β_c

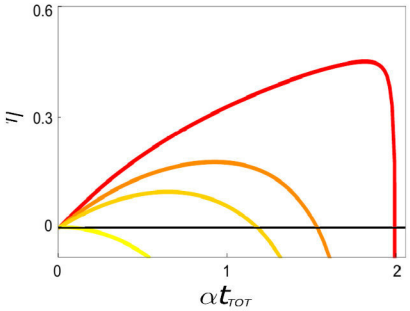

(e) Averaged efficiency ($\overline{\eta}$) vs. αt_{tot} for various σ

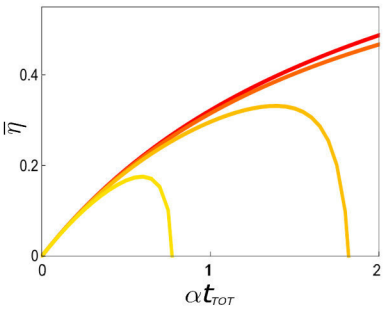

(f) Averaged efficiency ($\overline{\eta}$) vs. αt_{tot} for various β_h/β_c

Figure 3.10: Content taken by [41]. Averaged extractable work, power and efficiency as functions of αt_{tot}. In Figure 3.10(a), 3.10(c) and 3.10(e), we consider a fixed value for the temperature ($\beta_h/\beta_c = 0.5$) and vary σ. Different colours refer to different Gaussian widths: the red plots correspond to $\sigma^2 = 0.01$, the orange ones to $\sigma^2 = 0.5$, light orange ones to $\sigma^2 = 1$ and finally the (lowest) yellow curves refer to a flat distribution. In 3.10(b), 3.10(d) and 3.10(f) we take $\sigma^2 = 0.1$ and vary β_h/β_c, which, going from the red plots to the yellow ones, takes the values $\beta_h/\beta_c = 0.01, 0.31, 0.51, 0.71$.

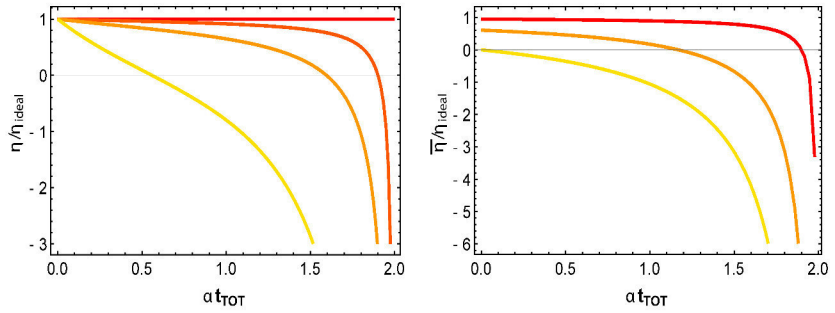

Figure 3.11: Content taken by [41]. At left, in Figure 3.11(a), the renormalized efficiency η/η_{ideal} as a function of the scaled total operation time, αt_{tot}, for different misalignments angles $\theta = 0, \pi/10, \pi/5, 2\pi/5$, at fixed temperature rapport $\beta_h/\beta_c = 0.5$. At right, in Figure 3.11(b), averaged efficiency $\bar{\eta}$ normalized with respect to the ideal efficiency obtained at $\theta = 0$. The average is taken over a Gaussian distributions with variances, $\sigma^2 = 0.1$, $\sigma^2 = 1$ and, at last, over a flat distribution. The temperature ratio is always $\beta_h/\beta_c = 0.5$.

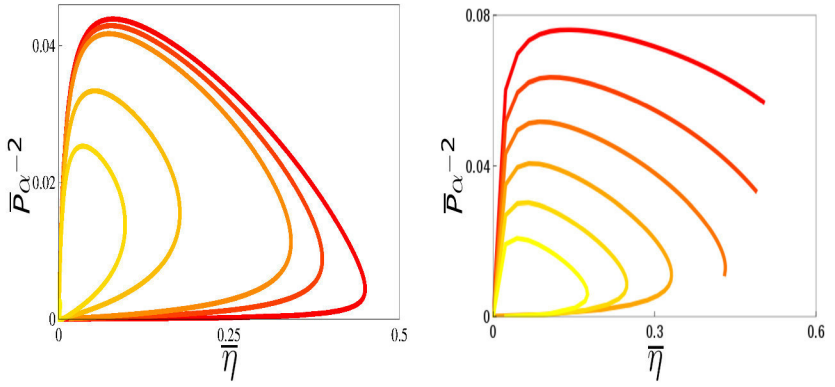

(a) $\mathcal{P}$ vs. η for various σ

(b) $\mathcal{P}$ vs.η for various β_h/β_c

Figure 3.12: Content taken by [41]. Relation between averaged power and averaged efficiency (respectively $\overline{\mathcal{P}}(t)$ and $\overline{\eta}(t)$) at the same time parameter αt_{tot}. In 3.12(a) we choose $\beta_h/\beta_c = 0.5$ and vary σ, which, from the outer to the inner curve changes as $\sigma^2 = 0.01, 0.05, 0.1, 0.5, 1$. In 3.12(b), on the right side, we fix $\sigma^2 = 0.1$ and starting from the outer to the inner curve we increase the reservoirs temperature ratio: $\beta_h/\beta_c = 0.02, 0.03, 0.04, 0.05, 0.06$.

Table 3.1: Content taken by [41]. Efficiency at maximum power at $\beta_h/\beta_c = 0.5$ and for different values of the Gaussian bell's width, optimal total cycle time, αt_{tot}^{MAX}, which $\overline{\mathcal{P}}$ attains its maximum.

σ^2	αt_{tot}^{MAX}	$\overline{\mathcal{P}}_{MAX}/\alpha^2$	$\overline{\eta}(\overline{\mathcal{P}}_{MAX})$
0.01	0.0882	0.0439	0.0775
0.05	0.0882	0.0429	0.0758
0.1	0.0882	0.0418	0.0737
0.5	0.0771	0.0334	0.0519
1	0.0340	0.0253	0.0340
10	0.0.220	0.0027	0.0220

Table 3.2: Content taken by [41]. Efficiency at maximum power for $\sigma^2 = 0.1$ for different temperature ratios β_h/β_c. The maximum power $\overline{\mathcal{P}}_{MAX} = \overline{\mathcal{P}}(t_{tot}^{MAX})$ is obtained for the times αt_{tot}^{MAX} second column.

β_h	αt_{tot}^{MAX}	$\overline{\mathcal{P}}_{MAX}/\alpha^2$	$\overline{\eta}(\overline{\mathcal{P}}_{MAX})$
2.1	0.175	0.0761	0.1420
3.1	0.125	0.0635	0.1056
4.1	0.1	0.0517	0.0862
5.1	0.075	0.0406	0.0660
7.1	0.05	0.0208	0.0447
9.1	0.025	0.0045	0.0224

and viceversa. Here from the maximum value of $\mathcal{P}$ we can extract the value of the efficiency at maximum power $\eta(\mathcal{P})$. Two sets of these data are reported in tables 3.3.2 and 3.2:

We approached the problem of the heat engine from a theoretial point of view, now we propose one experimental implementation by means of which it would be possible to realize the Otto cycle discussed so far and test our results. Such implementation is based on the apparatus proposed in [45]. The Otto cycle is made up by two different types of transformations, thus the proposed set-up has to be able to implement both of them. The physical system we propose is an optical one, and, in particular, we propose to encode the qubit into the polarization degrees of freedom of a single photon coupled to its frequency degrees of freedom representing the

environment. In the following we address the implementation of the two types of branches separately, stressing the key points for both of them.
Let us introduce the adiabatic evolution. In our cycle, the general form of the unitary evolution operator is achieved by the time transformation:

$$U(t,0) = \mathcal{T} e^{-i\int_0^t dt' \, \mathbf{B}(t')\cdot\sigma} \tag{3.84}$$

We stress that for a fixed time $t^* = t$ the above operator can be expressed by the Euler angles as:

$$U(t^*,0) = e^{-i\frac{\psi^*}{2}\sigma_z} e^{-i\frac{\theta^*}{2}\sigma_x} e^{-i\frac{\phi^*}{2}\sigma_z} \tag{3.85}$$

Eqn. (3.85) is very useful for our purpose because the single rotation of angle ψ^*, θ^* and ϕ^*, appearing in it, can be implemented in the optical setup manipulating the photon, as rotations of the polarization degrees of freedom of this latter. In this case, by choosing the basis$\{|H\rangle, |V\rangle$ of horizontal and vertical polarization of the photon, we can perform the wanted rotations by means of properly chosen phase retarders.
The isochoric transformation requires more care. Ideally, at the end of the transformation we could get the state:

$$\rho = \frac{1}{2\cosh(\beta(E_e - E_g)/2)} \left(e^{-\beta E_e} |e\rangle\langle e| + e^{-\beta E_g} |g\rangle\langle g| \right) \tag{3.86}$$

where $|e\rangle$ and $|g\rangle$ are the eigenstates of the Hamiltonian, which does not change during the transformation, and β is the inverse temperature of the thermal bath which allows the qubit to thermalize. No coherences are present at the end of the process as we can see from the above equation. The idea, as we said, is to exploit the spatial degrees of freedom of the photon as an effective bath for its polarization. We have not a thermal reservoir but here we try to emulate the dynamics of the thermalization which will lead the a Gibbs like state. The coupling between the polarization and the frequency degrees of freedom (the environment) is achieved by exploiting the birefringent property of a quartz plate. The effect of the latter on a photon, passing throughout it, is to phase-shift both the components of the polarization by an amount proportional to the number of photons per mode. Now, after such shifting, if we look only at the polarization degrees of freedom, that formally means to trace out the spatial part of the photon, the dynamics of the polarization turns out to be driven by the following dynamical map, obtained by developing the Limbland master equation for the system, between an initial state ρ_i to a final state ρ_f:

$$\rho_f = \frac{1}{2}\left((1+z)\rho_i + (1-z)\sigma_z \rho_i \sigma_z\right) \tag{3.87}$$

where the parameter z can be tuned from $z = 1$ (identity map) to $z = 1$(complete decoherence). Indeed expression (3.87) describes the decoherence process of the photon polarization state due to the interaction with the effective bath of the spatial degrees of freedom (the frequencies of above). Because of our assumption of complete thermalization we will always assume $z = 1$. We can thus exploit this mechanism in order to engineer the thermalization in the following way. At first let us assume that the inverse temperature of the bath we want to mimic is β. Such inverse temperature will be given by:

$$\beta = -\frac{1}{E_e - E_g} log\left(\frac{1 - p_g^{(f)}}{p_g^{(f)}}\right) \quad \text{with} \quad \frac{1}{2} \leq p_g^{(f)} < 1 \tag{3.88}$$

where $p_g^{(f)}$ is the population of the ground state at the end of the process, that is when the state has null off diagonal elements. Through the latter equation we can determine the population of the lowest energy level after the system is completely thermalized. Let us write the initial state (which in turn corresponds to the final state of the adiabatic transformation preceding the isochoric one) as:

$$\rho_i = \frac{1}{2}\mathbb{I} + \left(\frac{1}{2} - p_0^{(i)}\right)\sigma_z + b_x\sigma_x + b_y\sigma_y \tag{3.89}$$

At this level we rotate the initial state so to have the "right" populations of excited and ground levels according to the effective temperature eqn. (3.88) we want to mimic. Thus we get:

$$\rho'_f = \frac{1}{2}\mathbb{I}\left(\frac{1}{2} - p_2^{(f)}\right)\sigma_z + b'_x\sigma_x + b'_y\sigma_y \tag{3.90}$$

Now tracing over the frequencies by the decoherence dynamics in eqn. (3.87) we get $b'_x = b'_y$:

$$\rho_f = \frac{1}{2}\left(\frac{1}{2} - p_2^{(f)}\right)\sigma_z \tag{3.91}$$

Eqn. (3.91) concludes the isochoric transformation.

Chapter 4

Introduction to Topological Order

Hereafter we will approach the field of topological order. Born some decades ago, it deals with new sates of matter and thus it opened the doors to new physics and possible novel technological applications in various fields, in particular in quantum computation. The aim of this chapter is to introduce the main concepts that are behind this kind of order of matter also making some examples. In the next chapter 5 we will focus on a specific model for topological superconductors, that is the Kitaev model and at the end, in chapter 6, we will define the main topological invariants that are tools useful to characterize topological phases.
The most common examples of classical state of matter are the ones of gas, liquid, or solid. Now we can note that different states of matter are distinguished, one respect to each other, by their own internal structures. These internal structures are called *orders*. We can think to the correlation functions as elements to depict the order of the state. For instance the atoms in a gas are very uncorrelated, but in a solid they are frozen at almost fixed positions and their relative distance (internal structure) is successfully depicted by the positional correlation function. In addition, many other states of matter have been discovered. We cite superfluids, ferro and antiferromagnets, and liquid crystals. In all the above examples the various orders are associated with the symmetries of the system, i.e. again its internal structure. Symmetries are very useful for the description of the states of matter. Since, at this level, we focus on positional order then the symmetry we address is the translational symmetry. Indeed, with such symmetry, we immediately have a difference between solid and (for instance) gas. A gas remains the same under a translation, of the reference frame, of any distance inside the system, while a crystal remains the same only under a translation of a integer number of lattice steps.

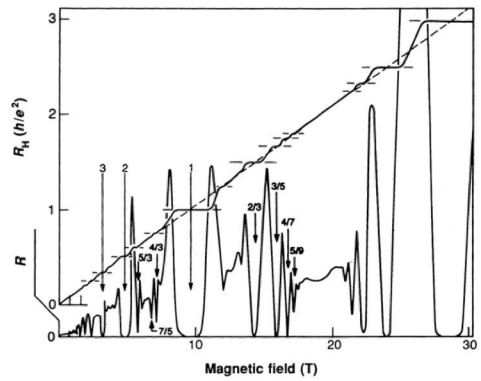

Figure 4.1: Picture taken from the public official webpage *www.nobelprize.org/nobel_prizes/physics/laureates/1998/press.html*. Values of longitudinal resistance and the ones of Hall resistance are reported. At various values of filling factor, longitudinal resistance goes to zero and the hall resistance gets some plateau. When the filling factor assumes integer values we get the standard integer quantum hall effect, otherwise when such filling factor is fractional we get the fractional quantum hall effect.

The two orders are different because the two states (gas and solid) have different symmetries. The freezing of the atoms of a gas to form a crystal reduces the continuous translational symmetry to a discrete translational one. A general theory of orders and their transitions has been developed and it works for a big number of states of matter. The main contribution to this theory was given by L. D. Landau.
Now we introduce a different kind of orders, the topological orders. Their characterization is not based on the translational symmetry but on another kind of internal structure related to their quantum nature and, as it will be clearer later, we need topological concepts to distinguish between the new universality classes. In introducing this new orders we proceed by historical steps as reported in [1] and [46]. The starting point of this new research coincides with the work in [47] in which the authors report the discovery of fractional quantum Hall effects. In this work electrons were confined between two different semiconductors so to form a $2D$ electron gas (2DEG). Then a strong magnetic field ($\sim$ 30 Tesla) has been applied and the gas has been cooled at $T \sim 1$ K. In this regime an electron lattice was expected to appear but it did not. What was found is however a new state of matter, the *fractional quantum Hall* state. Telling at coarse grain, in the effect that they discovered, the Hall conductance has a series of quantized plateau corresponding to fractional values of the quantum conductance $\sigma_Q = e^2/h$. It has a lot of new properties. The most important one is about the electron density in terms of filling

factor ν (as in the standard quantum Hall effect). The filling factor is defined as the ratio of the electron density n and the density of the flux quanta of the applied magnetic field B:

$$\nu = \frac{\text{electron density}}{\text{density of magnetic flux quanta}} = \frac{nhc}{eB} \tag{4.1}$$

It has been found that ν can be given by rational numbers: $\nu = 1, 1/3, 2/3, \ldots$. For integer filling factors we recover the the integral quantum Hall (IQH) states, described by Landau theory and discovered by Klitzing [48], on the other hand the ones with fractional filling factors are called FQH states. Hereafter we will address only $\nu = 1/m$ filling factor FQH effects, indeed we are interested in its topological nature and not in a complete description of the effect. To describe the appearing of FQH states requires a new theory that goes beyond the Landau theory, i.e. beyond the standard symmetries of the system. FQH states represent a new states of matter and we need new concepts to describe them, these newness are the *topological orders*. In [49] Laughlin approached the problem of FQH states giving a first interpretation of FQH effects. The new internal structure, for characterizing the FQH states, is the way in which the electrons are strongly correlated one with each other and this way is described by the filling factor. This quantum correlations substitutes the positional order used until now.
Let us try to visualize these correlations. A very easy and clear treatment is given in [46]. A single electron in a magnetic field always moves on a circular path (cyclotron motions). Since the electron, in quantum regime, is described by a wave function then the cyclotron motion is quantized such that now the initial circular path has to contain an integer number of wave length. Hereafter, since the treatment is done at quantum level, the word "path" will be used as substitution for main value of positional observable, as done for the case of the electron orbital of the preceding example. The number, n, of wave lengths for going around the path coincides with the Landau level occupied by the electron. At low temperatures, the electrons always stay in the first Landau level so that $n = 1$. If we have many electrons, as in the case of a 2DEG, they also go around each other. Now Fermi-Dirac statistics imposes that, in doing this second motion, an odd number of wave lengths is taken to recover the whole path. This will reflect on the filling factor, whose denominator is often odd. At last such motion follows another condition: due to the Coulomb repulsion, each electron tries to stay as far as possible from each other. Summarizing, all the electrons collectively move following these three rules:

- All electrons move (cyclotron motion) in the first Landau level
- In moving one around each other, the electrons take an odd number of steps

- Because of the Coulomb repulsions that stay away from each other as far as it is possible

In this scenario the electrons are strongly correlated and, the nature of first and second point (wave mechanics conditions about non destructive interference and fermionic statistic) allow for the quantumness of the correlations. If we assume that in the system this three rules are respected, then only one global moving pattern is permitted. Such pattern corresponds to the topological order in a FQH state. Different moving patterns corresponds to different topological orders of a FQH state.
The important aspect we are interested about is the link between the quantum nature of the correlations and the topology of some space, in particular the subspace generated by the system ground states. The degeneracy of the FQH ground states depends on the topology of the space that they generate [51, 52, 53]. It is this link with the topological nature of the system ground state that gives the name "topological" to this particular kind of quantum orders. The degeneracy we addressed is not a consequence of the Hamiltonian symmetries. It is in fact resistant against perturbations that destroy the symmetries of the system. To change the ground state degeneracy is possible only by changing the topological order that in this case means by changing the moving patterns of correlated electrons. It follows that such degeneracy is a good quantum number to measure the topological order, i.e. to know what kind of pattern the system has. Since we dealt only with an example of quantum order (although it is very powerful to introduce the new order) we now give a more general description of topological order.
At first we examine more carefully the orders in ordinary states of matter, i.e. at finite temperatures, thus when the quantumness of the system is affected. We will refer to these orders as *classical orders*. At finite temperatures, the full description of a system is mathematically given in terms of a probability distribution. Indeed to describe the positional order of the particles in a system, we can use the probability distribution $P(r_1, r_2, \dots r_N)$ where r_i indicates the spatial coordinate of the i-th particle and N is the total number of the particles. P continuously changes as we change some state parameter as temperature, pressure, and other some external conditions. However, systems described by different probabilities P can have similar properties and thus we say that they show the same phase. We group all those similar probability distributions into a single class, which is called a *universality class* (this concept will be formally approached in chapter 6). If we continue to change the external conditions then it can happen a radical change in the properties of the system. In this case we say that there is a phase transition. To pass from a phase to another one means that the system is described by a different classical order. The probability distributions, describing the system before and after the

transition, belong to different universality classes. As an example we can consider the phase transition between a liquid and a crystal. By a formal point of view the two states are respectively described by different distributions P_l and P_c. Now from these probability we introduce the correlations functions [50]:

$$\begin{cases} G_l(r_1, r_2) = \int \Pi_{i=3}^{N} dr_i \, P_l(r_1, \dots r_N) \\ G_c(r_1, r_2) = \int \Pi_{i=3}^{N} dr_i \, P_c(r_1, \dots r_N) \end{cases} \tag{4.2}$$

The positional correlation functions give the probability to find a particle in position r_2 given that we assume a particle to be at position r_1. Give a phase transition, the internal order that we address, is generally represented, according to the system we deal with, by a physical extensive variable that we label *order parameter*. Such order parameter is proportional to some derivate of the free energy of the system, assumed to be at equilibrium before and after the transition, $G(T, P) = U - TS + PV$ or $G(T, H) = U - TS + \mu_B H$ for magnetic systems. Giving some example of order parameters we have, for the phase transition liquid-gas, the difference between the density of the two phases, $\Psi = \rho_{liq} - \rho_{gas}$ or, looking at the degree of disorder in the orientation of a spin lattice in the ground state of the Ising model, the magnetization defined as $M = -(\partial G/\partial H)N/V$. In a transition, order parameters can vary with discontinuity or continuity at the transition point p_0. These two trends respectively define a first order and a second order phase transition. Thus, for first order transitions, we have discontinuous first order derivates of the state's free energy at the transition point:

$$\begin{aligned} \left.\frac{\partial G_1}{\partial T}\right|_{p_0} &\neq \left.\frac{\partial G_2}{\partial T}\right|_{p_0} \\ \left.\frac{\partial G_1}{\partial P}\right|_{p_0} &\neq \left.\frac{\partial G_2}{\partial P}\right|_{p_0} \\ \left.\frac{\partial G_1}{\partial H}\right|_{p_0} &\neq \left.\frac{\partial G_2}{\partial H}\right|_{p_0} \end{aligned} \tag{4.3}$$

Pedices 1 and 2 refer to the state of the system before and after the transition. For second order transitions we have continuous first order derivates but discontinuous second order ones that eventually diverge.
About these latter it is possible to classify them by means of *critical exponents*. Let us assume to have a thermodynamic variable described by a function $F(t)$, that is continuous and positive near the critical temperature T_C, where the variable t is the reduced temperature $t = (T - T_C)/T_C$. We define the critical exponent of such

variable as:

$$\lambda = \lim_{t \to 0} \frac{\ln(F(t))}{\ln(|t|)} \tag{4.4}$$

From the above relation we have that $F(t) \sim |t|^{\lambda}$, where $\sim$ stands for asymptotic limit that is $t \to 0$. At the critical point, that is the transition point for the second order transitions, the thermodynamic variables generally diverge or are null. Usually divergent thermodynamic variables are the magnetic susceptibility χ_H or the specific heat at fixed volume C_V. Critical exponent do not dependent by the particular interactions of the system. They depend on few parameters as the dimensions of the system or the symmetry of the order parameter. We get the same critical exponents for every system that has such same properties. By this point of view critical exponents show a universal character.
Finally we can define the *universality classes*. Each class includes all the systems that shows the same critical exponents.

Summarizing, about the classical order, we can itemize the following points as characterizing properties:

- Classical order is a property of the probability distribution $P(r_1, r_2, \ldots r_N)$ (directly linked to the symmetries of the system as we can see in eqns. (4.2)) in the $N \to \infty$ limit. Thus classical order describes the structures in terms of positive functions with infinite number of variables

- Distributions belonging to the same universality class have the same classical order. We group systems with similar distributions P

- Different universality classes are determined by the symmetries of the distributions. Symmetries are the central tool to characterize systems according to classical order

The aspect that classical orders (and the universality classes) are characterized by symmetries is fundamental for the Landau theory of classical orders and phase transitions. It is important to underline that this theory deals with systems at finite temperature. Although this latter is a strong theory, it does not describe all the classical orders. Indeed for instance the Kosterliz-Thouless phase transition does not change any symmetry.
Since strong quantum correlations appears at zero temperature we need a theory able to describe this regime. We need to define a new concept of order characterized by different properties respect to the classical one. We will call such new orders of quantum states at zero temperature *quantum orders*. This quantum orders are properties the ground state wave functions of the system since at $T \sim 0$ the state is collapsed on the ground state subspace. Furthermore classical and quantum order

are linked together by relations introduced in the postulates of quantum mechanics which link the system wave function to the probability distribution characterizing the considered particles. Indeed a classical order is a property of the probability distribution P, where this latter is a function of N coordinates of the particles. A quantum order is a property of ground state wave function ψ which is a complex function of N coordinates of the particles. P and ψ are then related by:

$$P(r_1, \dots r_N) = |\psi(r_1, \dots r_N)|^2 \tag{4.5}$$

Thus, although the square modulus delete some information about the wave function ψ, we can use classical order to describe approximatively well a quantum system. It is then also clear that the characterization, by classical order, misses the phase of ψ which brings the quantumness of the state as in the case of Berry phase. Then as for the classical orders, quantum orders are grouped in universality classes of ground state wave functions. If we change the parameters of the system Hamiltonian then the ground state wave function changes continuously too. Thus if some ground states have similar properties then we say that they describe the same phase and belong to the same universality class. States in the same universality class have the same quantum order. However, changing the interaction by a large amount can lead to a quantum phase transition, which reflects the fact the the system changes universality class.
Returning to the topological order introduced before for the FQH effect we realize that, since it is a property of 2DEG at zero temperature, then such topological order is particular kind of quantum order. A quantum phase transition stands when we change quantum universality class. Between these classes there are some of them that show another difference respect to the one of critical exponents; the Brillouin zones of each system states, over which are defined the ground states of the systems, have different topology when changing from a class to another. We will later explain better this aspect. Now noting that different FQH states have the same spatial symmetries we can understand why we need topological order to characterize this effect. By Landau theory we deleted some important information brought into ψ. When we consider the ground state wave function ψ instead $P = |\psi|^2$, we find different quantum orders. Let us note that topological orders and quantum orders are general properties of any states at zero temperature that is when quantum effects are important. We want to report that the concept of topological order was first introduced for spin liquids [51]. Then the first experimental observation of quantum order is reported in [54] with the discovery of superconducting state (in 1911), indeed a superconductor cannot be characterized by breaking symmetries. For general systems we can characterize the orders by addressing the ground state space. In chapter 6 we will give a series of measures of topological orders (as the

one given for the case of FQH ground states), i.e. topological invariants, that claim if the order is topological or not (topologically non trivial or trivial).

Chapter 5

The Kitaev Chain

Here we consider one of the most interesting model which shows a topological order, the Kitaev chain [5]. This model describes a 1D p-wave superconductor. Such system is though as a superconducting wire that, under certain conditions, has a gapped bulk together with zero energy excitations (in the thermodynamic limit) localized at the edges of the system. Such states are topological states whose characteristics will be analyzed later. We can anticipate that they are robust against disorder [55, 56], local perturbations [57] and the field operators corresponding to them undergo nonabelian statistics that can be used to perform quantum computation [58]. This model made of a chain of spinless fermions can be mapped to the Ising model by means of Jordan-Wigner transformations [59]. It has been introduced in 2000, from the theoretical point of view, but feasible realizations of the Kitaev chain or variations of it have been also recently proposed [60] [61] [62]. An experimental signature of Majorana zero modes as been reported in [63]. Recently the dynamics of such states has also been addressed [64].

5.1 Bogoliubov-de Gennes equations

Let us consider a generic 1D superconducting system whose Hamiltonian H has the following form [65]

$$H = \sum_{i=1}^{N} \left[-\mu_i \left(a_i^\dagger a_i - \frac{1}{2} \right) \right] + \left[\sum_{j>i} \left(-t_{i,j} a_i^\dagger a_j + \Delta_{i,j} a_i^\dagger a_j^\dagger \right) + h.c. \right] \quad (5.1)$$

In the above Hamiltonian, parameters $t_{i,j}$ and $\Delta_{i,j}$ are generally complex numbers. They respectively describe hopping and pairing of Dirac fermions on a one-dimensional lattice. On the other hand μ_i are assumed to be real, they represent

the site energies, i.e. the chemical potential of the fermions at the i-th site. Operators $\{a_j\}$ and $\{a^\dagger\}$ are defined on the Fock space of the whole system and, they respectively destroy and create a fermion at the i-th site. However we will formally define the Fock state and the action of such operators. Since we describe fermions then Fermi-Dirac statistics is assumed:

$$\{a_i^\dagger, a_j\} = \delta_{ij} \tag{5.2a}$$

$$\{a_i^\dagger, a_j^\dagger\} = \{a_i, a_j\} = 0 \tag{5.2b}$$

Then, indicating with $|0\rangle$ the state in a Fock space where no fermion is present, the vacuum state, we define such state by the action of the a_is on it:

$$a_i|0\rangle = 0 \tag{5.3}$$

Then $a_i^\dagger$ acts on $|0\rangle$ as:

$$a_i^\dagger|0\rangle = |1\rangle_i \tag{5.4}$$

where ket $|1\rangle_i$ means the there is a fermion at site "i". $N = \sum_i n_i = \sum_i a_i^\dagger a_i$ is the number operator, counting the fermions appear in a Fock state, and a generic eigenstate of such operator has the form:

$$|\{n\}\rangle = \prod_{i\in\{n\}} a_i^\dagger|0\rangle \tag{5.5}$$

Since Hamiltonian (5.1) in quadratic in a and $a^\dagger$ then it can be diagonalized by Bogoliubov transformations. This is what we will do but, at first, we need to rewrite H in Nambu representation, that is we double the space including *halls* together with particles:

$$H = \frac{1}{2}(a_1^\dagger, a_2^\dagger, ..., a_N^\dagger, a_1, ..., c_N) \underbrace{\begin{pmatrix} \hat{h}_{i,j} & \hat{\Delta}_{i,j} \\ \hat{\Delta}_{i,j}^\dagger & -\hat{h}_{i,j}^* \end{pmatrix}}_{=H_0} \begin{pmatrix} a_1 \\ a_2 \\ \vdots \\ a_{N-1}^\dagger \\ a_N^\dagger \end{pmatrix} \tag{5.6}$$

H_0, in the above equation, has dimensions $2N$x$2N$ instead of NxN (doubling of the space). Moreover Matrix $\hat{\Delta}$ is antisymmetric, in fact:

$$\sum_{i,j} \Delta_{i,j} a_j a_i = \sum_{i,j} \Delta_{j,i} a_j a_i = \sum_{i,j} \Delta_{j,i}(-a_i a_j) \tag{5.7}$$

and if it were symmetric we would have this latter term equal to zero implying $\Delta_{i,j} = \Delta_{j,i} = 0 \,\forall\, i, j$ because of the independence of the set $\{a_i\}$. It follows that $\hat{\Delta}^T = -\hat{\Delta}$ is the only possibility to allow H to be hermitian.
The only symmetry we required in writing H is the particle-hole symmetry. We will check it in few algebraic passages. We write the particle-hole operator for lattice Hamiltonian in Nambu representation as:

$$C = \begin{pmatrix} 0 & \mathbb{I} \\ \mathbb{I} & 0 \end{pmatrix} k \tag{5.8}$$

C is antiunitary and k is the operator of complex conjugation, thus:

$$\begin{aligned} CH_0C^{-1} &= \begin{pmatrix} 0 & \mathbb{I} \\ \mathbb{I} & 0 \end{pmatrix} k \begin{pmatrix} \hat{h} & \hat{\Delta} \\ \hat{\Delta}^\dagger & -\hat{h}^* \end{pmatrix} \begin{pmatrix} 0 & \mathbb{I} \\ \mathbb{I} & 0 \end{pmatrix} k \\ &= \begin{pmatrix} \hat{\Delta} & -\hat{h} \\ \hat{h}^* & -\hat{\Delta}^* \end{pmatrix} \begin{pmatrix} 0 & \mathbb{I} \\ \mathbb{I} & 0 \end{pmatrix} \\ &= \begin{pmatrix} -\hat{h} & \hat{\Delta}^T \\ \hat{\Delta}^* & \hat{h}^* \end{pmatrix} \\ &= -H_0 \end{aligned} \tag{5.9}$$

This symmetry is due to the Nambu representation we used. In doubling the space we also doubled the degrees of freedom of the system. In the following we will opportunely use such symmetry to eliminate this redundancy. Now we directly give the general solutions for the diagonalization of the system Hamiltonian (5.1), according to the Bogoliubov formalism and then, we will see the symmetry properties of the H_0's eigenstates due to eqn. (5.9).

We look for a canonical transformation that takes a set of $2N$ Dirac operators, $\left\{a_j, a_j^\dagger\right\}$ (that appear in the form (5.1)), and sends it into a set of $2N$ Dirac operators, $\left\{\tilde{a}_n, \tilde{a}_n^\dagger\right\}$, for whose the system Hamiltonian assumes the canonical form:

$$H_{can} = \sum_n \epsilon_n \tilde{a}_n^\dagger \tilde{a}_n + \text{const.} \tag{5.10}$$

We write this new operators as linear combination of the old set of operators

$$\begin{cases} \tilde{a}_n &= \sum_{j=1}^{N} \left(u_{n,j} a_j + v_{n,j} a\dagger_j\right) \\ \tilde{a}_n^\dagger &= \sum_{j=1}^{N} \left(v_{n,j}^* a_j + u_{n,j}^* a\dagger_j\right) \end{cases} \tag{5.11}$$

and look for the coefficients $\{u_{n,j}\}$ and $\{v_{n,j}\}$ of the writing (5.11) satisfying the canonical condition, i.e. operators $\{\tilde{a}_n\}$ an $\left\{\tilde{a}_n^\dagger\right\}$ have to satisfy the Fermi-Dirac statistic. Vectors $\mathbf{u}_n = (u_{n,1}, \ldots, u_{n,N})$ and $\mathbf{v}_n = (v_{n,1}, \ldots, v_{n,N})$ will be the wave functions of the quasiparticle and anti quasiparticle corresponding to the mode n-th. We define the unitary operator U as:

$$U = \begin{pmatrix} \left\{\mathbf{u}_n^T\right\} & \left\{\mathbf{v}_n^\dagger\right\} \\ \\ \left\{\mathbf{v}_n^T\right\} & \left\{\mathbf{u}_n^\dagger\right\} \end{pmatrix} \tag{5.12}$$

thus eqns. (5.11) can be rewritten as:

$$\begin{pmatrix} \tilde{a}_1 \\ \tilde{a}_2 \\ \vdots \\ \tilde{a}_{N-1}^\dagger \\ \tilde{a}_N^\dagger \end{pmatrix} = \underbrace{U^{-1}}_{=U^\dagger} \begin{pmatrix} a_1 \\ a_2 \\ \vdots \\ a_{N-1}^\dagger \\ a_N^\dagger \end{pmatrix} \tag{5.13}$$

Defining $\mathbf{a} \stackrel{d}{=} (a_1, \ldots, a_N, a_1^\dagger, \ldots, a_N^\dagger)^T$, we can write:

$$\begin{aligned} H &= \frac{1}{2}\tilde{\mathbf{a}}^\dagger H_0 \mathbf{a} \\ &= \frac{1}{2}\tilde{\mathbf{a}}\, U^\dagger H_0 U \tilde{\mathbf{a}} \\ &= \frac{1}{2}\tilde{\mathbf{a}}^\dagger \begin{pmatrix} \epsilon_1 & 0 & \ldots \\ 0 & \ddots & 0 \\ 0 & \ldots & \epsilon_{2N} \end{pmatrix} \tilde{\mathbf{a}} \end{aligned} \tag{5.14}$$

Now we see as the particle-hole symmetry characterize the eigenvector of H_0 (that form the unitary matrix U). We define $v_n = (\mathbf{u}_n, \mathbf{v}_n)^T$ and looking at eigenvalues equations for H_0 we have:

$$H_0 v_n = \epsilon_n v_n \rightarrow C H_0 C^{-1} C v_n = C v_n \epsilon_n \rightarrow H_0 C v_n = -\epsilon_n C v_n \tag{5.15}$$

Thus if v_n is an eigenvector of H_0 with eigenvalue ϵ_n then $C v_n$ is again eigenvector with opposite energy $-\epsilon_n$. Our spectrum is symmetric respect to the zero of the

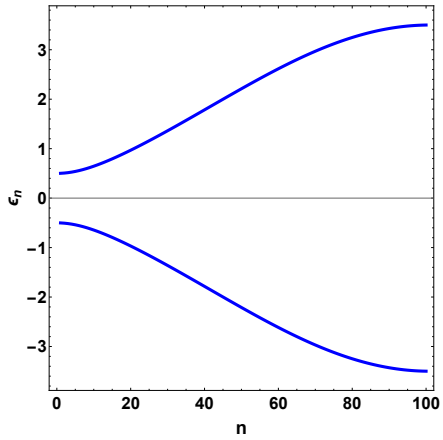

Figure 5.1: For a Hamiltonian with 100 lattice sites then 200 energy values accour. Due to the particle-hole symmetry the H spectrum is symmetric respect the the zero of the energy. For each positive eigenvalues ϵ then it exists a correspondent eigenvalues $-\epsilon$.

energy. H, written in terms of quasiparticle operators, is:

$$\begin{aligned} H_{can} &= \frac{1}{2}\,\tilde{\mathbf{a}}^{\dagger} \begin{pmatrix} \epsilon_1 & 0 & \dots & 0 & 0 \\ 0 & \ddots & 0 & \dots & 0 \\ 0 & \dots & \epsilon_N & 0 & \dots \\ \vdots & 0 & \dots & -\epsilon_1 & \dots \\ 0 & 0 & \dots & 0 & \ddots \end{pmatrix} \mathbf{a} \\ &= \frac{1}{2}\sum_{n=1}^{N} \epsilon_n \left(\tilde{a}_n^{\dagger}\tilde{a}_n - \tilde{a}_n\tilde{a}_n^{\dagger}\right) \\ &= \sum_{n=1}^{N} \epsilon_n \left(\tilde{a}_n^{\dagger}\tilde{a}_n - \frac{1}{2}\right) \end{aligned} \tag{5.16}$$

The vacuum state of H_{can}, $|\tilde{0}\rangle$, the state where no quasiparticle is present, is now defined as:

$$\tilde{a}_n|\tilde{0}\rangle = 0 \,\forall\, n = 1, \dots, N \tag{5.17}$$

The ground state, $|gs\rangle$, of the system is the Fock state with lowest energy. It corresponds to the one counting all the holes. It answers to:

$$\tilde{a}_n|gs\rangle = 0 \quad \text{for all } \tilde{a}_n \text{ appearing in } H_{can} \tag{5.18}$$

We can see that, of course, the vacuum state is a ground state of the system according to eqns. (5.17) and(5.18). Indeed the generic operator $\tilde{a}_n$ destroys the n-th mode particle but equivalently creates an hole (anti-particle) of mode n. Eqn. (5.17) says that the state $|\tilde{0}\rangle$ counts all the holes since adding another hole, a_n, gives as result 0 ($a_n^2 = 0$ because of Fermi-Dirac statistics). The the ground state energy is:

$$H|gs\rangle = -\frac{1}{2}\sum_{n=1}^{N}\epsilon_n|gs\rangle \rightarrow \epsilon_{gs} = -\frac{1}{2}\sum_{n=1}^{N}\epsilon_n \tag{5.19}$$

Remember that $\epsilon_n \geq 0$ in the above expression.
Now if we consider the case in which some of the ϵ_ns are zero, then they come in pairs because of the particle-hole symmetry. For simplicity let us consider the case in which only two solutions are zero. Then the eigenvectors of H_0 relative to $+\epsilon = -\epsilon = 0$, respectively $v_{\epsilon=0}$ and $v_{-\epsilon=0} = Cv_{\epsilon=0}$ are degenerate. In this scenario we can rotate the basis of such zero energy subspace, always remaining in it. Opportunely choosing this rotation as:

$$\tilde{v}_1 = \frac{1}{2}\left(v_{\epsilon=0} + Cv_{\epsilon=0}\right) \tag{5.20a}$$

$$\tilde{v}_2 = \frac{1}{2i}\left(v_{\epsilon=0} - Cv_{\epsilon=0}\right) \tag{5.20b}$$

the resulting transformed eigenstates are invariant under particle-hole symmetry:

$$C\tilde{v}_1 = \tilde{v}_1 \tag{5.21a}$$

$$C\tilde{v}_2 = \tilde{v}_2 \tag{5.21b}$$

The transformed field operators corresponding to the collective excitations at zero energy are then:

$$\gamma_1 = \sum_{j=1}^{N}(\tilde{v}_1)_j a_j + (\tilde{v}_1)_{j+N}a_j^\dagger \tag{5.22a}$$

$$\gamma_2 = \sum_{j=1}^{N}(\tilde{v}_2)_j a_j + (\tilde{v}_2)_{j+N}a_j^\dagger \tag{5.22b}$$

They are hermitian, as in can be seen by analysing $\gamma_1^\dagger$ (things are similar for $\gamma_2^\dagger$):

$$\begin{aligned}\gamma_1^\dagger &= \sum_{j=1}^{N}(\tilde{u}_1)_j^* a_j^\dagger + (\tilde{v}_1)_j^* a_j \\ &= \sum_{j=1}^{N}(\tilde{v}_1)_j a_j^\dagger + (\tilde{u}_1)_j a_j \\ &= \gamma_1\end{aligned} \tag{5.23}$$

where in the last passage, in the above equation, we used the property of invariance under particle-hole symmetry. Then we add that:

$$[\gamma_{1,2}, H] = 0 \tag{5.24}$$

At this level we can introduce the concept of Majorana Zero Mode operator γ (MZM) [66]. It is a fermionic operator that squares to $\mathbb{I}$, thus it is hermitian and commutes with the Hamiltonian of the system:

$$\gamma \quad \text{is a fermionic operator} \tag{5.25a}$$

$$\gamma^\dagger = \gamma \tag{5.25b}$$

$$[\gamma, H] = 0 \tag{5.25c}$$

Conditions (5.25a) and (5.25b) alone define a Majorana fermion. It can be shown that operators $\gamma_{1,2}$ follow a fermionic statistic (since their anticommutator is proportional to the identity), although different from the Fermi-Dirac one. Counting also last point, eqn. (5.25c), we can claim that such $\gamma_{1,2}$ are MZM. Unluckily conditions (5.25) are too idealized to be achievable for real systems. Generally for finite length systems the two MZM, that will be localized modes, overlap and this interaction gives rise to non null energy excitation, then:

$$[\gamma, H] \sim e^{-\chi/\xi} \tag{5.26}$$

where χ is a length scale and ξ is a correlation length associated with the Hamiltonian. In the limit $\chi \to \infty$ or $\xi \to 0$ we get eqns. (5.25).

5.2 The Kitaev Model

Now we use the results obtained in the preceding section to approach the Kitaev model introduced in [5]. Here we deal with a 1 D topological superconductor. We will define the general form for the Majorana operators, as combinations of Dirac fermion operators. Then we will diagonalize the system Hamiltonian in terms of such Majorana operators. At the end we will see that the system allows for MZMs localized at the edge of the 1 D wire.
The Hamiltonian introduced by Kitaev is:

$$H_{Kit} = \sum_j \Big[-\mu\Big(a_j^\dagger a_j - \frac{1}{2}\Big) - w_0(a_j^\dagger a_{j+1} + a_{j+1}^\dagger a_j) + \Delta a_j a_{j+1} + \Delta^* a_{j+1}^\dagger a_j^\dagger \Big] \tag{5.27}$$

The above Hamiltonian considers only first neighbors interactions. Then the hopping term, w_0, is chosen to be real, in this case the whole Hamiltonian is invariant under time reversal symmetry. Now we define a new set of operators, i.e. the Majorana operators, by the following set of transformations:

$$\begin{cases} c_{2j-1} = a_j + a_j^\dagger \\ c_{2j} = \dfrac{a_j - a_j^\dagger}{i} \end{cases} \quad \text{with } j = 1, \dots, N \tag{5.28}$$

Majorana fermions satisfy the relations:

$$\{c_i, c_j\} = 2\delta_{i,j} \tag{5.29a}$$

$$c_j^\dagger = c_j \tag{5.29b}$$

We got a chain of $2N$ sites and each site l is associated with the operator c_l that is a Majorana fermion. Indeed the conditions in the set of equations (5.29) era equal to eqns. (5.25a) and (5.25b). An important relation between Dirac and Majorana fermions, according to the definitions (5.28), is:

$$a_j^\dagger a_j = \frac{1}{2}(\mathbb{I}_j + i c_{2j-1} c_j) \tag{5.30}$$

Now let us return the system Hamiltonian. Since it is quadratic it can be written, in terms of Majorana operators, in the form:

$$H = \tfrac{i}{4} \textstyle\sum_{l,m} A_{l,m} c_l c_m \quad A_{l,m} = A_{l,m}^* = -A_{m,l} \tag{5.31}$$

In fact addressing H_{Kit}, we obtain:

$$H_{Kit} = \frac{i}{2} \sum_j \Big[-\mu c_{2j-1} c_{2j} + (w_0 + \Delta) c_{2j} c_{2j+1} + (-w_0 + \Delta) c_{2j-1} c_j \Big] \tag{5.32}$$

and the form (5.31) is achieved by choosing an antisymmetric A matrix such that $A_{2j-1,2j} = -\mu$, $A_{2j,2j+1} = (w_0 + \Delta)$ and $A_{2j-1,j} = -w_0 + \Delta$. We stress that the pairing term is generally complex, $\Delta = |\Delta| e^{i\theta}$, but the physics of the system is not affected by the phase θ. Indeed it can be eliminated from the Hamiltonian (5.32) by putting such phase parameter into the definition of Majorana operators as:

$$\begin{cases} c_{2j-1} = \exp\left(i\frac{\theta}{2}\right) a_j + \exp\left(-i\frac{\theta}{2}\right) a_j^\dagger \\ c_{2j} = -i \exp\left(i\frac{\theta}{2}\right) a_j + i \exp\left(-i\frac{\theta}{2}\right) a_j^\dagger \end{cases} \tag{5.33}$$

By this way we can substitute Δ with $|\Delta|$. Now we proceed to find out a writing, in terms of Majorana operators, for expressing the canonical form (5.10). We proceed by defining a set of Majorana operators according to eqns. (5.28) but now we choose as Dirac operators the set appearing in the canonical Hamiltonian (5.10):

$$\begin{cases} \tilde{a}_n = \frac{1}{2}\left(b'_n + b'_n\right) \\ \tilde{a}_n^\dagger = \frac{1}{2}\left(b'_n - ib''_n\right) \end{cases} \tag{5.34}$$

By means of this definition we get:

$$\begin{aligned} H_{can} &= \frac{i}{2}\sum_{n=1}^{N} \epsilon_n b'_n b''_n \\ &= \text{diag}_n \begin{pmatrix} 0 & \epsilon_n \\ -\epsilon_n & 0 \end{pmatrix} \\ &\doteq \begin{pmatrix} 0 & \epsilon_1 & 0 & \dots & 0 \\ -\epsilon_1 & 0 & 0 & \dots & 0 \\ \vdots & 0 & \ddots & 0 & \dots \\ 0 & \dots & 0 & 0 & \epsilon_N \\ 0 & \dots & 0 & -\epsilon_N & 0 \end{pmatrix} \end{aligned} \tag{5.35}$$

We know that the block form (5.35) is ensured because of the properties of A [67]. Indeed if A a real and skewsymmetric transformation then it exists a real and orthogonal transformation, W ($WW^T = W^TW = \mathbb{I}$), such that:

$$A_J = WAW^T = \text{diag}_n \begin{pmatrix} 0 & \epsilon_n \\ -\epsilon_n & 0 \end{pmatrix} \tag{5.36}$$

where $\{\epsilon_n\}$ are the coefficients of the spectrum of A, $\{\pm i\epsilon_n\}$. Thus at the end we have:

$$H_{can} = \sum_n \epsilon_n \left(\tilde{a}_n^\dagger \tilde{a}_n - \frac{1}{2}\right) = \frac{i}{2}\sum_n \epsilon_n b'_n b''_n \tag{5.37}$$

Operators $\{b'_n\}$ and $\{b'_n\}$ will be linear combinations of $\{c_j\}$ ($j = 1, \dots, 2N$):

$$\begin{pmatrix} b'_1 \\ b''_1 \\ \vdots \\ b'_N \\ b''_N \end{pmatrix} = W \begin{pmatrix} c_1 \\ c_2 \\ \vdots \\ c_{2N-1} \\ c_{2N} \end{pmatrix}$$

The orthogonality of W preserves the algebra of the set and its reality ensure the hermiticity of $\{b'^{,''}_m\}$, it is a canonical transformation. To check it let γ_k and $\gamma_{k'}$ be two generic operators belonging to $\{b'_k\}$ and $\{b''_k\}$. Then the anticommutator relations are preserved:

$$\begin{aligned}\{\gamma_k, \gamma_{k'}\} &= \left\{ \sum_{j=1}^{2N} W_{k',j}\gamma_j, \sum_{j=1}^{2N} W_{k,i}\gamma_i \right\} \\ &= \sum_{i,j=1}^{2N} W_{k,j} W_{k',i} \{\gamma_j, \gamma_i\} \\ &= 2\sum_{i=1}^{2N} W_{k,i} W^T_{i,k'} \\ &= 2\delta_{k,k'}\end{aligned} \tag{5.38}$$

and also the hermiticity condition holds:

$$\gamma_k^\dagger = \sum_{i=1}^{2N} W^*_{k,,i}\gamma_i^\dagger = \sum_{i=1}^{2N} W_{k,,i}\gamma_i = \gamma_k \tag{5.39}$$

In chapter 7 we give the explicit form linking the elements of matrix W to U for a generic system with long range interactions and generally broken time reversal symmetry. The time reversal case can be obtained as specific case of the generally broken time reversal one.
Returning to our case, what is very interesting, looking at Hamiltonian (5.32), is that if we choose $\mu = 0$ and $w = \Delta = 1$ for open boundary conditions, then such Kitaev Hamiltonian (5.32) reads:

$$H = -iw_0 \sum_{j=1}^{N-1} c_{2j} c_{2j+1} \tag{5.40}$$

Now defining another set of Fermi operator as follows:

$$\begin{cases} \tilde{a}_j &= \frac{1}{2}(c_{2j} + ic_{2j+1}) \\ \tilde{a}_j^\dagger &= \frac{1}{2}(c_{2j} - ic_{2j+1}) \end{cases} \tag{5.41}$$

it becomes:

$$H = 2w_0 \sum_{j=1}^{N-1} \left(\tilde{a}_j^\dagger \tilde{a}_j - \frac{1}{2} \right) \tag{5.42}$$

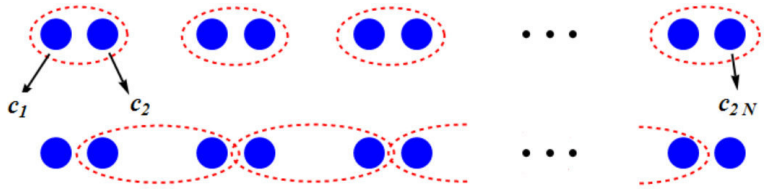

Figure 5.2: Trivial and non trivial topological phase. The high image show a normal link between two MFs of the same physical site. The other picture shows as two MFs of different site link together according to the Hamiltonian (5.42).

A fermionic state does not enter in the Hamiltonian, in fact c_1 and c_{2N} remain unpaired. Such fermion excitation will have zero energy since it does not appear in eqn. (5.42). This missing fermion state is defined by such unpaired Majorana operators [68]:

$$\begin{cases} \tilde{a}_N = \frac{1}{2}(c_1 + ic_{2N}) \\ \tilde{a}_N^\dagger = \frac{1}{2}(c_1 - ic_{2N}) \end{cases} \tag{5.43}$$

Note that the whole set as soon defined $\{\tilde{a}_j\}_{j=1}^N$ satisfies the Fermi-Dirac algebra. For an usual s-wave superconductors we have a single ground state with even parity, here the situation changes just because this missing fermion in Hamiltonian (5.42). We have two degenerate ground states (since the state counting the missing fermion, at zero energy, satisfies the ground state condition eqn. (5.18)) with different parity. Indeed the vacuum state, that is also our first ground state, has zero quasi particles thus it has even parity $P(|gs\rangle_0 = |\tilde{0}\rangle) = (-1)^{\#(qp)} = 1$. Otherwise the state $|gs\rangle_1 = \tilde{a}_N^\dagger|\tilde{0}\rangle$ has one quasiparticle excitation thus its parity is odd, $P(\tilde{a}_N|\tilde{0}\rangle) = (-1)^1 = -1$. Since by a unitary transformation we do not change the number of fermions in the system then also the parity of the state remain unchanged. It follows that $|\tilde{0}\rangle$ is made by a superposition of Fock states counting an even number of fermions (the fermions addressed in Hamiltonian (5.27)) and $|gs\rangle_1$ is made by states with an odd number of the same preceding fermions. It is then useful to introduce the parity operator:

$$P = \prod_j (-ic_{2j-1}c_{2j}) \tag{5.44}$$

where the operators $\{c_i\}$ are again the ones appearing in Hamiltonian (5.27). Operator (5.44) counts the parity of a general many body Fock state. Note that the combination $(-ic_{2j-1}c_{2j}) \doteq \begin{pmatrix} 1 & 0 \\ 0 & -1 \end{pmatrix}$ measures the parity of the j-th fermion state, it is defined on a bidimensional space spanned by states $|0\rangle_j$ and $|1\rangle_j$, the first

ket has parity 1 and the latter -1. Because of the algebra defined in eqn. (5.29), $\{c_i, c_j\} = 2\delta_{i,j}$, it is possible to rewrite P as:

$$\begin{aligned} P &= (-ic_1c_2)\dots(-ic_{2N-1}c_{2N}) \\ &= (-i)^N c_1c_2\dots c_{2N} \\ &= (-i)^N(-1)^{2N-2}c_2c_3\dots c_1c_{2N} \\ &= (-ic_2c_3)\dots(-ic_1c_{2N}) \end{aligned} \tag{5.45}$$

The last term in the above equation, $(-ic_1c_{2N})$, is just the parity operator of the fermion that does not appear in Hamiltonian (5.42). We have:

$$(-ic_1c_{2L})|gs\rangle_0 = |gs\rangle_0 \quad \text{and} \quad (-ic_1c_{2L})|gs\rangle_1 = -|gs\rangle_1 \tag{5.46}$$

This paremetrical regime for Hamiltonian (5.32), characterized by the presence of unpaired Majorana fermions at the end of the wire, belongs to a topological phase, topological invariants, that we will define in the next section, are non trivial. For topologically trivial regime we have not zero energy modes and no localized states is present (see for istance the case $\Delta = w_0 = 0$ and $\mu < 0$ in (5.32)). Then we also claim that no topological phase can be gotten for closed boundary conditions. Indeed in this latter case the interaction between the last Majorana fermion of the wire and the first one allows for an extra term in the Hamiltonian effectively depicted as $H_{eff} \propto (i/2)uc_{2N}c_1$ thus, it provides a non null amount of energy for the fermion excitation. We have not anymore unpaired Majorana zero modes at the edge of the wire. The case just examined, $w_0 = |\Delta| = 1$ and $\mu = 0$ is a very particular case. In general MZM appear in the topological phase as a generic linear combination of the initial Majorana fermions $\{c_j\}$. To look at their form we proceed by diagonalizing Hamiltonian (5.32) and imposing the existence of zero energy solutions, under the assumption of OBC (open boundary conditions). The Bogoliubov transformations, in the Majorana picture, for the Kitaev Hamiltonian give zero energy solutions as:

$$\begin{cases} b' = \sum_j \left(\alpha'_+ x_+^j + \alpha'_- x_-^j\right) c_{2j-1} \\ b'' = \sum_j \left(\alpha''_+ x_+^{-j} + \alpha''_- x_-^{-j}\right) c_{2j} \end{cases} \tag{5.47}$$

with j going from one to N, $\alpha'^{,''}_{\pm}$ being parameters , successively linked together because of the OBC and:

$$x_\pm = \frac{-\mu \pm \sqrt{\mu^2 - 4w_0^2 + 4|\Delta|^2}}{2(w_0 + \Delta)} \tag{5.48}$$

Imposing OBC we get:

$$\begin{cases} \alpha'_+ \underbrace{x_+^0}_{=1} + \alpha'_- \underbrace{x_-^0}_{=1} = 0 \\ \alpha''_+ x_+^{-(N+1)} + \alpha''_- x_-^{-(N+1)} = 0 \end{cases} \quad \text{or} \quad \begin{cases} \alpha''_+ \underbrace{x_+^0}_{=1} + \alpha''_- \underbrace{x_-^0}_{=1} = 0 \\ \alpha'_+ x_+^{-(N+1)} + \alpha'_- x_-^{-(N+1)} = 0 \end{cases} \tag{5.49}$$

to be taken in the limit $N \to \infty$. If $2|w_0| < |\mu|$ we have two possible conditions for $x_\pm$: or $|x_+| < 1$ and $|x_-| > 1$ or $|x_+| > 1$ and $|x_-| < 1$. Thus imposing the normalization condition on the coefficients in (5.47) we find out that only one of the coefficients α'_+ or α''_+ in the expression of b', or α'_- or α''_- in b'', is non zero but, according to both the sets in (5.49), the other coefficient has to be zero. It follows that there is no zero modes in the system. On the other hand if $2w_0 > |\mu|$ and $\Delta \neq 0$ then $|x_+|, |x_+| < 1$ and, repeating the same reasoning as in the preceding case OBC are fulfilled as well as the normalization condition.The good OBC, in this case, are the one in the left system in (5.49). We find that the system allows for two Majorana zero modes localized at the edge of the wire, b' at the left edge at b'' at the right one. They decrease in amplitude going toward the bulk and for finite length wire this allows for some overlap between them providing some amount of energy that destroy the zero mode regime. For finite length wire the system is in fact described by the effective Hamiltonian:

$$H_{eff}^{fl} \propto \frac{i}{2} t b' b'' \quad t \propto e^{-L/l_0} \tag{5.50}$$

where $l_0^{-1} =$ is the smallest between $|\ln |x_\pm||$. In the last case, for $-2w_0 > |\mu|$ and $\Delta \neq 0$, we have $|x_+|, |x_+| > 1$ and zero modes are always allowed but now the modes b' and b'' flip, the right side set in (5.49) is considered.

Chapter 6

Non Trivial Topology for the Reciprocal Lattice Space

In this chapter we will see how the topology enters in the description of the ground state wave functions and how MZM are directly linked to the appearing of non trivial topology.
When we tell about a topological phase transition we address a particular kind of quantum phase transition. Standard universality classes approach, defined via critical exponents for the quantum systems, always works when identifying a change in quantum order. Now we want to go deeper in the characterization of quantum order change by addressing the topological order. Thus we build up another kind of classes, the (topological) equivalence classes. As result some of the quantum orders also have nontrivial topological properties. These latter constitute a subset of the universality classes defined in the last chapter. We introduce the basic concepts of topology, used later, by considering to have many figures and we ask to ourselves when we can consider two or more of them to be equivalent. Obviously the answer depends on the definition we give about equivalence. For instance, in elementary geometry the equivalence between two figures is given by congruence, but this is a too stringent definition for our aims; so we introduce the *topological equivalence*. We say that two figures are topologically equivalent if we can deform one of them into the other by means of continuous deformation. In a formal way the equivalence relation we adopt is the *homeomorphism*:

Definition 1 *Let X_1 and X_2 be topological spaces. A map $f : X_1 \to X_2$ is a* ***homeomorphism*** *if it is continuous and it has an inverse $f^{-1} : X_2 \to X_1$ which is also continuous.*

If there exists an homeomorphism between X_1 and X_2 then X_1 is said to be homeomorphic to X_2 and viceversa. Now we can think to divide the whole set of topolog-

ical spaces into *equivalence classes* according to whether it is possible to connect the spaces between themselves by homeomorphisms. When it is possible we say that they belong to the same equivalence class. In symbols, we say $\sim$ to be the homeomorfism and we define a generic equivalent class $[a]$ by:

$$[a] = \{x \in X | x \sim a\} \tag{6.1}$$

Although the division in classes is conceptually well defined it is operatively difficult to do, that is why we introduce the concept of *topological invariants*. Topological invariants are the quantities which are conserved under an homeomorphism [69]. Also in this case, it is very hard to find all of them for each space, so what we can say is that if two different topological spaces has different topological invariants they are not homeomorphic to each other, so they do not belong to the same equivalence class. Sometime we choose to lose in formality and leave the relation of homeomorphism for the one of "homotopy type"; that is to say we do not require the map linking the two space to be reversible. We can have a continuous map f going from S_1 (the first space) to S_2 (the second space) which is not reversible and another continuous map g going S_2 to S_1. What we are interested for is to identify the various topological phases of a physical system. So we try to characterize a state by means of a topological invariant, defined in the following according to the discrete symmetries of the system, and we check, for different values of state parameters, such topological invariant's values.
Generally, in differential topology, One concerns with topological invariants associated with smooth manifolds. Now for a periodic system, thought to be in the thermodynamic limit, the k space (the first Brillouin zone) is a smooth manifold. Then the invariants of all TSM are defined on it ([70, 71]). Since the topological phase is linked to the appearing of MZMs in the system and such modes are necessarily obtained for OBC it is very strange that the bulk properties give information about edge states (the k space is achieved imposing closed boundary conditions that is equivalent to looking at the bulk). However this is the way by which the scientific community has proceeded Thus we introduce the Hamiltonian H for the closed system written in terms of Fourier transform of Dirac fermions $\{a_j, a_j^\dagger\}_{j=1}^N$. Here we assume periodic boundary conditions (PBC) when we close the system so that:

$$a_{j+N} \sim a_j \quad \forall j = 1, \dots, N$$

Now we define a new set of $2N$ operators $\{a_\kappa, a_\kappa^\dagger\}$ as:

$$\begin{cases} a_k = \frac{1}{\sqrt{N}} \sum_j a_j e^{-i\kappa j a} \\ a_k^\dagger = \frac{1}{\sqrt{N}} \sum_j a_j^\dagger e^{i\kappa j a} \end{cases} \tag{6.2}$$

where a in the exponentials is the lattice step length, j goes from 1 to N and, according to PBC, $\kappa = k\,2\pi/a$ with $k = 1, \ldots, N$ are the reciprocal lattice vectors. The system Hamiltonian can be then written as:

$$H = \frac{1}{2} \sum_{\kappa \in 1B.Z.} \left({a_\kappa}^\dagger, a_{-\kappa} \right) H(\kappa) \begin{pmatrix} a_k \\ a_{-k}^\dagger \end{pmatrix} \tag{6.3}$$

The ground state of the system can be expressed by the action of operators in (6.2) and the Hamiltonian parameters. Thus addressing such state (expected to be occupied at low temperatures) we aim to check some change of the topology of the first Brillouin zone, that is our manifold.
Now that we have the manifold, the main point is what is the appropriate invariant for the system. The classification of topological phases, thus the choice of a good topological invariant, is done by considering the symmetries of the Hamiltonian as time reversal $\mathcal{T}$, particle-hole $\mathcal{C}$ and chiriality $U = \mathcal{T} \circ \mathcal{C}$ one [71][72]. Generally, about these three symmetries, we have:

$$\mathcal{T}^2 = \pm\mathbb{I} \quad \mathcal{C}^2 = \pm\mathbb{I} \tag{6.4}$$

but in our cases (spinless fermions) $\mathcal{T}^2 = \mathcal{C}^2 = \mathbb{I}$. Remembering that we deal with a 1 D system, always undergoing to particle-hole symmetry, then the cataloguing in topological classes takes the time reversal Hamiltonians into the BDI class and, the one with no time reversal symmetry into the D class. They group 1 D system with particle-hole symmetry and respectively time reversal symmetry and broken time reversal. There are two principal topological invariants which correspond to integer numbers, $\mathbb{Z}$ and $\mathbb{Z}_2$, respectively for classes BDI and D. Such invariants are the winding number and the pfaffian invariant. In the following we will define such topological invariants.

6.0.1 $\mathbb{Z}$ Invariant

Let us consider the case of a 1D p-wave topological superconductor whose Hamiltonian, assuming periodic boundary conditions, shows particle-hole and time reversal symmetry:

$$H(-\kappa)^* = H(\kappa) \tag{6.5}$$

then:

$$H(k) = \begin{pmatrix} \epsilon(k) - \mu & i\Delta(k) \\ -i\Delta(k) & \mu - \epsilon(k) \end{pmatrix} \tag{6.6}$$

whit real elements. A god topological invariant for the phase is the *winding number*, that can be defined using Anderson pseudospin vector [73]:

$$\vec{d}(k) = \Delta(k)\mathbf{j} + (\epsilon(k) - \mu)\mathbf{k} \tag{6.7}$$

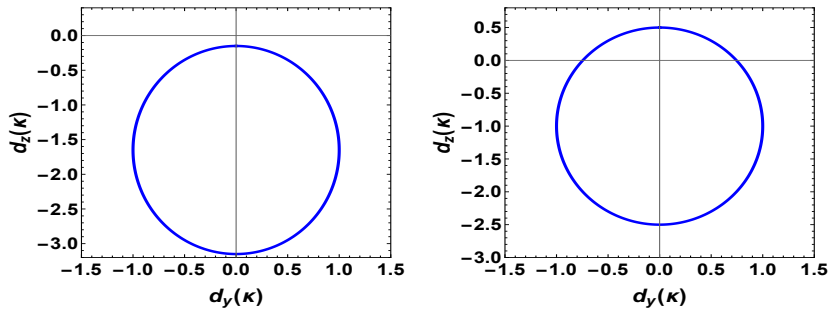

Figure 6.1: Two example of $\vec{d}(k)$ (unormalized) in the $y-z$ plane for the Kitaev model. At left a trivial topological phase with $W=0$ instead, on the right side, a topological phase with one MZM per edge ($W=\pm 1$)

so that $H(k) = \vec{d}(k)\cdot\vec{\sigma}$ with $\vec{\sigma}$ being the vector of Pauli matrices. Now we normalize $\vec{d}(k)$:

$$\hat{d}(k) = \cos(\theta(k))\mathbf{j} + \sin(\theta(k))\mathbf{k} \tag{6.8}$$

With $\cos(\theta(k)) = \Delta(k)/|\vec{d}(k)|$ and $\sin(\theta(k)) = (\epsilon(k)-\mu)/|\vec{d}(k)|$. Now if we consider the momentum vectors (reciprocal lattice vectors), assuming periodic boundary conditions, they form a ring T^1. The unit vector $\hat{d}(k)$ lives on a unit circle S^1 and so the mapping $\theta(k)$ is a map $\theta(k) : T^1 \to S^1$. About this mapping we consider its fundamental group as topological invariant [74] (in two dimensions we would have a classification of mapping from T^2 to S^2 always by means of winding number [75]):

$$\begin{aligned} W &= \oint \frac{d\theta(k)}{2\pi} \\ &= \int_{-\pi}^{\pi} d\kappa \, \frac{\partial \hat{d}_z(\kappa)}{\partial \kappa} \partial \hat{d}_y(\kappa) \end{aligned} \tag{6.9}$$

It says to us how many times $\hat{d}(k)$ turns around $(0,0)$ in the $y-z$ plane, while running over the whole first Brillouin zone. Moreover the change in MZM number at each end of the wire is given also by W, In particular we have $W = \#(b') - \#(b'')$ at the left edge of the wire (1DTSC case) [56].

6.0.2 $\mathbb{Z}_2$ Invariant

If our system Hamiltonian is not time reversal invariant, then symmetry is reduced to $\mathbb{Z}^2$. We cannot use anymore the Winding number as topological invariant. A good topological invariant, introduced in [5] is the *Pfaffian invariant*. The author

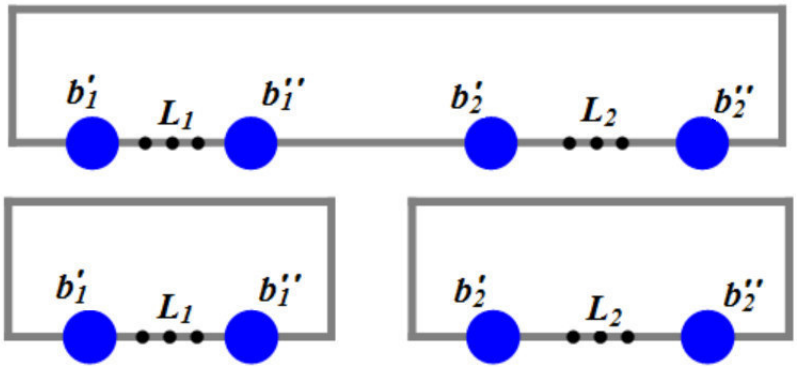

Figure 6.2: Two different ways to close two different chain showing MZM at their own edges. Or we close each on on it self or we link the right edge of the first chain to the left edge of the other one and then we do the same changing the role of the first and second chain.

introduces the the Majorana number $\mathcal{M}(H) = \pm 1$ associated with the Hamiltonian H where this latter has a unique ground state. For Hamiltonians that exhibit Majorana bound states, in the case of open boundary conditions, then $\mathcal{M}(H)$ takes the value 1, which corresponds to a nontrivial topology. Then, if we consider two chains of lengths L_1 and L_2 (the number of sites per chain coincides with their length), it can be shown that the Majorana number is related to the fermionic parity P of the ground state of a closed chain of length $L = L_1 + L_2$ by the following relation:

$$P(H(L_1 + L_2)) = \mathcal{M}(H)P(H(L_1))P(H(L_2)) \tag{6.10}$$

whatever option, for closing the two chains together, we choose (see Figure 6.2). Now we give the definition of the Pfaffian of a skewmatrix A, in terms of the total antisymmetric tensor $\epsilon_{i_1,\ldots,i_{2n}}$, as:

$$Pf(A) = \frac{1}{2^n n!}\epsilon_{i_1,\ldots,i_{2n}} A_{i_1,i_2} \ldots A_{i_{2n-1},i_{2n}} \tag{6.11}$$

In our case, if A is the matrix characterizing the Majorana representation of the system Hamiltonian,t hen it is shown that

$$P(H) = \mathrm{sgn}\{Pf(A)\} \tag{6.12}$$

Combining together eqns. (6.10) and (6.12) we get:

$$\mathcal{M} = \mathrm{sgn}\{Pf(A)\} \tag{6.13}$$

Indicating with $\tilde{A}(k)$ the Fourier transform of skewmatrix A expression the last expression can be rewritten as:

$$\mathcal{M} = \mathrm{sgn}\{Pf(\tilde{A}(0))Pf(\tilde{A}(\pi))\} \tag{6.14}$$

The reciprocal lattice point (we are in a 1 D space) $\kappa = \pi$ exists only if the number of lattice sites is even and this is just the case we consider. Points $\kappa' = 0$ and $\kappa'' = \pi$ are special since, because the PBC, we have $0 \sim$ and $\pi \sim -\pi$. Furthermore looking at the diagonal form (5.36) it is immediate that:

$$Pf(A_J) = \prod_{n=1}^{N} \epsilon_n > 0 \tag{6.15}$$

Using the relation:

$$Pf(\underbrace{WAW^T}_{=A_J}) = Pf(A)det(W) \tag{6.16}$$

together wit eqn. (6.13) we get:

$$\mathcal{M} = det(W) = \pm 1 \tag{6.17}$$

If now we take in consideration the Fourier transform $\tilde{W}(k)$ of W, then such transform is block diagonal and we have:

$$\begin{aligned} \mathcal{M} &= \Pi_k det(\tilde{W}(k)) \\ &= \Pi_{k=-k} det(\tilde{W}(k)) \\ &= det(\tilde{W}(0))det(\tilde{W}(\pi)) \end{aligned} \tag{6.18}$$

The reality of W implies $\tilde{W}(k)^* = \tilde{W}(k)$. Since $\tilde{W}(k)$ is unitary for all k then:

$$det(\tilde{W}(k)) = e^{i\varphi k} \tag{6.19}$$

Always because of the reality constrain then $\varphi k = \varphi k(mod 2)$ holds, and this latter implies that φk is quantized to integer multiples of π at the k points 0 and π. Therefore the invariant is expressed as:

$$\mathcal{M} = (-1)^{\frac{\varphi_0 - \varphi_\pi}{\pi}} \tag{6.20}$$

The determinant of $\tilde{W}(k)$ is a continuous function of k so the phase change $\Delta\varphi = \varphi_0\varphi$ can be written as in the following:

$$\Delta\varphi = i \int_0^\pi \left[d_\kappa(\ln(\det(\tilde{W}(\kappa)))) \right] d\kappa \tag{6.21}$$

At last Pfaffian invariant is related top the quantized Zak-Berry phase, Φ_{ZB}, by [76]:

$$\Delta\varphi = \Phi_{ZB} \tag{6.22}$$

There exist another $\mathbb{Z}^2$ topological invariant. Indeed under the assumption that, in the whole k space, the spectrum is fully gapped for all k points, we can define [**?**]:

$$\nu = \mathrm{sgn}\{H(0)H(\pi)\} \tag{6.23}$$

Such invariant gives the the parity of the number of MZM at the end of the system.

Chapter 7

Long Range Kitaev Model

In this chapter we consider a generalized Kitaev chain model taking into account long range interactions (in hopping and pairing), finding the conditions under which Majorana zero modes (MZM) or massive edge modes (MEM) can appear, in the presence or in the absence of time reversal symmetry (TRS). In particular we obtain that for TRS Hamiltonians many MZM per edge appear when interactions counts a finite number of neighbors. By breaking TRS such number of Majorana modes is reduced to one, moreover, extended critical regions appear in the phase diagrams. For the case of all-neighbor interactions (true long range interactions), together with MZM, we get also MEM. Finally we discuss the cases in which MZM are obtained for a finite length of the wire. Such cases are important for their possible experimental implementations via cold atoms or optical devices. Theoretical extensions of Kitaev model was already proposed for counting more neighbors interactions for hopping and superconducting pairing between Dirac fermions of the wire [56][61][73][77][78][79][80][81].
For the case of a simply extended Kitaev model, counting a finite number of neighbor interactions, the main result has been the possibility to find many MZM per edge, in the presence of time reversal symmetry. Situation changes if TRS is broken, these breaking allows tunneling between edge modes removing MZM from zero energy levels (symmetry protection is removed) and creating Dirac fermion states with non-zero energies and leaving the system in a topologically trivial phase [73]. In this situation it has been shown that we can have at maximum one MZM per edge [56]. In this latter case a good topological invariant is the $\mathbb{Z}^2$-valued invariant ν, defined in the next section, which is related to the parity of the number of Majorana fermions per edge. Recent developments consider all neighbors interactions and show the presence of massive edge modes [77][79][80]. It has been shown that for such long range models one finds, for certain parametric regimes,

area law violation and the breaking down of the conformal symmetry for closed boundary conditions. Here, instead, we systematically study the role of hopping and pairing ranges and TRS for the characterization of the topological phases by means of topological invariants and exact diagonalization. We then present and discuss several phase diagrams which can be drawn, corresponding to different situations. Finally we generalize the transfer matrix approach useful to derive the ground state for a generic number of neighbors.

7.1 Long Range Hamiltonian with Algebraic Decay in Hopping and Pairing

We propose a long ranged Kitaev chain model taking into account r neighbor interactions in hopping and pairing separately as well as combined together We assume both of these interactions to be algebraically decreasing with lattice distance between two different lattice sites. Algebraic decay of long ranged pairing alone has been well studied in [77], in the limit of infinitely long interaction, it shows, for certain physical regimes, Majorana zero modes and massive edge modes identified as topological massive Dirac fermions (TMDF) in [80].The Hamiltonian we introduce, similar to the one of [79], is the following:

$$H = \sum_{j=1}^{N} \left(-\mu \left(a_j^\dagger a_j - \frac{1}{2} \right) \right) + \sum_{l=1}^{r} \sum_{j=1}^{N-r} \left(-w_l d_l^{-\alpha} a_j a_{j+l}^\dagger + \Delta d_l^{-\beta} a_j a_{j+l} + \text{h.c.} \right) \quad (7.1)$$

In eq.(7.1) N is the number of lattice sites of the wire whose length is L, μ is the site chemical potential, w_l and Δ_l are the hopping and p-wave superconducting pairing terms which let the $j-th$ lattice site with the site $(j+l)-th$ interact. Phase factor in Δ (such term is generally complex) can be gauged out as shown in [5], on the other hand w_l is assumed to have the form $w_l = w_0 e^{i\varphi l}$ with real φ and w_0. Index l runs over the neighbors sites and d_l is defined as in [77]:

$$\begin{cases} d_l = l & \text{if} \quad l \leq N/2 \\ d_l = N - l & \text{if} \quad l > N/2 \end{cases} \quad (7.2)$$

for closed boundary conditions or we assume $d_l = l$ for OBC. Exponents α and β, that characterize the decreasing of long range effects, are assumed to be positive or null. At least set $\{a_j\}$ satisfy Fermi-Dirac statistic. Now we will focus on the

discrete symmetries of the system's Hamiltonian which will help us further. Hamiltonian H in (7.1) is sent in $-H$ under particle-hole transformation. Calling C the operator flipping particles in holes and viceversa we have:

$$C^{-1}HC = -H \tag{7.3}$$

Eq. (7.3) stands for each choice we make for state parameters. The situation changes if we look at time reversal symmetry; we use reciprocal lattice to test this discrete symmetry. So at first we close the chain into a ring so that position $j + N \sim j \quad \forall j = 1, \dots, N$ and we choose periodic or antiperiodic boundary conditions (we will explain later why this dilemma) for Dirac operators, i.e. $a_{j+N} = \pm a_j \, \forall j$. Then we define a new set of operators $\{a_\kappa\}$ by:

$$a_j = \frac{1}{\sqrt{N}} \sum_{\kappa \in B.Z.} a_\kappa e^{-i\kappa j} \tag{7.4}$$

with

$$\kappa = \begin{cases} \frac{2\pi k}{N} & \text{for PBC} \\ \frac{2\pi k + \pi}{N} & \text{for ABC} \end{cases} \tag{7.5}$$

and we rewrite H in terms of new Dirac fermions operators:

$$\begin{aligned} H_{PBC-ABC} = & \\ &= \sum_\kappa \begin{pmatrix} a_\kappa^\dagger & a_{-\kappa} \end{pmatrix} \Bigg\{ \sum_l \left[l^{-\alpha} w_0 \sin(\varphi l) \sin(\kappa l) \right] \mathbb{1} \\ &+ \left(-\frac{\mu}{2} - \sum_l \left[l^{-\alpha} w_0 \cos(\varphi l) \cos(\kappa l) \right] \right) \boldsymbol{\sigma_z} \\ &+ \left(\Delta \sum_l l^{-\beta} \sin(\kappa l) \right) \boldsymbol{\sigma_y} \Bigg\} \begin{pmatrix} a_\kappa \\ a_{-\kappa}^\dagger \end{pmatrix} = \\ &= \sum_\kappa \begin{pmatrix} a_\kappa^\dagger & a_{-\kappa} \end{pmatrix} H_0(\kappa) \begin{pmatrix} a_\kappa \\ a_{-\kappa}^\dagger \end{pmatrix} \end{aligned} \tag{7.6}$$

In eq.(7.6), both for PBC or for ABC, time reversal condition $H_0(-\kappa)^* = H_0(\kappa)$ is satisfied only if we consider real hopping terms w_l, thus if $\varphi = 0, \pi$. In the next sections we will analyze both situations, TR and broken TR Hamiltonian, separately. Now let's focus on what happen when we close the chain. PBC/ABC dilemma materializes if there are finite size effects. In [77], ABC are assumed to preserve pairing terms in H, otherwise this choice destroys hopping terms for finite

N and $r \geq N/2$. For $r < N/2$ no problem arises, as both choices preserve interaction terms and invariance for discrete translations. Closed chains for ABC and PBC are however always different. For finite r we can solve the dilemma by looking at the expression of $H_0(\kappa)$ in reciprocal space, where terms like $\cos\left(l\left(\frac{2\pi k}{N}+\frac{\pi}{N}\right)\right)$ and $\sin\left(l\left(\frac{2\pi k}{N}+\frac{\pi}{N}\right)\right)$ go to $\cos\left(l\left(\frac{2\pi k}{N}\right)\right)$ and $\sin\left(l\left(\frac{2\pi k}{N}\right)\right)$ for $N \to \infty$ if l remains finite. Instead, if we consider an infinite number of interacting neighbors (always in the thermodynamic limit), function d_l will always be always l and the above terms in (7.6) take into account polylogarithm functions $Li_\alpha(e^{\pm i\kappa l})$ where κ already belongs to a continuum so the dilemma doesn't stands. In the thermodynamic limit, PBC or ABC give the same H.
System's topological phase is described by different topological invariants according to time reversal symmetry standing. In the case in which such symmetry stands we ill use the winding number in eqn. (6.9), otherwise we will address the topological invariant ν in (6.23).

7.2 Finite Neighbors Number Chain: Topological Phase Diagrams

Here we focus on the case of finite neighboring interactions and will give topological phase diagrams (TPD) for each case we will address. At first we allow the hopping term to be long ranged despite the pairing interaction is considered to be at first neighbors, then the opposite case is assumed. At the end we allow both of them to be long ranged and, for this case, we analyze the topological phase in TR and broken TR regime.

7.2.1 long ranged hopping: Time Reversal Regime

We will now analyze eq.(7.1) in the limit of only long ranged hopping, i.e. $\beta \to \infty$, for finite r. In Figure 7.1 we observe topological regime ($\mathbb{Z} = \pm 1$) to enlarge as the inverse of penetration length (α^{-1}) of the hopping term grows up. The result we found about this specific Hamiltonian is consistent with the one obtained in [80]. Only one MZM per edge can be found and this aspect can be understood since the dependence of pairing term on κ goes as $\sin(\kappa)$ and not as $\sin(l\kappa)$ ($l = 1, \ldots, r$). Thus, after moving over all the first Brillouin zone in κ-space, the winding vector can only makes at maximum one circle around $(0, 0)$. To better show this aspect we report in Figure 7.2(a) all the spanned points in $y - z$ plane by the unormalized winding vector $\mathbf{d}(\kappa) = \left(0, \Delta\sin(\kappa), (-w_0)\sum_l l^{-\beta}\cos(l\kappa)\right)$.

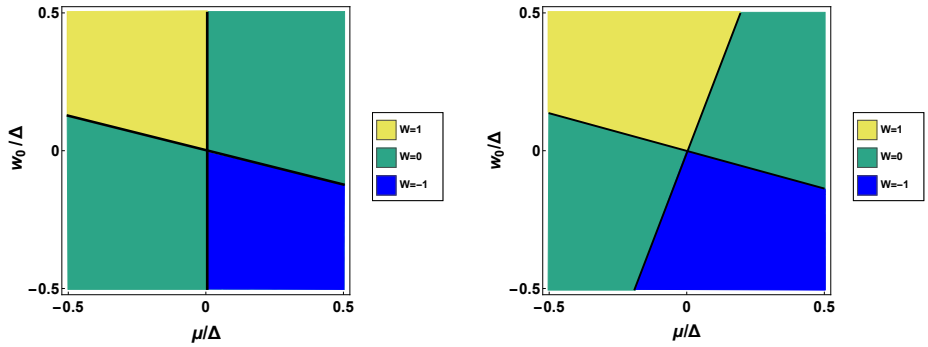

(a) $r = 2 \quad \alpha = 0 \quad \beta \to \infty$ (b) $r = 2 \quad \alpha = 0.3 \quad \beta \to \infty$

Figure 7.1: Phase diagram, showing the values of W as in the legend, for $r = 2$ with growing α in the limit of $\beta \to \infty$, i.e. only long ranged hopping. Topological regime enlarges for $\alpha \to \infty$ where Kitaev model regime is obtained.

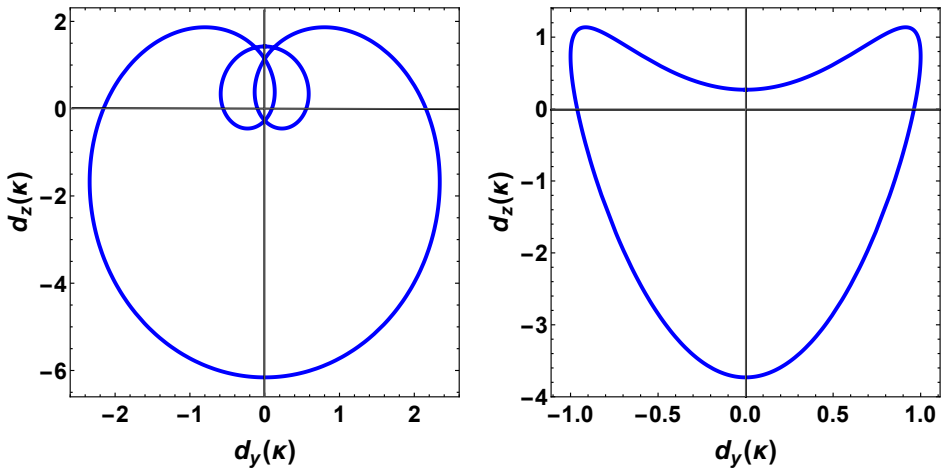

(a) $r = 2 \quad \alpha = 0.7 \quad \beta \to \infty$ (b) $r = 3 \quad \alpha = \beta = 0.1$

Figure 7.2: Unormalized winding vector for $\beta \to \infty$, $\alpha = 0.7$ and $r = 2$ in Figure 7.2(a) and $\alpha = \beta = 0.1$ and $r = 3$ in Figure 7.2(b). In both figures $\mu/\Delta = 1$ and $w_0/\Delta = 2$. In the first case the graphic can turns around $(0, 0)$ at maximum once but, on the other hand graphics in the second figure can makes 1 or 3 twists around the origin.

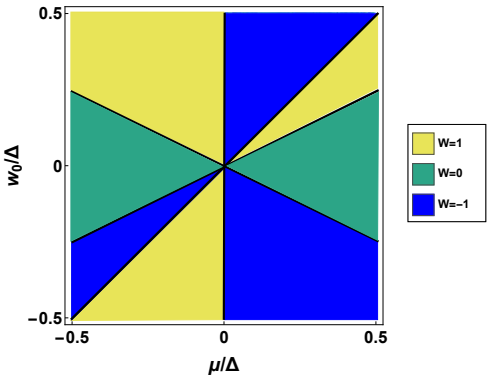

(a) $r = 3 \quad \beta = 0 \quad \alpha \to \infty$

Figure 7.3: TPD of H with only long-ranged pairing; values of W are reported. In Figure 7.3(a) we note phase diagram has a strange alternating topological invariant but the regime where 1 MFs per edge appears is the same as in the Kitaev chain model limit ($\beta \to \infty$)

7.2.2 Long Ranged Pairing: Time Reversal Regime

Now we get $\alpha \to \infty$ so to analyze H in the regime of only long ranged pairing. Again the winding number, as before, takes the values $0, \pm 1$. We note an alternation, inside the topological regime, of values ± 1 for $\mathbb{Z}$. This behaviour, not present in only long ranged hopping Hamiltonian, is more emphatic as r increases (we are always assuming r to be finite) and it disappears as $\beta \to \infty$, in which case we will obtain the well known topological phase diagram for Kitaev model in [5]. However the topological region is the same as in the first neighbors Kitaev model. Indeed since $|W| = 0, 1$ then such W is equivalent ν. Addressing the expression of this latter, we have that $H_0(0, \pi) = d_z(0, \pi)$ for our case are the same as in the case of the standard Kitaev chain. As a consequence the presence of MZM, characterizing the topological phase, is given by the same parametric regime for both cases.

7.2.3 Long Ranged Pairing and Hopping: TR and BTR Symmetry

We will now look at physical effects on topological phase considering long ranged hopping and pairing at the same time. We assume $\beta = \alpha$ at first in the regime of TR symmetry and then in the more realistic case of broken TR.

Time Reversal Case

In Figure 7.4 we show how the increasing of α destroys MZM at the edge of the wire. For $\alpha = 0$ we can obtain $|W_{MAX}| = r$ which tells us that we have r MZM per edge [75], for $\alpha \to \infty$ we recover the standard Kitaev chain model. However, changing α, or other parameters such modes are created or destroyed in pair for each edge, with the only exception of the appearing of $W = 1$ regime for each r we choose (even or odd). We will explain this appearing-disappearing" behaviour using the particle-hole symmetry. Indeed, for each eigenvalue ϵ_n we must have another eigenvalue $-\epsilon_n$, so MZM have to be created or destroyed in couples. Let's assume we destroy theme, then the thought can also be applied to the reverse process. For each couple of states moved away from zero there will be a gap Σ_n in the spectrum. This effect can be described, as done in [5], by an efficient Hamiltonian $V_{eff} \propto -(t_{eff}/2)\tilde{a}_n^\dagger \tilde{a}_n$ where t_{eff} describes the overlap between two MZM. Such overlap is due to the finite characteristic penetration length, ξ, of MZM. If such $\xi = 0$ this discussion about overlap is not valid. Now it is reasonable to think this overlap effect is greater between two functions whose peaks are close to each other, i.e. between two MZM lying in the same side of the wire. As a result in loosing MZM we delete two of them per time for each edge. Nevertheless, topological phase with $|W| = 1$ is always present. As we will show in the next section, the system admits $W = \pm 1 \, \forall \, r$ with Hamiltonian identically singular for certain parameters choice. Such choice is $\mu = 0$ and $|w_l| = |\Delta_l| \, \forall \, l = 1, \ldots, r$. This Hamiltonian admits one MZM at each edge of the wire. It is just the topological nature of these modes (their robustness), which tells us that some regions exist, around this point in the parameters space, in which such topological phase is maintained. Therefore the $|W| = 1$ phase is somehow protected. To conclude the description of topological phase transitions, in going from $|W| = 1$ to $|W| = 0$ standard overlap between MZM at opposite edges occurs. As result we itemize:

- If r is even we can have 0, 1 or an even number of MZM per edge until this number can be just r

- If r is odd, we can have 0 or an odd number of MZM per edge until W can get the same value of r

We observed that an increasing of potential's penetration length $\xi = \alpha^{-1}$, for $\alpha < 1$, supports richer and richer topological phases, i.e. the appearing of many MZM per edge.

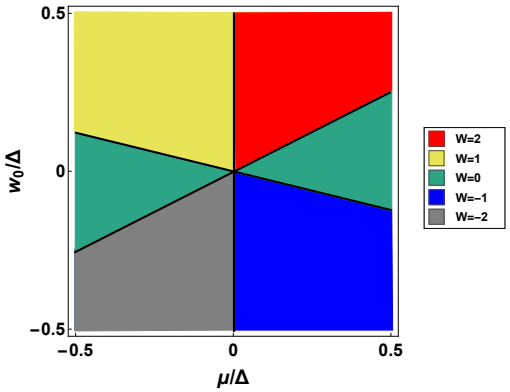

(a) $r = 2 \quad \alpha = 0$

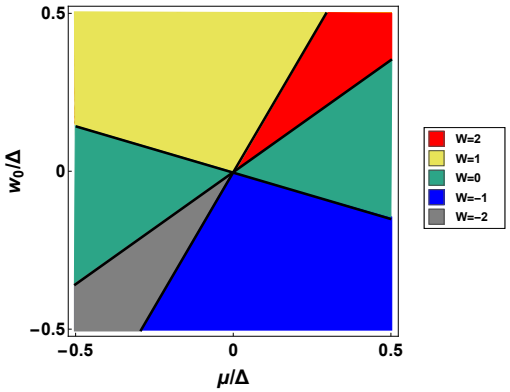

(b) $r = 2 \quad \alpha = 0.5$

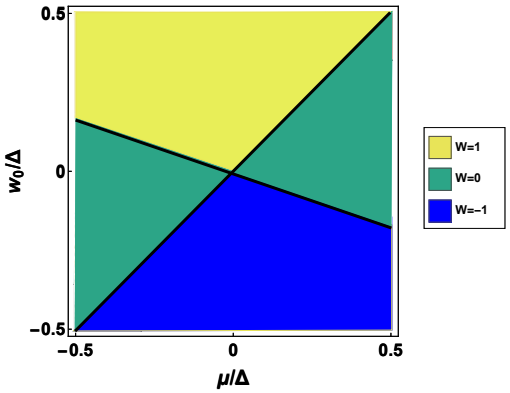

(c) $r = 2 \quad \alpha = 1$

Figure 7.4: W values with both hopping and pairing are long ranged with $\alpha = \beta$ and $r = 2$. Only for $\alpha < 1$ we can have two MZM per edge. Regions where these are obtained decrease as α grows up. Kitaev first neighbors model is obtained for $\alpha \to \infty$.

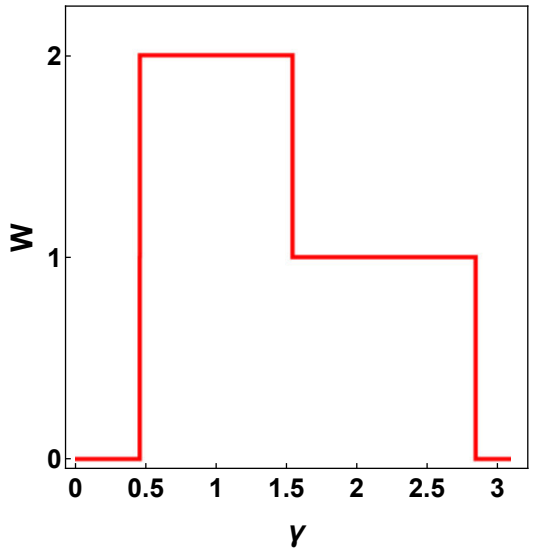

(a) $r = 2 \quad \alpha = \beta = 0$

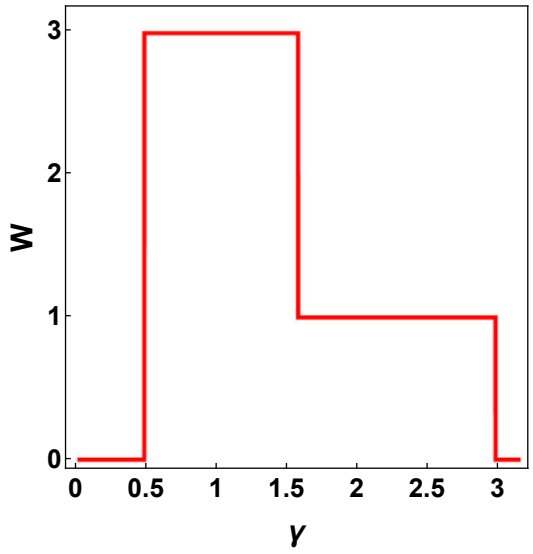

(b) $r = 3 \quad \alpha = \beta = 0$

Figure 7.5: TPD for two different r neighbors Kitaev chain; in Figure 7.5(a) $r = 2$ and in Figure 7.5(b) $r = 3$. State parameters are $\alpha = \beta = 0$, so that hopping and pairing are both long ranged with a flat potential and we choose $\mu/\Delta = 0.1\cos(\gamma)$ and $w_0/\Delta = 0.1\sin(\gamma)$ with $\gamma \in [0, \pi]$. Such angle is reported on the x axis, on the other side we report on y axis the relative winding number W. For $\gamma \in [\pi, 2\pi)$ the phase diagram is antisymmetric, to the above ones, respect to $\gamma = \pi$. For some regimes we have $W = r$ in both situations. The legend shows that ABC and PBC give the same results, such graphics are obtained via numerical calculations of W on reciprocal lattices of $100\ \kappa$ sites.

Broken Time Reversal Case

Including broken time reversal effects implies coupling between odd as well as even index Majorana operators so that, as explained in [56], only topological phase with an odd W, in TRS regime, will survive because of particle-hole symmetry of the spectrum. BTR is induced by non null φ_l in eqn. (7.1). Here we check the effects of two different forms of this parameter, $\varphi_l = \varphi_0 \, \forall \, l = 1, \ldots, r$ and $\varphi_l = \varphi_0 l$ with $l = 1, \ldots, r$. We find almost the same training of topological phase with respect to the state parameters (see Figure 7.6). 2D regions, in which the gap closes, are present for both cases. Then the parametric regime, including topological states, reduces as φ_0 increases and completely disappears for $\varphi_0 = \pi/2$.

7.3 Infinite Neighbors Number Long Ranged Chains: Topological Phase Diagrams

Here, as done in [80] and [79], we will approach the regime $r = N \to \infty$ but we will explore the case of long ranged hopping and pairing separated as well as together in TRS and broken TRS. We will obtain massive edge mode states as predicted in [79] and [80]. We want to underline that it is important to know the trend of such phase to know the potency of an experimental implementation of such Hamiltonian in order to use topological behaviour of MZM and MTDF.

7.3.1 Long Ranged Pairing: TR and BTR Symmetry

In this section we will divide the study of H into three parts: the case where the inverse penetration length of the pairing potential (β) is smaller than one, the case in which it lies between 1 and 2 and finally the case in which it is greater than 2. As before we will approach time reversal and broken time reversal cases separately

Time Reversal Case

Under TR symmetry, the three regimes of β addressed before respectively correspond to the regime where H and its derivates are not defined in $\kappa = 0$, only the derivates of H are not defined in $\kappa = 0$ and both Hamiltonian and its derivates are defined over all Brilloiun zone, $\kappa \in [-\pi, \pi]$. For $\alpha < 2$ and time reversal Hamiltonian, the winding number W is defined as indefinite integral [80] but, due to the point $\kappa = 0$, it takes semi integer values for $\alpha < 1$. $W = 1/2$ topological phase (red region in Figure 7.7) as well as the coexistence of MZM and MEM in the region $1 < \alpha < 1.5$ and $-2 < \mu < 2$ has been already focused in [80]. Here, about

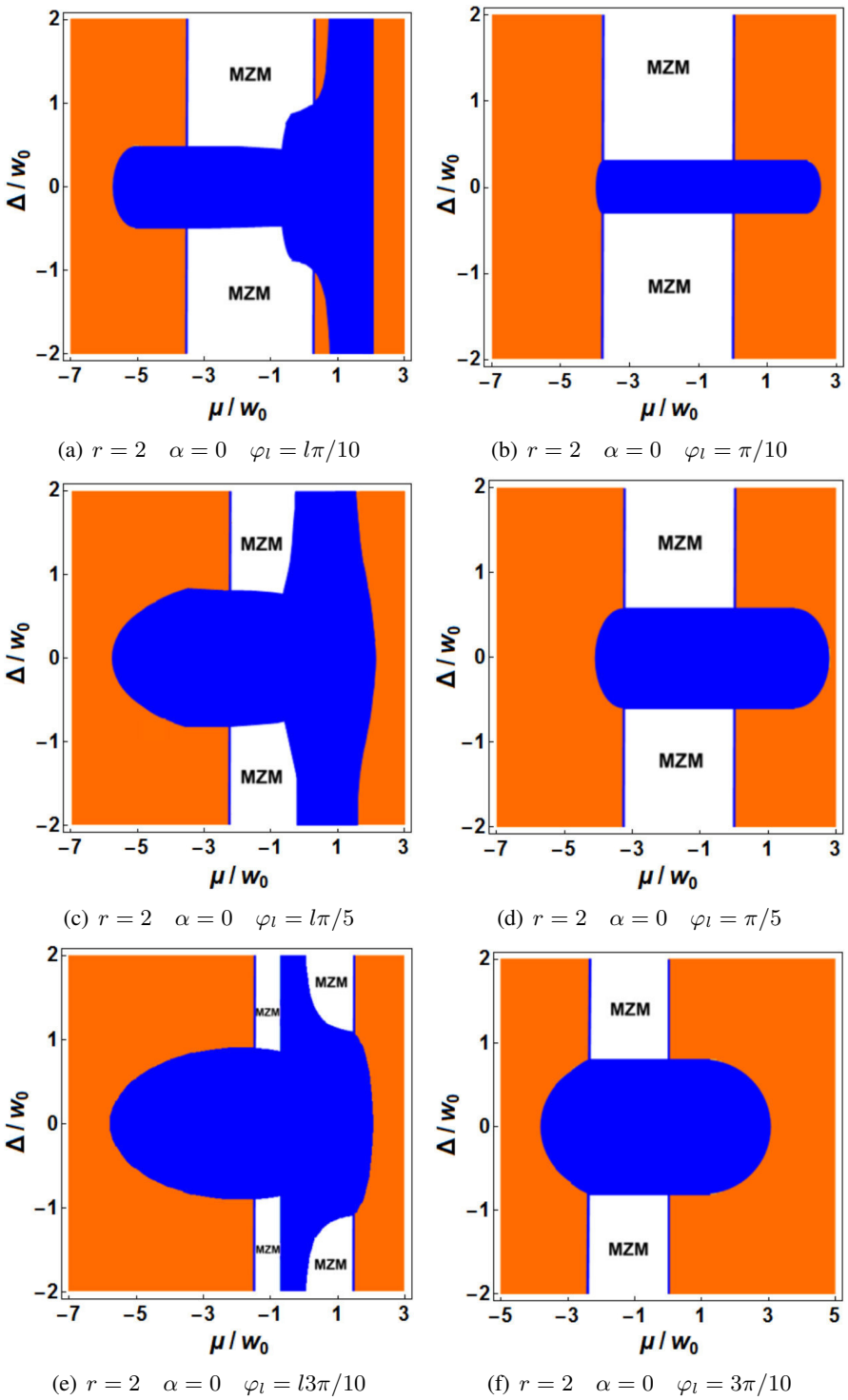

(a) $r = 2 \quad \alpha = 0 \quad \varphi_l = l\pi/10$

(b) $r = 2 \quad \alpha = 0 \quad \varphi_l = \pi/10$

(c) $r = 2 \quad \alpha = 0 \quad \varphi_l = l\pi/5$

(d) $r = 2 \quad \alpha = 0 \quad \varphi_l = \pi/5$

(e) $r = 2 \quad \alpha = 0 \quad \varphi_l = l3\pi/10$

(f) $r = 2 \quad \alpha = 0 \quad \varphi_l = 3\pi/10$

Figure 7.6: Topological phases for $\alpha = 0$ in a second neighbors interacting chain. White regions host MZM, instead in the orange zones no edge mode is present, here topological phase is trivial. μ and Δ are normalized to w_0. Introducing complex hopping delete phases with an even number of MZM per edge and, critical lines become two dimensional critical regions represented in blue. In Figure 7.6(b), Figure 7.6(d) and Figure 7.6(f) we consider only a complex hopping term like $w_l = w_0 e^{i\varphi_l} = w_0 e^{i\varphi_0}$ (constant φ per each l-th neighbors), on the other hand in Figure 7.6(a), Figure 7.6(c) and Figure 7.6(e) long range effects act also on the

this latter region, we give a more precise collocation of such massive and massless edge modes according to the parametric regime. Then it is really interesting to note that we have MEM also in the $W = 0$ and $W = 1$ regions for points closed to $(-2, 1)$ in Figure 7.7 in the region with the blue star. We justify this assertion showing the mass and gap scaling for some of these points in Figure 7.8. Here the value of winding number is difficult to achieve thus we do not report any value. Returning on Figure 7.8 we note, see Figure 7.8(d) and 7.8(f), that gaps are present not only between the lowest energy level and the excited ones. There are gaps between the second and the third level and so on up to level 3 and 4 in Figure 7.8(d) and 4 and 5 in Figure 7.8(f). For the mass scaling, extrapolation has been done by standard "Mathematica" command. thus it just gives a qualitative idea about how the trend is. In panels Figure7.8(e) and Figure7.8(f) the scaling stops at $N = 4000$ since we clearly see how the gap does not change anymore and how the mass tends to zero. Indeed we get a mass $\Lambda_0 < 0.001$ and the raport between the masses at two consecutive lattice site numbers does not seem to converge to 1, indicating that such mass tends to zero. On the other hand in panels Figure7.8(a) and 7.8(c) such raport tends to 1 indicating that a finite mass for the ground state exists and that the thermodynamic limit is almost achieved, but only at $N \sim 10000$. No conclusion about the form of such trends has been done.
About blue region we have $W = -1/2$ thus it is topologically non equivalent to the trivial phase with $W = 0$; winding number is different thus they are not equivalent. The last note that we report is about Figure 7.8(e). Indeed here a linear dependence of Λ_0 in $1/N$ seem to stand. It is just the case since if the mass were zero then, assuming $\Lambda_0(1/N)$ to be analytical, we would have

$$\lim_{1/N\to 0} \frac{\Lambda_0(1/N)}{\Lambda_0(1/(2N))} = 2^m \tag{7.7}$$

where m is the leading order for the Taylor series of Λ_0 closed to $1/N \to 0$. In our case such ratio tends to 2 implying that the leading order is the first one. We see a linear dependence.

Broken Time Reversal Case

In broken TR case, however, we cannot use TI ν in the regime $\alpha < 1$ since $H(0) = d_z(0)$ is not defined there. What we propose below is a TPD made by considering the presence of gapped bulk and the values of the mass of lower positive H_0's eigenvalue (the mass Λ_0 addressed before) for various points in the region $\alpha < 1$, together with the values of ν for the region $\alpha > 1$. The presence of gapped bulk gives information on the presence of edge modes that can be massive or massless. We then know this last information by performing the mass scaling

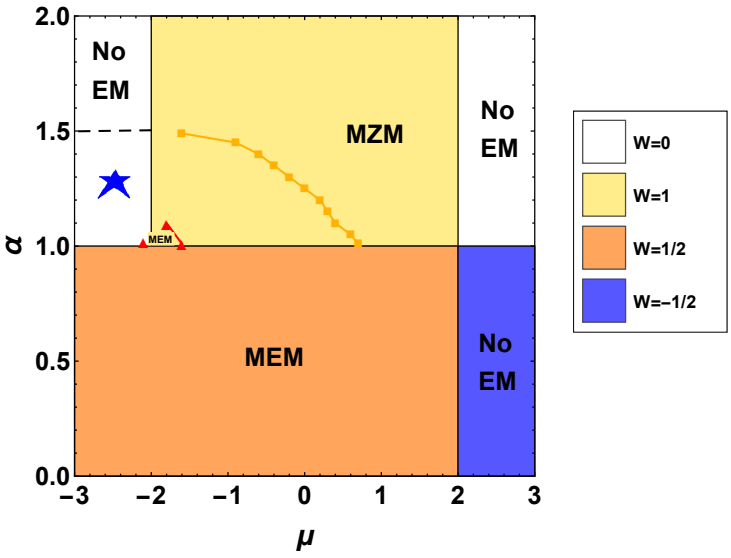

Figure 7.7: TPD for only long ranged pairing in TR regime. Peculiar appearing of massive edge modes (MEM) pictured by red triangles in the regions with $W = 1$, where we aspected MZM, and $W = 0$. Winding number seems not to be able to well describe the transitions toward MEM phase. At the proximity of critical point (-2,1) we can find massive edge modes moving toward every direction we want. Yellow squares represent edge modes whose masses are quite smaller than 10^{-3} by numerical diagonalization of H_0 considering a lattice of $N = 4000$ sites; they are good candidate to be MZM. At their right masses are smaller and smaller. The red region shows the presence of massive edge modes and the blue one has not peculiar characteristic about the spectrum, however it has non trivial topological behaviour due to the non null value of TI W. In the region with the star symbol gap scaling difficulty converges up to $N \sim 10^4$, thus cannot give any information about the presence of edge modes. $\Delta = 2w_0$ has been assumed.

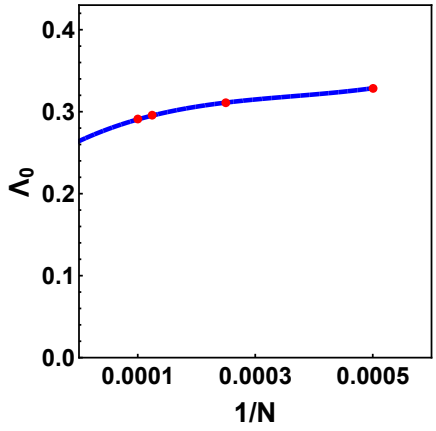

(a) Mass scaling - $\mu = -2.1$ and $\alpha = 1.02$

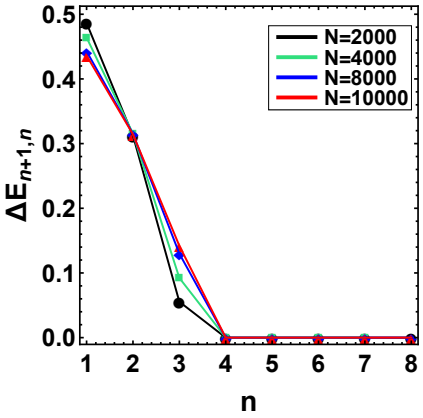

(b) Gap scaling - $\mu = -2.1$ and $\alpha = 1.02$

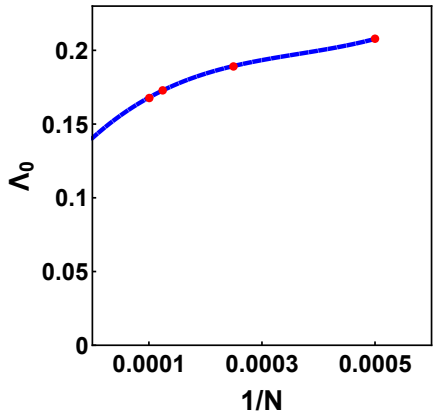

(c) Mass scaling - $\mu = -1.8$ and $\alpha = 1.1$

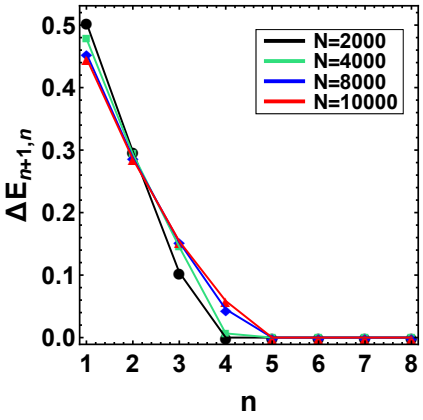

(d) Gap scaling - $\mu = -1.8$ and $\alpha = 1.1$

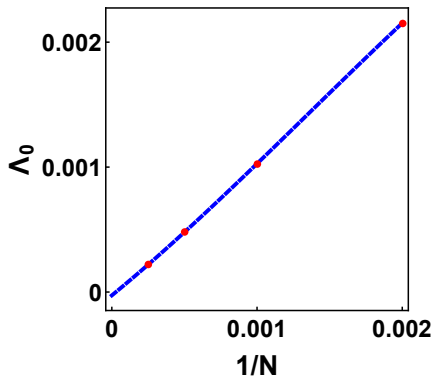

(e) Mass scaling - $\mu = 0$ and $\alpha = 1.25$

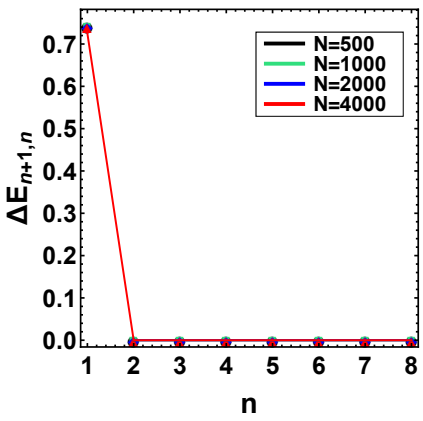

(f) Gap scaling - $\mu = 0$ and $\alpha = 1.25$

Figure 7.8: Mass and gap size scaling for two points respectively at $W = 1$ and $W = 0$ (TR regime for only long ranged pairing) showing finite masses and gapped bulks. In Figure7.8(b) and Figure7.8(d) we find a gap not only between the first level and the bulk but also the second, the third and the fourth level are separated from the bulk. An analogue result is found for broken TR case. $\Delta = 2w_0$ has been assumed.

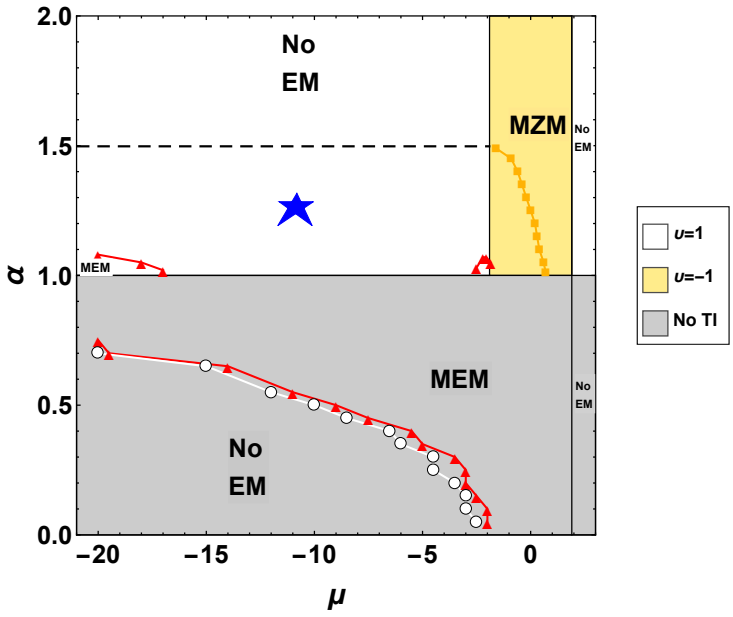

Figure 7.9: TPD for the case long ranged pairing in BTR symmetry with $\varphi = \pi/10$. MEM, for $\alpha < 1$, are almost destroyed by time reversal symmetry breaking but for $\alpha > 1$ they seems to be more robust. In the latter regime, we find MEM in the same regions they were for the time reversal case. The critical lines $\mu = \pm 2$ close one toward the other. ν is not defined for $\alpha < 1$ thus, in this case, the critical line dividing MEM from No EM phase has to lie between the lines depicted by red triangles (MEM) and white circles (No EM). Again, in $\nu = 1$ region with the star symbol, gap scaling does not converge up to $N \sim 10^4$. Also for this case $\Delta = 2w_0$.

for $\Lambda_0(N) = \min\{E_n(N) > 0\}$ as said before. We give this TPD in Figure7.9 made by assuming $\varphi_l = \pi/10$ in the Hamiltonian (7.1) with $r = N \to \infty$. The region over $\alpha = 1$, where MEM exist, seems to be greater than in the TRS case. This is really strange since breaking TR destroys edge modes or at least leave them as they were before the breaking. However critical lines $\mu = \pm 2$ move toward $\mu = 0$ as $\varphi \to \pi/2$, as we found for the finite neighbors case. Finally MEM in the region $\mu < -2$ and $\alpha < 1$ are drastically reduced. Then in Figure 7.10 we show how the TR breaking destroys edge modes. We address $\alpha = 1.3$ and observe a gradual reduction of the edge modes regime while $\varphi_l = \varphi_0$ grows up. Such edge mode region will completely disappear for $\varphi_0 = \pi/2$.
Again the lower energy levels discretize more and more while getting the thermo-

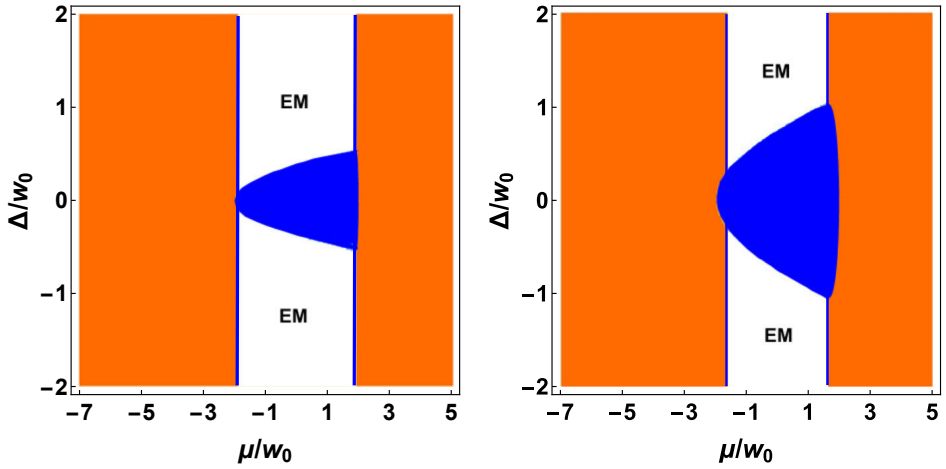

(a) Long ranged pairing: $\alpha = 1.3 \quad \varphi = \pi/10$ (b) Long ranged pairing: $\alpha = 1.3 \quad \varphi = \pi/5$

Figure 7.10: TPD for $\alpha = 1.3$ in the case of only long range in paring with BTR symmetry, $\varphi = \pi/10, \pi/5$. TI ν has been addressed. White region corresponds to $\nu = -1$ and the orange one to $\nu = 1$. Although for $\nu = -1$ we can say that edge modes appear, this is not the case for the $\nu = 1$. In the right side $\nu = 1$ zones there is no edge mode but, in the left zones mass scaling does not converge up to $N \sim 10^4$, thus no information can be gotten. As φ increases non trivial phase reduces. Blue regions are critical regions where gap closes.

dynamic limit.

7.3.2 Long Ranged Hopping and Pairing Together: TR and BTR Symmetry

It is immediate to consider long ranged pairing and hopping together as done in [79]. We propose TPD showing the trend of topological invariants and edge modes. Also in this case TI are not always able to show the crossing from massless to massive edge modes and viceversa.

Time Reversal Case

For TR symmetry, winding number in (6.9) is really difficult to numerically integrate because of non analyticity in $\kappa = 0$ for $\alpha < 1$ thus, also for TRS Hamiltonian, we use ν as TI in Figure 7.11. Again we find massive and massless edge modes for $\alpha < 1$. Their presence has been proved by operating mass and gap scaling for

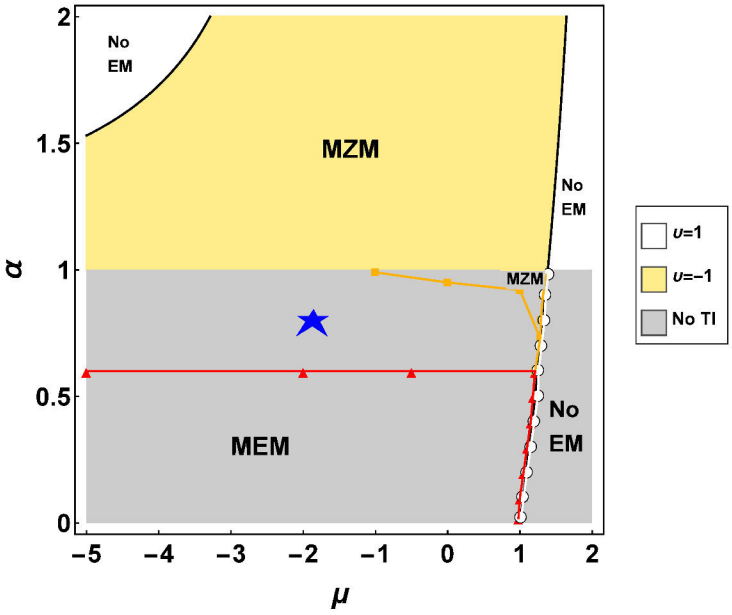

Figure 7.11: TPD for the case of both long range in hopping and paring regime under TR symmetry. TI delineates the separation between trivial and non trivial topological phases only for $\alpha > 1$. The crossing from massless to massive edge modes as well as the crossing between No edge modes phase to MZM or MEM phase can be checked only by mass ad energy gap scaling for each point of TPD. Again in the region signed by the star, gap scalings do not easily converge and we do not know in there are edge modes. Other state parameters have been chosen to be $\Delta = 2w_0$

each point reported in Figure 7.11. Then, for $\alpha > 1$, ν can well characterize the topological phase, showing the presence of MZM and trivial states.

Broken Time Reversal Case

Again we address two different kinds of time reversal symmetry breaking: at first we assume non null phase for the hopping term as $\varphi_l = \varphi_0$ and then we assume $\varphi_l = \varphi_0 l$. About the first case, breaking TRS has the effect to gradually delete the topological phase for $\alpha > 1$ but MEM and MZM, for $\alpha < 1$, show resistance against the growing of φ_0. This last behaviour is different from the one observed in the case of only long range in pairing where for instance MEM are rapidly destroyed in this region. Finally edge modes completely disappear for $\varphi = \pi/2$ as we aspected.

It is also interesting to refer the case $\varphi_l = \varphi_0 l$. In this scenario, as showed in Figure 7.12, MEM and MZM are found in the region $\alpha < 1$. However that gap and mass scaling are difficult to perform in this regime for small value of μ. Convergence to fixed value for mass and gap are not gotten also by means of simulations with ten thousand lattice points, thus it is good to explore this region in future works. Finally we underline that MZM are rapidly destroyed for small values of μ, $\mu \leq -3$ and $\alpha > 1$.

For some example of mass and gap scaling about this latter case, see Figure 7.13. Again the the interpolation for the mass scaling graphics has been done by running a "Mathematica" command thus, it gives only a qualitative trends. If the mass becomes smaller and smaller while $N \to \infty$ and the raport between two consecutive values, at different N, does not converge to 1, we are quite sure that such value goes to zero. When the raport converge to 1 than we are quite sure that a non null value for the mass is obtained and the thermodynamic limit has been achieved. As we can see that, according to the state parameters, the thermodynamic limit is obtained at different high values of N.

7.4 MZMs Wave Functions

In this section we will investigate MZMs wave functions. We will obtain the modes of zero energies in the thermodynamic limit (infinite lattice sites in a wire of length $L = Na$ where a is the lattice step set equal to one $a = 1$) or when such number is finite. In this way we hope to generalize the discussion about the first neighbors model done in [5]. Each result that we will give has been supported by numerical calculations in diagonalizing H_0.

At first we will point out the main features of the generic formalism. We can write

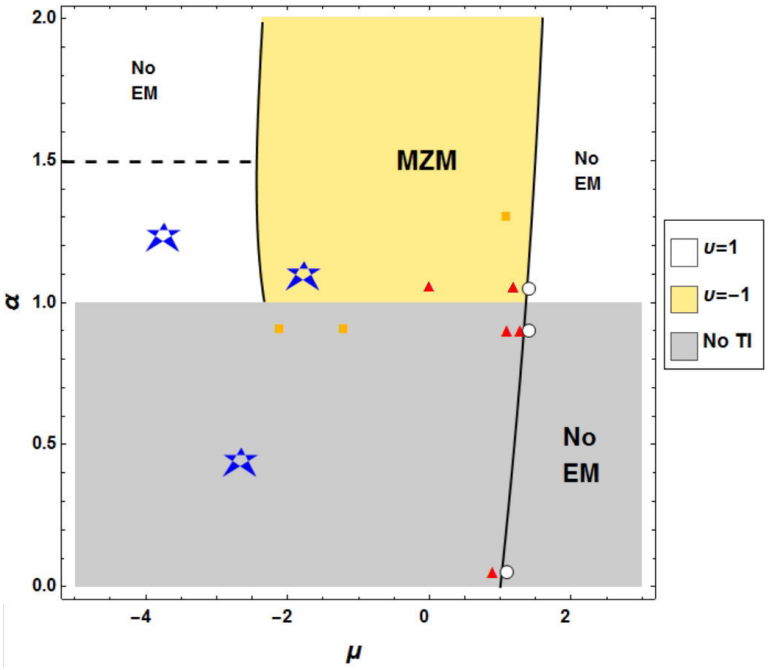

Figure 7.12: Here long range in both hopping and pairing and BTR regime with $\varphi_l = l\pi/4$. The left and right side critical lines are respectively given by $\kappa = 0$ and π. As μ decreases, thermodynamic limit is not gained numerically. Energy gaps between levels do not converge to fixed values also for $N = 9000$ lattice sites. Again $\Delta = 2w_0$

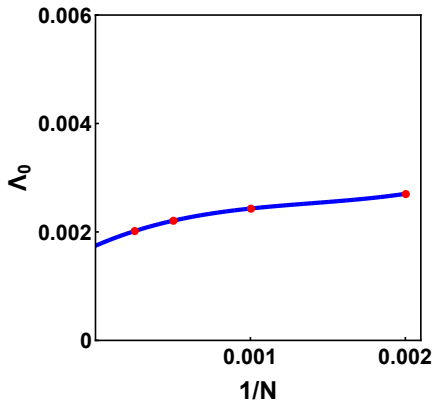

(a) Mass scaling - $\mu = 1.3$, $\alpha = 0.9$ and $\varphi_0 = \pi/10$

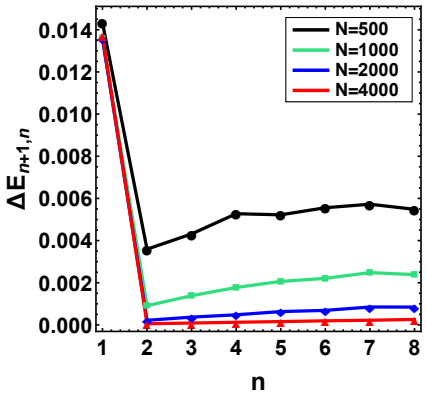

(b) Gap scaling - $\mu = 1.3$, $\alpha = 0.9$ and $\varphi_0 = \pi/10$

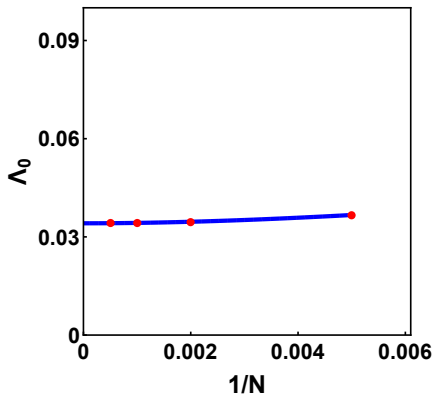

(c) Mass scaling - $\mu = 1.4$, $\alpha = 0.9$ and $\varphi_0 = \pi/10$

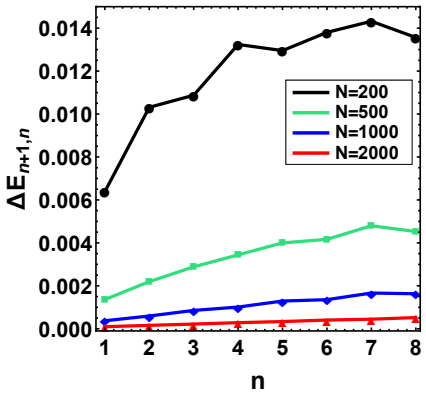

(d) Gap scaling - $\mu = 1.4$, $\alpha = 0.9$ and $\varphi_0 = \pi/10$

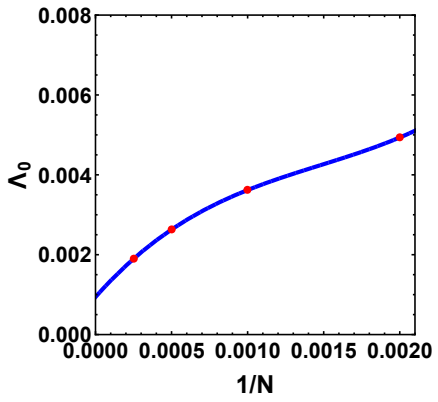

(e) Mass scaling - $\mu = 1.2$, $\alpha = 1.05$ and $\varphi_0 = \pi/10$

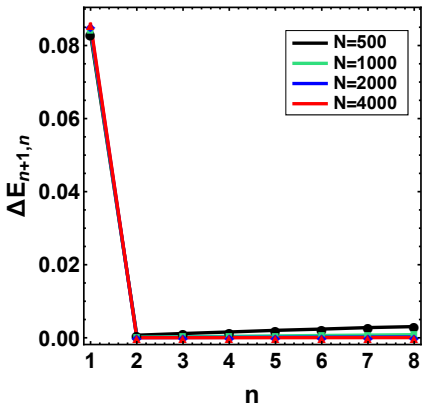

(f) Gap scaling - $\mu = 1.2$, $\alpha = 1.05$ and $\varphi_0 = \pi/10$

Figure 7.13: Mass and gap scaling to evidence the presence of MEM as well as topologically trivial modes in the TPD for long range hopping and paring regime in BRT symmetry with $\varphi_l = l\pi/10$ for three points in Figure 7.12. Calculating the reports between the masses at different lengths of the chain we have that in Figure 7.13(a) and Figure 7.13(e) they tend to 1 as the modes were massive. For sure we have edge mode as the gaps are well in evidence for them.

our H in terms of Majorana operators, defined as:

$$\begin{cases} c_{2j-1} = a_j + a_j^\dagger \\ c_{2j} = \frac{1}{i}\left(a_j - a_j^\dagger\right) \end{cases} \tag{7.8}$$

with

$$\begin{cases} \{c_l, c_m\} = 2\delta_{l,m} & \forall\, l, m = 1, \dots, N \\ c_j^\dagger = c_j & \forall\, j = 1, \dots, 2N \end{cases} \tag{7.9}$$

Thus:

$$\begin{aligned} H = & \\ & = \begin{pmatrix} a_1 & \dots & a_N & a_1^\dagger & \dots & a_N^\dagger \end{pmatrix} H_0 \begin{pmatrix} a_1 \\ \vdots \\ a_N \\ a_1^\dagger \\ \vdots \\ a_N^\dagger \end{pmatrix} \\ & = \frac{i}{2}\Bigg\{ \sum_j \Bigg[(-\mu) c_{2j-1}c_{2j} + \sum_{l=1}^{r} (-w_0) l^{-\alpha} \\ & \qquad \Big(\sin(\varphi)\big(c_{2j-1}c_{2(j+l)-1} + c_{2j}c_{2(j+l)}\big) \\ & \qquad + \cos(\varphi)\big(c_{2j-1}c_{2(j+l)} - c_{2j}c_{2(j+l)-1}\big) \\ & \qquad + |\Delta|\big(c_{2j-1}c_{2(j+l)} + c_{2j}c_{2(j+l)-1}\big)\Big) \Bigg] \Bigg\} \\ & = i \sum_{s,t} c_s A_{s,t} c_t \end{aligned} \tag{7.10}$$

The matrix H_0 is hermitian ($H_0^\dagger = H_0$) and it can be diagonalized by means of unitary transformations:

$$U H_0 U^\dagger = \begin{pmatrix} \epsilon_1 & 0 & \dots & 0 \\ 0 & \ddots & 0 & \dots \\ \vdots & \ddots & -\epsilon_1 & \ddots \\ 0 & \dots & 0 & \ddots \end{pmatrix}_{2N \times 2N}$$

The right side of the above equation is due to the particle-hole symmetry of the Hamiltonian, $C^{-1} H_0 C = -H_0$ where $C = k(\sigma_x)_{2N\text{x}2N}$ and k is the complex

conjugation operator. On the other hand the operator A, in the last passage of eqn. 7.10, is real and antisymmetric so that:

$$WAW^T = diag_\lambda \begin{pmatrix} 0 & \epsilon_\lambda \\ -\epsilon_\lambda & 0 \end{pmatrix}$$

where $\{\pm\epsilon_\lambda\}$ are eigenvalues of H_0 (the set of A's eigenvalues is $\{\pm i\epsilon_\lambda\}$) and W is a real orthogonal matrix: $WW^T = W^TW = \mathbb{I}$ [67].
U and W are transformations which respectively transform the sets $\{a_j, a_j^\dagger\}_{j=1}^N$ and $\{c_j\}_{j=1}^{2N}$:

$$\begin{pmatrix} \tilde{a}_1 \\ \vdots \\ \tilde{a}_N \\ \tilde{a}_1^\dagger \\ \vdots \\ \tilde{a}_N^\dagger \end{pmatrix} = U^\dagger \begin{pmatrix} a_1 \\ \vdots \\ a_N \\ a_1^\dagger \\ \vdots \\ a_N^\dagger \end{pmatrix} \qquad \begin{pmatrix} b_1 \\ \vdots \\ b_{2N} \end{pmatrix} = W \begin{pmatrix} c_1 \\ \vdots \\ c_{2N} \end{pmatrix} \tag{7.11}$$

Diagonal form of H, written by means of Dirac fermion or Majorana operators, is:

$$H = \sum_n \epsilon_n \left(\tilde{a}_n^\dagger \tilde{a}_n - \frac{1}{2} \right) = \frac{i}{2} \sum_n \epsilon_n b_{2n-1} b_{2n} \tag{7.12}$$

Assuming that U and W are canonical we have:

$$\left\{ \tilde{a}_n^\dagger, \tilde{a}_m \right\} = \delta_{n,m} \quad \text{and} \quad \{\tilde{a}_n, \tilde{a}_m\} = 0 \,\forall\, n, m = 1, \ldots, N$$
$$\left\{ b_n^\dagger, b_m \right\} = 2\delta_{n,m} \,\forall\, n, m = 1, \ldots, 2N$$

The two sets above are linked by:

$$\begin{cases} b_{2n-1} = \tilde{a}_n + \tilde{a}_n^\dagger \\ b_{2n} = \frac{1}{i} \left(\tilde{a}_n - \tilde{a}_n^\dagger \right) \end{cases}$$

Now, in our case, H is always quadratic and it can be diagonalized by means of Bogoliubov transformations; the matrix U is the Bogoliubov transformations matrix. We can think to write the new $\tilde{a}_n$s as a combination of the first set of operators a_j by means of two sets of functions $\{u_{n,j}\}$ and $\{v_{n,j}\}$:

$$\tilde{a}_n = \sum_{j=1}^N \left(u_{n,j}^* a_j + v_{n,j}^* a_j^\dagger \right) \tag{7.13}$$

with $\sum_{j=1}^{N}\left(|u_{n,j}|^2+|v_{n,j}|^2\right)=1\,\forall\, n=1,\dots,N$. Thus we write $U^\dagger$ as:

$$U^\dagger=\begin{pmatrix} u^*_{1,1} & \dots & u^*_{1,N} & v^*_{1,1} & \dots & v^*_{1,N}\\ \vdots & & \vdots & \vdots & & \vdots\\ u^*_{N,1} & \dots & u^*_{N,N} & v^*_{N,1} & \dots & v^*_{N,N}\\ v_{1,1} & \dots & v_{1,N} & u_{1,1} & \dots & u_{1,N}\\ \vdots & & \vdots & \vdots & & \vdots\\ v_{N,1} & \dots & v_{N,N} & u_{N,1} & \dots & u_{N,N}\end{pmatrix} \tag{7.14}$$

and by means of eq. (7.11) and canonical transformations assumption we can link W to U:

$$\begin{cases} W_{2n-1,2j-1} &= \frac{1}{2}\left(u_{n,j}+u^*_{n,j}+v_{n,j}+v^*_{n,j}\right)\\ W_{2n-1,2j} &= \frac{i}{2}\left(-u_{n,j}+u^*_{n,j}+v_{n,j}-v^*_{n,j}\right)\\ W_{2n,2j-1} &= \frac{i}{2}\left(u_{n,j}-u^*_{n,j}+v_{n,j}-v^*_{n,j}\right)\\ W_{2n,2j} &= \frac{1}{2}\left(u_{n,j}+u^*_{n,j}-v_{n,j}-v^*_{n,j}\right)\end{cases} \tag{7.15}$$

or viceversa:

$$\begin{cases} u^*_{n,j}=\frac{1}{2}\Big(W_{2n-1,2j-1}+W_{2n,2j}+i\big(W_{2n,2j-1}-W_{2n-1,2j}\big)\Big)\\ v^*_{n,j}=\frac{1}{2}\Big(W_{2n-1,2j-1}-W_{2n,2j}+i\big(W_{2n,2j-1}+W_{2n-1,2j}\big)\Big)\end{cases} \tag{7.16}$$

In eqns. (7.15), if we assume TR symmetry, then $W_{2n,2j-1}=0$ and $W_{2n-1,2j}=0$; in this case we will call $\phi_{n,j}=W_{2n-1,2j-1}$ and $\psi_{n,j}=W_{2n,2j}$ for next developments. Looking for MZMs, we are interested in spectrums with null energies, so in systems with degenerate ground states. Such modes can be obtained in two different situations, in the first case they are modes appearing in the thermodynamic limit, in the second case (for particular parametric regimes) they can be observed with finite lattice number of fermions. In the following sections we will analyze these two cases.

7.4.1 MZMs Wave Functions in the Thermodynamic Limit

We will now take a picture of MZMs wave functions via transfer matrix approach. We will compare the results with the ones of numerical calculations for the eigenstates of H_0. We will write Bogoliubov equations for the system and check for the existence of MZMs in the thermodynamic limit thus eliminating the system's finite size effects. When these effects are present we have non null energy states and non degenerate even ground state for the system. The condition of zero energy

will be obtained in the limit $N \to \infty$ and $a \to 0$ with L constant that is the thermodynamic limit. Developing Bogoliubov formalism in terms of W's elements, we have:

$$\begin{aligned}
\epsilon_n W_{2n-1,2j-1} = \\
&= (-\mu) W_{2n,2j} + \sum_{l=1}^{r} l^{-\alpha} \Bigg[(-w_0) \cos(l\varphi) \\
&\quad \left(W_{2n,2(j+l)} + W_{2n,2(j-l)} \right) \\
&\quad + (-w_0) \sin(l\varphi) \left(W_{2n,2(j+l)-1} + W_{2n,2(j-l)-1} \right) \\
&\quad + |\Delta| \left(W_{2n,2(j+l)} + W_{2n,2(j-l)} \right) \Bigg]
\end{aligned} \tag{7.17a}$$

$$\begin{aligned}
\epsilon_n W_{2n-1,2j} = \\
&= \mu W_{2n,2j-1} + \sum_{l=1}^{r} l^{-\alpha} \Bigg[w_0 \cos(l\varphi) \\
&\quad \left(W_{2n,2(j-l)-1} + W_{2n,2(j+l-1)} \right) \\
&\quad + w_0 \sin(l\varphi) \left(W_{2n,2(j-l)} + W_{2n,2(j+l)} \right) \\
&\quad - |\Delta| \left(W_{2n,2(j-l)-1} - W_{2n,2(j+l)-1} \right) \Bigg]
\end{aligned} \tag{7.17b}$$

$$\begin{aligned}
\epsilon_n W_{2n,2j-1} = \\
&= \mu W_{2n,2j-1} + \sum_{l=1}^{r} l^{-\alpha} \Bigg[w_0 \cos(l\varphi) \\
&\quad \left(W_{2n-1,2(j+l)} + W_{2n-1,2(j-l)} \right) \\
&\quad + \sin(l\varphi) w_0 \left(W_{2n,2(j+l)-1} - W_{2n-1,2(j-l)-1} \right) \\
&\quad + |\Delta| \left(W_{2n,2(j+l)} + W_{2n,2(j-l)} \right) \Bigg]
\end{aligned} \tag{7.17c}$$

$$\begin{aligned}\epsilon_n W_{2n,2j} = \\ &= (-\mu) W_{2n-1,2j-1} + \sum_{l=1}^{r} l^{-\alpha} \Bigg[(-w_0)\cos(l\varphi) \\ &\quad \left(W_{2n-1,2(j-l)-1} + W_{2n-1,2(j+l)-1}\right) \\ &\quad + (-w_0)\sin(l\varphi)\left(W_{2n-1,2(j-l)} - W_{2n-1,2(j+l)}\right) \\ &\quad + |\Delta|\left(W_{2n-1,2(j-l)-1} - W_{2n-1,2(j+l)-1}\right)\Bigg]\end{aligned} \tag{7.17d}$$

Resolution Via Transfer Matrix for TR Symmetry

For $\varphi = 0$, thus if Hamiltonian is time reversal, terms $W_{2m-1,2i} = W_{2m,2i-1} = 0$ and then, for $\epsilon_n = 0$, $W_{2m,2i}$ and $W_{2m-1,2i-1}$ decouple. Such is the case that we will approach. Using $\phi_{n,j}$ to indicate $W_{2n-1,2j-1}$ and $\psi_{n,j}$ for $W_{2n,2j}$ and considering that we can have several MZMs per edge (r at maximum), we can write:

$$\phi^{(0)}(j) = \sum_{l=1}^{\#(MZM\,per\,edge)} C_l \phi_{l,j} \tag{7.18a}$$

$$\psi^{(0)}(j) = \sum_{l=1}^{\#(MZM\,per\,edge)} D_l \psi_{l,j} \tag{7.18b}$$

where $\phi_{l,j}$ and $\psi_{l,j}$ are indipendent and $\phi^{(0)}(j)$ and $\psi^{(0)}(j)$ are the general superposition wave functions of such independent zero modes. These latter satisfy:

$$\begin{pmatrix} \phi^{(0)}(i+r) \\ \vdots \\ \phi^{(0)}(i-r+1) \end{pmatrix} = T \begin{pmatrix} \phi^{(0)}(i+r-1) \\ \vdots \\ \phi^{(0)}(i-r) \end{pmatrix} \tag{7.19a}$$

$$\begin{pmatrix} \psi^{(0)}(i-r) \\ \vdots \\ \psi^{(0)}(i+r-1) \end{pmatrix} = T \begin{pmatrix} \psi^{(0)}(i-r+1) \\ \vdots \\ \psi^{(0)}(i+r) \end{pmatrix} \tag{7.19b}$$

where

$$T = \begin{pmatrix} -\frac{\Delta_{r-1}+w_{r-1}}{\Delta_r+w_r} & \dots & -\frac{\mu}{\Delta_r+w_r} & \dots & \frac{\Delta_r-w_r}{\Delta_r+w_r} \\ 1 & 0 & \dots\dots\dots\dots & & 0 \\ 0 & 1 & 0 & \dots & \vdots \\ \vdots & \dots & \ddots & \ddots & 0 \\ 0 & \dots\dots\dots\dots & & 1 & 0 \end{pmatrix} \tag{7.20}$$

Generic solutions of (7.19) can be also written as:

$$\phi^{(0)}(j) = \sum_{s=1}^{2r} \alpha_s \lambda_s^j \tag{7.21a}$$

$$\psi^{(0)}(j) = \sum_{s=1}^{2r} \beta_s \lambda_s^{-j} \tag{7.21b}$$

where λ_s are eigenvalues of T (transfer matrix), coefficients α_s and β_s are independent and $j = 1, \ldots, N$.
It is important to note that such modes have to underline to OBC:

$$\begin{aligned} &\phi^{(0)}(0) = \cdots = \phi^{(0)}(1-r) = 0 \\ &\phi^{(0)}(N+1) = \cdots = \phi^{(0)}(N+r) \end{aligned} \tag{7.22a}$$

$$\begin{aligned} &\psi^{(0)}(0) = \cdots = \psi^{(0)}(1-r) = 0 \\ &\psi^{(0)}(N+1) = \cdots = \psi^{(0)}(N+r) \end{aligned} \tag{7.22b}$$

As we will see, all the OBC in (7.22) will be satisfied only in the thermodynamic limit.
For find the zero mode wave function we will proceed as follows. Assuming that the majority of the λ_l is such that $|\lambda_l| < 1$, we consider the modes ϕ_l localize at the left edge of the wire, thus also the ϕ_l modes localized at the opposite edge. Among eqns. (7.22) we take:

$$\phi(0) = \cdots = \phi(1-r) = 0 \tag{7.23a}$$

$$\psi(N+1) = \cdots = \psi(N+r) \tag{7.23b}$$

and verify the existence of generic zero energy modes solving eqns. (7.19) for $\phi^{(0)}$ and $\psi^{(0)}$, written in the form (7.21), counting only λ_l smaller than one in modulus, and underlying to eqns. (7.23). Following [56] we will call n_f the number of T's eigenvalues whose modules are smaller than one and r is the number of conditions we impose "per edge" on each one of $\phi^{(0)}$ and $\psi^{(0)}$. Thus we will have $\mathcal{N} = n_f - r$ linear independent zero modes in each side of the wire; i.e. the generic solutions in (7.21) will have $\mathcal{N}$ free parameters. The final writing will be of the form reported in eqns. (7.18). The λ_l greater than one in modulus has been not taken in consideration for the linear combinations eqns. (7.21) since it would be impossible to satisfy the normalization conditions for the wave functions.
In the opposite case, when the majority of λ_l is s.t. $|\lambda_l| > 1$, we can repeat the same procedure considering $\mathcal{N}' = n' - r$ MZM per edge with n' being the number of T's eigenvalues whose modules is greater than one, but imposing $\phi(N+1) =$

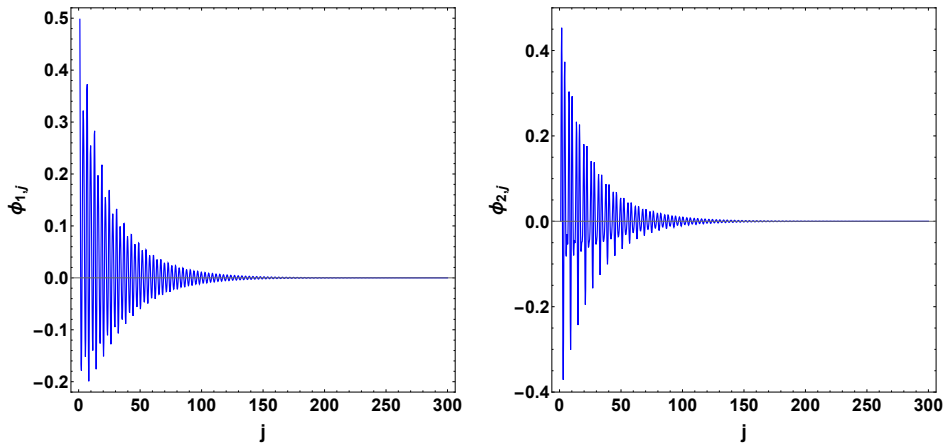

(a) $\phi_{1,j}$ (b) $\phi_{2,j}$

Figure 7.14: $\phi_{1-2,j}$ obtained by numerical calculations following the protocol explained in 7.4.1. We used $N = 150$, $\alpha = \beta = 0$, $r = 2$, and $\mu/|\Delta| = w/|\Delta| = 0.1$. In this regime we have two MZM per edge. The above functions are in the "left side" of the wire. Note $\phi_{1,j}$ is peaked on $j = 1$ but, $\phi_{2,j}$ is a bit shifted. We will obtain a similar result in section 7.4.2, where two MZM per edge are found on a finite sites lattice. The same situation is found considering generic r.

$\cdots = \phi(N+r) = 0$ and $\psi(0) = \cdots = \psi(1-r)$ instead of eq. (7.23). In both cases $\mathcal{N}$ or $\mathcal{N}'$ have to be positive. Furthermore, we will focus on the form of these wave functions. Because of the nature of T's eigenvalues, i.e. whether they are real or complex, we can have a simple decaying trend of MZM or an oscillatory decaying one. Indeed if at least one couple of λ_l is complex (complex roots have to come in pair) they will give an oscillatory decreasing of $\phi(j)$ and $\psi(j)$, which will take into account terms like:

$$\begin{aligned} \lambda_1^j + \lambda_2^j = \lambda_1^j + (\lambda_1^*)^j & \\ = |\lambda_1|^j (e^{i\theta_1 j} + e^{-i\theta_1 j}) & \\ = 2|\lambda_1|^j \cos(\theta_1 j) & \quad (7.24) \end{aligned}$$

If each considered λ_l is real, then MZM wave functions will only show a decaying trend - like λ_l^j. This result is analogue to the one in [74]. The last step of this protocol will be underlining that the ϕ_l and ψ_l that we get by the above procedure are not orthogonal and normalized. Thus we can proceed via Gramm-Smidth orthonormalization process.

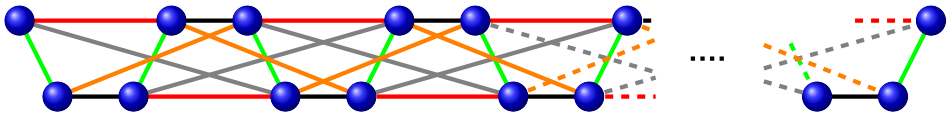

Figure 7.15: General second neighbors Hamiltonian (7.26). Gray and orange lines represent the second neighbors potentials, respectively $\Delta_2 - w_2$ and $\Delta_2 + w_2$. If both Δ_2 and w_2 are null the graph reduces to the Kitaev chain toy model.

7.4.2 Finite Length Lattice MZMs for r-Neighboring Interactions Hamiltonian

In [5] it is shown that we can have unpaired MZM also if lattice size is finite. We will generalize this result to r neighbors Kitaev Hamiltonian. We will work in TR regime. Hamiltonian of such system (OBC) written in terms of Majorana operators is:

$$H = \frac{i}{2}\Bigg[\sum_{j=1}^{N}(-\mu)c_{2j-1}c_{2j} + \sum_{l=1}^{r}\sum_{j=1}^{N-r}\Big((\Delta_l - w_l)c_{2j-1}c_{2j+2l} + (\Delta_l + w_l)c_{2j}c_{2j+2l-1}\Big)\Bigg] \tag{7.25}$$

Parameters w_l and Δ_l can take whatever value. First we will find such unpaired Majorana modes for the case $r = 2$ and then we will generalize it to r neighbors case. In this situation we have:

$$H = \frac{i}{2}\Bigg[\sum_{j=1}^{N}(-\mu)c_{2j-1}c_{2j} + \sum_{j=1}^{N-1}\Big((\Delta_1 - w_1)c_{2j-1}c_{2j+2} + (\Delta_1 + w_1)c_{2l}c_{2j+1}\Big) + \sum_{j=1}^{N-2}\Big((\Delta_2 - w_2)c_{2j-1}c_{2j+4} + (\Delta_2 + w_2)c_{2j}c_{2j+3}\Big)\Bigg] \tag{7.26}$$

We directly delete the contribute of some c_j if

- $\Delta_2 = \pm w_2 \neq 0$ and $\Delta_1 = w_1 = \mu = 0$
- $\mu = 0$, $\Delta_1 = \pm w_1 \neq 0$ and $\Delta_2 = \pm w_2 \neq 0$

Let us focus on these two cases separately and assume a positive hopping term w_2. In the first case Hamiltonian reduces to:

$$H = \sum_{j=1}^{N-2} i w_2 c_{2j} c_{2j+3} \tag{7.27}$$

now defining

$$\begin{cases} \tilde{a}_j = \frac{1}{2}\left(c_{2j} + i c_{2j+3}\right) \\ \tilde{a}_j^\dagger = \frac{1}{2}\left(c_{2j} - i c_{2j+3}\right) \end{cases} \quad \text{for} \quad j = 1, \ldots, N-2 \tag{7.28}$$

and

$$\begin{cases} \tilde{a}_{N-1} = \frac{1}{2}\left(c_3 + i c_{2L-2}\right) \\ \tilde{a}_{N-1}^\dagger = \frac{1}{2}\left(c_3 - i c_{2L-2}\right) \end{cases} \quad \text{and} \quad \begin{cases} \tilde{a}_N = \frac{1}{2}\left(c_1 + i c_{2L}\right) \\ \tilde{a}_N^\dagger = \frac{1}{2}\left(c_1 - i c_{2L}\right) \end{cases} \tag{7.29}$$

we have a whole set $\{\tilde{a}_j\}_{j=1}^N$ of Dirac fermions operators satisfying Fermi-Dirac algebra:

$$\left\{\tilde{a}_i, \tilde{a}_j^\dagger\right\} = \delta_{i,j} \quad \text{and} \quad \left\{\tilde{a}_i, \tilde{a}_j\right\} = \left\{\tilde{a}_i^\dagger, \tilde{a}_j^\dagger\right\} = 0 \tag{7.30}$$

For all $i, j = 1, \ldots, N$ that diagonalize H in (7.26).
Calling $|\tilde{0}\rangle$ the Fock state for where no quasi-particle is present, the vacuum state, we have:

$$\tilde{a}_j|\tilde{0}\rangle = 0 \,\forall\, j = 1, \ldots, N \quad \text{and} \quad \tilde{a}_j^\dagger|0_j\rangle = |1_j\rangle \tag{7.31}$$

thus the Hamiltonian has the form:

$$H = 2w_2 \sum_{j=1}^{N-2} \left(\tilde{a}_j^\dagger \tilde{a}_j - \frac{1}{2}\right) \tag{7.32}$$

It is important to note that eq. (7.32) and (7.27) do not contain respectively terms proportional to $\tilde{a}_{N-1,N}^\dagger \tilde{a}_{N-1,N}$ and $(-i)b_{1,3}b_{N,N-2}$. Terms missing in eq. (7.27), $(-i)b_{1,3}b_{2N,2(N-1)}$, are four Majorana zero modes which are unpaired (see Figure 7.4.2); the topological phase is non-trivial.

We will show that the ground state degeneracy goes as $2^2 = 4$. At first we will define $|gs\rangle$ to be ground state if and only if:

$$\tilde{a}_j|gs\rangle = 0 \,\forall\, j = 1, \ldots, N-2 \tag{7.33}$$

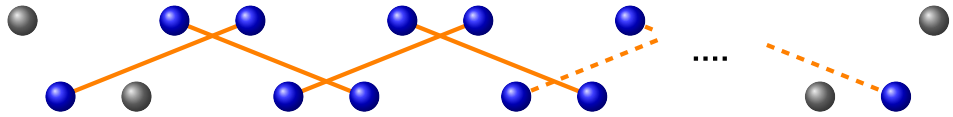

Figure 7.16: In this regime only terms proportional to $\Delta_2 + w_2 = 2w_2$ survive. All the links in the network disappear and the system is equivalent to $N-2$ noninteracting Dirac fermions made by two MFs of opposite chains. Such fermion's site energy is just $2w_2$. The four unpaired MFs are zero energy modes and all the rest of the states are degenerate with energies $2w$ or $-2w$.

Then we define P, the parity operator, as:

$$\begin{aligned} P &= \prod_{i=1}^{N}(-ic_{2j-1}c_{2j}) = (-ic_1c_2)\dots(-ic_{2N-1}c_{2N}) \\ &= (-ic_2c_5)(-ic_4c_7)\dots(-ic_3c_{2L-2})(-ic_1c_{2N}) \\ &= \prod_{i=1}^{N} P_j = \bigotimes_{j=1}^{N}\sigma_z^{(j)} \end{aligned} \tag{7.34}$$

P_j in eq. (7.34) counts the number of fermions (quasi-particles) that are in the j-th fermionic subspace. Note that in eq. (7.27) terms proportional to P_{N-1} and P_N miss and thus $[P_{N-1}P_N, H] = [P, H] = 0$; $P_{N-1}P_N$ and H have the same eigenstates.
There are fours states $|\psi\rangle$ diagonalizing $P_{N-1}P_N$: two states with one fermion either in the (N-1)-th or in the N-th subspace, another one with one fermion in both subspaces and the vacuum state. Indeed:

$$\begin{aligned} P_{N-1}P_N|\tilde{0}\rangle = & \\ &= 2\left(\frac{1}{2} - \tilde{a}^\dagger_{N-1}\tilde{a}_{N-1}\right)2\left(\frac{1}{2} - \tilde{a}^\dagger_{N}\tilde{a}_{N}\right)|\tilde{0}\rangle \\ &= |\tilde{0}\rangle \end{aligned} \tag{7.35a}$$

$$\begin{aligned} P_{N-1}P_N|1_{N-1,N}\rangle = & \\ &= 2\left(\frac{1}{2} - \tilde{a}^\dagger_{N-1}\tilde{a}_{N-1}\right)2\left(\frac{1}{2} - \tilde{a}^\dagger_{N}\tilde{a}_{N}\right) \\ &\quad \tilde{a}^\dagger_{N-1,N}|\tilde{0}\rangle \\ &= -|1_{N-1,N}\rangle \end{aligned} \tag{7.35b}$$

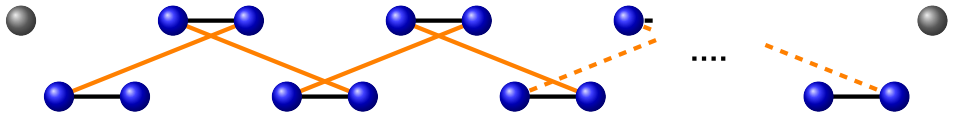

Figure 7.17: The above system is equivalent to a chain of $2N-2$ Majorana fermions interacting whit their first neighbors by alternate potentials, $\Delta_1 + w_1 = 2w_1$ and $\Delta_2 + w_2 = 2w_2$ plus two unpaired MFs at the ends of the chain.

$$\begin{aligned} P_{N-1}P_N|1_{N-1},1_N\rangle = \\ &= 2\left(\frac{1}{2} - \tilde{a}^\dagger_{N-1}\tilde{a}_{N-1}\right) 2\left(\frac{1}{2} - \tilde{a}^\dagger_N\tilde{a}_N\right) \\ &\quad \tilde{a}^\dagger_{N-1}\tilde{a}^\dagger_N|\tilde{0}\rangle \\ &= |1_{N-1},1_N\rangle \end{aligned} \tag{7.35c}$$

$|\tilde{0}\rangle$ and $|1_{N-1}1_N\rangle$ have even parity, $|1_{N-1}\rangle$ and $|1_N\rangle$ have odd parity. Such eigenstates satisfy also:

$$\tilde{a}_j|\tilde{0}\rangle = 0 \tag{7.36a}$$

$$\tilde{a}_j|1_{N-1,N}\rangle = -\tilde{a}^\dagger_{N-1,N}\tilde{a}_j|\tilde{0}\rangle = 0 \tag{7.36b}$$

$$\tilde{a}_j|1_{N-1},1_N\rangle = -\tilde{a}^\dagger_{N-1}\tilde{a}^\dagger_N\tilde{a}_j|\tilde{0}\rangle = 0 \tag{7.36c}$$

for each $j = 1, 2, \ldots, 2(N-1)$.
They are all ground states of the Hamiltonian; the system has four degenerate ground states. The subspace in which they live is made by a bidimensional even parity and a bidimensional odd parity subspace. This configuration is equivalent to a situation counting two second neighbors separated Kitaev chain each one showing one unpaired Majorana modes per edge. Considering r neighbors Hamiltonian we can say that having $\mu = \Delta_1 = w_1 = \cdots = \Delta_{r-1} = w_{r-1} = 0$ and $\Delta_r = w_r$ is equivalent to counting r separated and non interacting first neighbors Kitaev chains. Taking into account other non null w_l and Δ_l could mean letting these separated chains interact linking also some unpaired c_j we had before and thus such MZMs will disappear.

We will now look at the case $\mu = 0$, $\Delta_1 = w_1 \neq 0$ and $\Delta_2 = w_2 \neq 0$. In this regime only one unpaired Majorana fermion per edge is present (see Figure 7.17). It is important to also look at the system for an algebraic point of view.

Hamiltonian, in this regime, becomes:

$$\begin{aligned} H &= 2w_1 \sum_{j=1}^{N-1} c_{2j}c_{2j+1} + 2w_2 \sum_{j=1}^{N-2} c_{2j}c_{2j+3} \\ &= \underbrace{(-1)^{N-1}(2w_1) \sum_{j=1}^{N-1} c_{2j+1}c_{2j}}_{H^{(1)}} \\ &\quad + 2 \left(\underbrace{w_2 \sum_{j=1}^{N-2} c_{2j}c_{2j+3}}_{H^{(2)}} \right) \\ &= H^{(2)} + H^{(2)} + H^{(1)} \end{aligned} \tag{7.37}$$

$H^{(1)}$, the term counting first neighboring interactions between c_j, plays the role of an interacting potential between two split wires. The system becomes equivalent to one chain of MFs where each MF interacts with its neighbors with alternating potential $2w_1$ and $2w_2$. Otherwise it can be seen as two separated Dirac fermions chains ($2H^{(2)}$) interacting one with each other by the term $H^{(1)}$. Eqn. (7.37) is yet singular and two unpaired MFs are present in this regime. Generalizing such result and considering r neighbors interacting chains, we can have $1, 2, \ldots, r$ unpaired MFs per edge and to know in which state they are localized by the following logic:

- For $\mu = \Delta_1 = w_1 = \cdots = \Delta_{r-1} = w_{r-1} = 0$ and $\Delta_r = w_r \neq 0$ we have r MFs per edge and they are localized in $j = 1, 3, \ldots, 2r-1$ for the left side and in $j = 2N, 2N-2, \ldots, 2N-2r$ for the right side; there are $2r$ unpaired MFs in the chain ($j = 1, \ldots, 2N$). If $\Delta_r = -w_r$ then left and right side MZM flip.

- Choosing the same regime as in the preceding point but now choosing $\Delta_{r-1} = w_{r-1} = 0$ if $\Delta_r = w_r = 0$, or in $\Delta_{r-1} = -w_{r-1} \neq 0$ if $\Delta_r = -w_r \neq 0$, we will lose the innermost unpaired Majorana fermions in the chain; there are $2(r-1)$ unpaired MFs in the chain occupying the same position as before and so on.

- For $\Delta_l = \pm w_l \neq 0$ with $l = 1, \ldots, r$ and $\mu = 0$ we only have one MFs per edge in the chain, localized at the edge of the wire; $j = 1$ and $j = 2N$ if $\Delta_l = w_l$ or $j = 2$ and $j = 2N-1$ if $\Delta_l = -w_l$ ($j = 1, \ldots, 2N$)

Other topological phases are found, in above configurations, if we change the sign of some w_l, respect to Δ_l, in Hamiltonians. These phases show less MZM per edge than the ones itemized. Engineering such Hamiltonians would mean having rich topological phases with finite size lattices. We would also like to underline that for r neighbors chains we can obtain $\#(MZM\,per\,edge) = 1, 2, \ldots, r$ both if r is even and if r is odd.

7.5 Outlooks and conclusions

The goals obtained range from the characterization of appearing and disappearing of topological phase, for finite neighbors interaction chains, to the more general characterization of edge modes for infinitely long ranged Kitaev chains. Both for time reversal and broken time reversal symmetry has been approached.

At first we addressed the regime of finite neighbors and time reversal symmetry. In the case of only long ranged hopping, we found an increase of topological phase as the penetration length of the hopping term goes to infinity, $\xi = \alpha^{-1} \to \infty$. This trend is not intuitive. A similar result was obtained in [80] where an exponential decaying hopping term is assumed and it counts all the neighbors in the chain. We found that the same physics is achieved using an algebraic decaying hopping term and counting a finite number of neighbors for the interaction. Then we have reported that, if only long ranged pairing term, with a finite number of neighbors, is assumed, then the topologically non trivial region is the same as for the standard Kitaev chain. Although it does not change, we observe, inside such region, an alternating of positive and negative values for the winding number, $W = \pm 1$. This alternating trend increases with the number of neighbors taken in consideration for the pairing interaction. At last, assuming broken time reversal symmetry, we obtained the erasure of MZMs in the case we have an even number of such modes per edge. On the other hand we showed that, for an odd number (in our case one MZM per edge), the topological phase is reduced when the parameter φ_0, which induces such breaking, goes to $\pi/2$. These two trends was already predicted in [56]. Here we checked that it happens for both cases $\varphi_l = \varphi_0$ (assumed also in [56]) and $\varphi_l = l\varphi_0$ that we checked here. To assume such parameter, $\varphi_l = l\varphi_0$, allows for a more realistic treatment of the model and, it was not sure that now the condition $varphi_0 = \pi/2$ brought to the disappear of topological phase.
Then we gave the complete set of Bogoliubov equations for getting the general solutions of the system energy spectrum in the case of general broken time reversal symmetry. The simpler case of TR regime is obtained by choosing $\varphi_l = 0$ in such set of equations. We also gave the transformation linking the Majorana and Dirac quasiparticle operators for the canonical Hamiltonian.

Finally we showed how to obtain many MZMs per edge, using finite length chains. Although this is very difficult to improve experimentally, an implementation of such parametric regime can bring to advantages, since we get many topological (strong) states with a minimum overlap and using few lattice sites.

For the case of all neighbors interactions we give topological phase diagrams, recovering preceding and important results but also adding new information about the presence of massive and massless edge modes as well as not localized modes. This has been done for both TR and BTR regimes. The TR case was already addressed in literature but, the characterization by TPD of BTR symmetry is a new argument for such long range regime. In TR regime we have at maximum one MZM per edge. But if we address massive modes, MEMs, after looking at the gaps for the lower energy levels we note that for high penetration length for the hopping term, $\beta^{-1} \to \infty$, such levels are discrete. We have gaps between many levels in the lower region and then, for high enough energy levels, we find the energy band (look at Figure 7.8). When TRS is broken such characteristic disappears. Only one energy gap can be present. We have that the breaking of TR symmetry brings to an erasure of edge modes.
As last result we recall that for infinite long ranged chain, the description of topological phase transition, given only in terms of TI W and ν, seems not to be complete according to the mass and gap scaling we performed. Also if these latter does not change, we have appearing or disappearing of MZMs. A more detailed analysis of such regime is required to fully characterize phase diagrams showing massless or massive edge modes.
To better itemize all these results we present the following two tables in which we resume everything.

FINITE NUMBER OF NEIGHBORS

Time Reversal			**Broken Time Reversal**
Hopping	**Pairing**	**Hopping and Pairing**	**Hopping and Pairing**
We get only 1 MZM per edge for whatever number of neighbors for the interaction we assume. A growth of penetration lengths of the potentials implies that topological phase enlarges in the parameters space.	We get only 1 MZM per edge for whatever number of neighbors for the interaction we assume. We get the same topological phase as in the Kitaev model but, as the penetration length of the pairing term enlarges then the winding number flips between 1 and -1 more and more.	We get more and more MZMs per edge as the penetration lengths of the potentials increases. Such number at maximum equals the number of neighbors counted in the interactions.	Breaking TR symmetry then MZMs survive only if we had an odd number of such modes per edge in the time reversal regime. MZMs completely disappear for $\varphi_0 = \pi/2$.

INFINITE NUMBER OF NEIGHBORS

Time Reversal		**Broken Time Reversal**	
Pairing	**Hopping and Pairing**	**Pairing**	**Hopping and Pairing**
We can get only one MZM per edge thus we see a gap between the lower level and the bulk. Where massive modes are present we can have that many lower energetic levels discretize. We get many gaps. finally MZMs seems to disappear without any changing of topological invariants.	Same physics as for the case of only long range in pairing with infinite neighbors interactions and time reversal symmetry.	Only one level is bulk protected for every kind of edge mode, MZM or MEM. We would have passages from massless to massive edge modes without any change of TI ν. Every edge mode completely disappears for $\varphi_0 = \pi/2$.	Same physics as for the case of only long range in pairing with infinite neighbors interactions and broken time reversal symmetry.

Chapter 8

Single Electron Tunneling Devices

In this last chapter we give at first a general overview of the single electron tunneling process in electronic circuits. If the tunneling charge goes toward a very small component then, the Coulomb blockade regime can be achieved. It happens that the presence of the charge on a component, with very small sizes, allows the charging energy of such component (generally named "island") to prevent the tunneling of another charge carrier. Then we show as it is possible to use one electron tunneling circuits to harvest current from a gradient of temperature, standing between two components of the circuit, using quantum dot islands [82, 83]. Then we will underline the main difference between this latter case and the one in which the islands are made by metallic dots (usually copper). This represents our investigation to this field. Indeed quantum dots are generally made using semiconductors that are difficult to produce. On the other hand copper is easier to find and thus, it is interesting to investigate how one electron tunneling devices works using this kind of islands. Such circuits also represent the basis for further characterization of charge and heat transport including topological wires as components.

8.1 Coulomb Blockade

Single electron tunneling is a phenomenon appearing when, in a circuit, some insulating barrier that block the normal flow of charge carriers. Here after in this section, we assume a configuration such "normal metal-insulator-normal metal". If the insulating barrier is small enough then electrons tunneling is possible. In this case we indicate the component "metal-insulator-metal" as a *tunnel junction*. Furthermore if the size of the second normal metal (toward the electron tunnels) are very small, then also its capacitance C is reduced (generally to $C \sim 10^{-15}F$) and this allows for high charging energy E_c for such island. It happens that the

presence of an excess electron on the island generates a so high repulsive potential (that is charging energy $E_c \propto e^2/(2C)$ where C is the island selfcapacitance) that it blocks the tunneling of the other electrons. Usually the magnitude of such charging energy is found to be $E_c \sim 10^{-4}eV$. You can note that here we deal with the tunnel junctions as they were effective capacitors. This physical scenario is called *Coulomb blockade* and it is formally defined by the three following conditions [84]:

- The bias voltage V_{bias}, that moves the electron toward the island, must be small compared to the electron charge divided by the selfcapacitance C of the island, i.e. $V_{bias} < e/C$.
- $E_c >> kT$ that is, thermal fluctuations cannot allow the electron to flow into the island if this latter is already occupied
- The tunnelling resistance, R_T, that can be seen as a characteristic resistance of the device seen as a (quantum) capacitor in charge, must be great compared to the quantum resistance $R_Q = h/e^2(\ 26K\Omega)$.

The latter point comes from the requirement that after the tunneling, the electron spends on the island a time $t \sim R_T C$ greater compared to the time needed for tunneling: $\tau \sim \hbar/eV_{bias} \sim hC/e^2$. That is, the electron is localized on the island. By this way we know that only an electron per time is on the island because the other is blocked on the lead (the metallic terminal). Such scenario, induced by the Coulomb blockade, is addressed as *single electron tunneling* [84, 85].

By means of tunnel junctions, in the regime of single electron tunneling, we can build up two principal circuits: a single electron box and a single electron transistor (SET). In the first case we have an island, that can be a metallic island, as in the preceding case, or a quantum dot, linked to one metallic lead. In the case of a SET the island is linked to two lead terminals. In the following we address a circuit where a biased SET is capacitively coupled to a SEB where no bias is applied (see Figure 8.2).

8.2 Transition Rates

Here we give the transition rates for an electron tunneling phenomenon in a device such as a SEB or a SET. We address the case of an electron tunneling from the lead of some circuit into an island. We can think about an electron the tunneling from the upper left lead toward the upper island in Figure 8.2. The calculations will be performed in the regime where charging energy effects are relevant. At first we write down the whole Hamiltonian for the process, involving the tunneling event from the left lead to the (metallic) island. Then, considering the tunneling part of

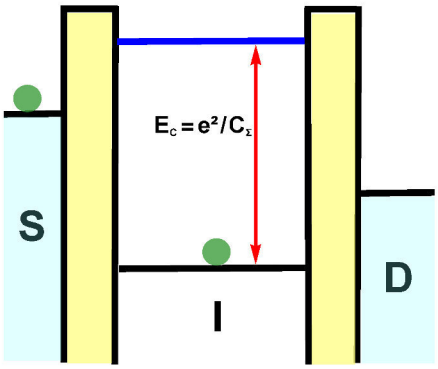

Figure 8.1: Tunnel junction in a Coulomb Blockade configuration. At left the source (S), at the centre the island (I), in which the low capacity induce huge separation between energetic levels, and at right the drain (D). Electrons (green balls) could jump across the potential walls by tunnel effect. At low temperature the presence of an electron in the island prevent to crossing of another one from the source because too much energy is now required to occupy the lowest free level.

the Hamiltonian as a perturbation, we proceed using Fermi golden rule for getting the transition rate for the addressed process [86].

The Hamiltonian that we will take in consideration counts the term for the metallic lead (the left one), the island, a tunneling term between these two components and the charging energy for the island that here we assume can host one electron at maximum. Thus we write:

$$H = \sum_{k,\sigma} \epsilon_k c^\dagger_{k,\sigma} c_{k,\sigma} + \sum_{q,\sigma} \epsilon_q c^\dagger_{q,\sigma} c_{q,\sigma} + \underbrace{\left[\sum_{\sigma,k,q} T_{q,k} c^\dagger_{q,\sigma} c_{k,\sigma} + h.c. \right]}_{H_{tun}} + H_{ch}(n) \quad (8.1)$$

The ϵs in the above writing are the energies of the conducting electrons and the term $T_{k,q}$ gives the strength of the tunneling between lead and island. This latter is assumed to be very little compared to the characteristic energies of the system such that we can treat it as a perturbation. The analogous Hamiltonian for the case of a quantum dot will count a term $\epsilon_{q,\sigma}$ instead of the whole sum (on q and σ) considered above for the energy levels of the island. In the case where a bias $2V$ is applied to the SET, and thus we measure a tension V between the left lead and the

metallic island, we can perform a unitary transformation:

$$H \to H' = U^\dagger H U - i\hbar U^\dagger \frac{\partial U}{\partial t} \tag{8.2}$$

where U is unitary and it is given by:

$$U = \prod_{k,\sigma} \exp\left(i\frac{e}{\hbar} V t c^\dagger_{k,\sigma} c_{k,\sigma}\right) \tag{8.3}$$

Thus recalling H' as H, we get:

$$H = \sum_{k,\sigma} (\epsilon_k + V)\, c^\dagger_{k,\sigma} c_{k,\sigma} + \sum_{q,\sigma} \epsilon_q c^\dagger_{q,\sigma} c_{q,\sigma} + \sum_{\sigma,k,q} T_{q,k} c^\dagger_{q,\sigma} c_{k,\sigma} + h.c. + H_{ch}(n) \tag{8.4}$$

The tunneling term would acquire a phase factor that we dropped because it does not imply any important physics under our assumptions. In the more general case, where some environment Hamiltonian is added to our system, we must be care about such phase as stressed in [86]. Now, using Fermi golden rule, we directly get the rate for such tunneling electron:

$$\Gamma_{i,f} = \frac{2\pi}{\hbar} |\langle f| \sum_{\sigma,k,q} T_{q,k} c^\dagger_{q,\sigma} c_{k,\sigma} |i\rangle|^2 \delta\left[E_f - E_i\right] \tag{8.5}$$

where i and f are the unperturbed initial and final states of the system, respectively before and after the tunneling event:

$$|i\rangle = |n^i_{k_1}, \ldots, n^i_{q_1}, \ldots\rangle \tag{8.6}$$

$$|f\rangle = |n^f_{k_1}, \ldots, n^f_{q_1}, \ldots\rangle \tag{8.7}$$

The energies, in the Dirac delta, E_i and E_f, are respectively the whole initial and the final energies of the system. With such delta we require energy conservation in the tunneling process. They can be written as:

$$E_i = \sum_{\sigma,k} (\epsilon_k + V) + \sum_{\sigma,q} \epsilon_q + H_{ch}(0) \tag{8.8}$$

and

$$E_f = E_i - (\tilde{\epsilon}_k + V) + \tilde{\epsilon}_q - H_{ch}(0) + H_{ch}(1) \tag{8.9}$$

where, in E_f, we deleted the contribution of an electron in the left lead and added the one of an electron in the island respect to E_i.

Since we are interested in the whole transition rate from the left lead to the island we have:

$$\Gamma_{L,I} = \sum_{i,f} P(|i\rangle)\Gamma_{i,f} \tag{8.10}$$

To calculate the above expression, at first we address the energy conservation required in the Dirac delta. According to our Hamiltonian we have:

$$E_i - E_i = f = \epsilon\tilde{k} - \epsilon_{\tilde{q}} + eV - \underbrace{(H_{ch}(n+1) - H_{ch}(n))}_{\delta H_{ch}} \tag{8.11}$$

Then, including also the temperature, as a parameter, in the characterization of the probability distribution for the initial states (remember that it is linked to the Fermi-Dirac distribution for the conducting electrons), we rewrite $p(|i\rangle)$ as $P_\beta(|i\rangle)$. Therefore the transition rate has the form:

$$\Gamma_{L,I} = \sum_{i,f} P_\beta(|i\rangle)\frac{2\pi}{\hbar}|\langle f| \sum_{\sigma,k,q} T_{q,k} c^\dagger_{k,\sigma} c_{k,\sigma}|i\rangle|^2 \delta\left[\epsilon\tilde{k} - \epsilon_{\tilde{q}} + eV - \delta H_{ch}\right] \tag{8.12}$$

It is now important to underline that, given the form of the tunneling Hamiltonian, the only states $|i\rangle$ and $|f\rangle$ that give non null contribution to $\Gamma_{L,I}$, when they close in braket the tunneling term, have the form:

$$\begin{cases} |i\rangle & = |\dots, 1_{k,\sigma}, \dots\rangle|\dots, 0_{q,\sigma}, \dots\rangle \\ |f\rangle & = |\dots, 0_{k,\sigma}, \dots\rangle|\dots, 1_{q,\sigma}, \dots\rangle \end{cases} \tag{8.13}$$

An electron, in the left lead, is destroyed leaving a hole with its same quantum numbers and another electron is then created in the island. Here, in the island, at the same time we destroy an hole with the same quantum numbers of the created electron.
With this in mind, the above expression for the rate assumes the form:

$$\frac{2\pi}{\hbar} \sum_{\sigma,k,q} P_\beta(|k\rangle)(1 - P_\beta(q))|T_{q,k}|^2 \delta\left[\epsilon_k - \epsilon_q + eV - \delta H_{ch}\right] \tag{8.14}$$

where now the probability P_β coincides with the Fermi-Dirac distribution. The passage to the last expression can be easily checked assuming two states bands for both the left lead and the island.
Now we perform the passage from the discrete case to the continuum:

$$\Gamma_{L,I} \simeq |T|^2 \frac{2\pi}{\hbar} 2 \int d\epsilon_k \int d\epsilon_q \varrho(\epsilon_k)\varrho(\epsilon_q) P_\beta(|k\rangle)(1 - P_\beta(q)) \\ \delta\left[\epsilon_k - \epsilon_q + eV - \delta H_{ch}\right] \tag{8.15}$$

where we have assumed that $|T_{q,k}| \sim |T| \,\forall\, k, q$. Furthermore the product between the two densities of electron states ϱ is almost constant at low temperature and this is our case. Since we assume very low temperatures then transitions happen between electrons that have almost the Fermi energy, thus we get:

$$\Gamma_{L,I} \simeq |T|^2 \frac{2\pi}{\hbar} 2\varrho(\epsilon_L^F)\varrho(\epsilon_I^F) \int d\epsilon_k \int d\epsilon_q P_\beta(|k\rangle)(1 - P_\beta(q)) \\ \delta\left[\epsilon_k - \epsilon_q + eV - \delta H_{ch}\right] \quad (8.16)$$

The constant before the integral can be riexpressed as $1/(e^2 R_T)$ where R_T is the tunneling resistance:

$$R_T = \frac{\hbar}{4\pi e^2 \varrho(\epsilon_L^F)\varrho(\epsilon_I^F)|T|^2} \quad (8.17)$$

Thus, eliminating the Dirac delta in the integral, we get the general form for $\Gamma_{L,I}$:

$$\Gamma_{L,I} = \frac{1}{e^2 R_T} \int d\epsilon \, f_{T_L}(\epsilon)\left(1 - f_{T_I}(\epsilon - \Delta E)\right) \quad (8.18)$$

In the simple case where lead and island have the same temperature $T = T_L = T_I$ we get:

$$\Gamma_{L,I} = \frac{1}{e^2 R_T} \frac{\Delta E}{\exp\{-\Delta E/kT\} - 1} \quad (8.19)$$

8.3 Heath-to-Current Harvesting

Here we consider the three-terminal circuit in Figure 8.2, that has been addressed in [82], where the two island are quantum dots. By opportunely choosing the temperatures of the leads, as well as the other state parameters, we can allow for heat-to-currert harvesting. Given a temperature gradient, between the system (SET) and the gate (SEB), we can produce some charge current into the system at zero bias voltage (Seebeck effect). We will proceed, to describe such effect, by writing the equations for the circuit, treating the tunneling junctions 1, 2 and g as effective capacitors. Then we will obtain the electrostatic energies and thus the charging energies of the two quantum dot islands. These latter will be taken into account for the form of the transition rates of such system. We will solve the master equation, for the occupation probabilities of the islands, finding the stationary solutions and finally, we will find a relation between the rate of heat exchanged, between system and gate, and the charge current into the system. It is such relation that shows how we can have current at zero bias voltage due to heat flow between the quantum dots.

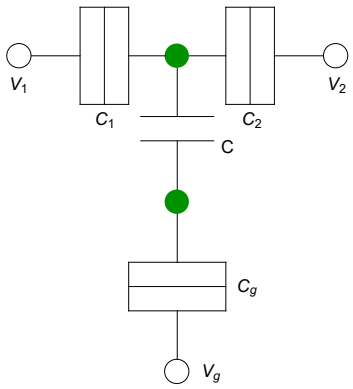

Figure 8.2: The whole circuit is made by two quantum dots (green disks), the system dot above and the gate dot down The gate dot is connected by a tunnel junction, of capacitance C_g to a gate voltage V_g. The system dot is connected in the same way to two terminals at different voltage, V_1 and V_2. The two subsystem are capacitively coupled together by a normal capacitor of capacitance C.

From the second Kirchoff law, the set of equations for the circuit is:

$$\begin{cases} Q_s &= C_1 \underbrace{(\phi_s - V_1)}_{-Q_1} + C_2 \underbrace{(\phi_s - V_2)}_{+Q_2} + C \underbrace{(\phi_s - \phi_g)}_{Q} \\ Q_g &= C_g \underbrace{(\phi_g - V_g)}_{-Q_g} + C \underbrace{(\phi_g - \phi_s)}_{+Q} \end{cases} \tag{8.20}$$

where ϕ_s and ϕ_g are the potentials on the system and gate islands and Q_s and Q_g are the excesses of charge on them. They can be expressed as $Q_s = qn_s$ and $Q_g = qn_g$ (q is the charge of the charge carriers). V_1, V_2 and V_g are respectively the potentials at the left, right and gate terminals and C_1, C_2 and C_g are the capacitances of the respective tunnel junctions. At last, C is the capacitance of the capacitor which couples system and gate. Solving the set of eqns. 8.20 respect to ϕ_s and ϕ_g we get:

$$\begin{cases} \phi_s(Q_s, Q_g) &= \left(\frac{1}{C_1+C_2+C-\frac{C^2}{C+C_g}} \right) \left[Q_s + C_1 V_1 + C_2 V_2 + \left(\frac{C}{C+C_g} \right) (Q_g + C_g V_g) \right] \\ \phi_g(Q_s, Q_g) &= \frac{(C+C_1+C_2)Q_g + C(Q_s+C_1V_1+C_2V_2) + C_gV_g(C+C_1+C_2)}{CC_g+C_1(C+C_g)+C_2(C+C_g)} \end{cases} \tag{8.21}$$

Now defining $C_{\Sigma_s} = C_1 + C_2 + C$, $C_{\Sigma_g} = C + C_g$ and $\tilde{C} = \left(C_{\Sigma_s} C_{\Sigma_g} - C^2 \right) / C$

the above set can be rewritten as:

$$\begin{cases} \phi_s(Q_s, Q_g) &= \left(\frac{1}{C\tilde{C}}\right)\left(C_{\Sigma_s}(Q_s + C_1V_1 + C_2V_2) + C(Q_g + C_gV_g)\right) \\ \phi_g(Q_s, Q_g) &= \left(\frac{1}{C\tilde{C}}\right)\left(C(Q_s + C_1V_1 + C_2V_2) + C_{\Sigma_g}(Q_g + C_gV_g)\right) \end{cases} \tag{8.22}$$

That gives a concise form for the potential of the two quantum dots, given the excess charges Q_s and Q_g on the islands.

Then we have that the electrostatic energy for the quantum dot system is given by:

$$U(Q_s, Q_g) = \int_0^{Q_s} dQ'_s\, \phi_s(Q'_s, Q_g) + \int_0^{Q_g} dQ'_g\, \phi_g(Q_s, Q'_g) \tag{8.23}$$

while the charging energy, $U_{s-g,Q_{g-s}}$, that we are interested in, is the change of electrostatic energy, in the system (s) or in the gate (g), when an electron tunnels into this latter and when there is an excess of charge, Q_g or Q_s, in the other dot. Thus, scaling Q_s and Q_g over q, we have:

$$\begin{cases} U(0,0) = 0 \\ U(0,1) = \left(C_{\Sigma_g}\left(q + 2C_1V_1 + 2C_2V_2\right) + 2CC_gV_g\right)\left(q/(2C\tilde{C})\right) \\ U(0,1) = \left(2C(C_1V_1 + C_2V_2) + C_{\Sigma_s}(q + 2C_gV_q)\right)\left(q/(2C\tilde{C})\right) \\ U(1,1) = \Big(C_{\Sigma_g}(q + 2C_1V_1 + 2C_2V_2) + 2C(2q + C_1V_1 + C_2V_2 + C_gV_g) \\ \qquad = \quad + C_{\Sigma_s}(q + 2C_gV_g)\Big)\left(q/(2C\tilde{C})\right) \end{cases} \tag{8.24}$$

for the electrostatic energies, the following set for the charging energies:

$$\begin{cases} U_{s,0} = U(1,0) - U(0,0) = U(1,0) \\ U_{s,1} = U(1,1) - U(0,1) = U_{s,0} + 2q/\tilde{C} \\ U_{g,0} = U(0,1) - U(0,0) = U(0,1) \\ U_{g,1} = U(1,1) - U(1,0) = U_{g,0} + 2q/\tilde{C} \end{cases} \tag{8.25}$$

The amount $E_c = U_{\alpha,1} - U_{\alpha,0} = 2q/\tilde{C}$ with $\alpha = s$ and g, is fundamental for the working of the engine. It represents the exchanged energy between system and gate when a charge carrier tunnels into one of the two dots and it will leave it only after another charge carrier has occupied the other dot.

Furthermore such charging energies appear in the transition rates. They can be calculated via Fermi golden rule as done in section 8.2 and they reads:

$$\Gamma^{-}_{l,n} = \Gamma_{l,n} f\left[(E_{\alpha,n} - qV_l)/(kT_l)\right] \tag{8.26a}$$

$$\Gamma^{+}_{l,n} = \Gamma_{l,n} - \Gamma^{-}_{l,n} \tag{8.26b}$$

Here we used the notation $\Gamma^{\pm}_{\alpha,n}$ to indicate that in the dot α there is an electron tunneling outside (+) or inside (-) while, in the other dot there is one (n=1) or zero (n=0) electrons. Furthermore, in eqns. (8.26), $\Gamma_{l,n}$ is a function depending on the properties of the tunneling junction l of a terminal and on the occupation number of the other dot. Then $E_{l,n} = \epsilon_\alpha + U_{\alpha,n}$, with ϵ_α, is the bare energy for the dot α and, f indicates the Fermi-Dirac distribution function:

$$f(x) = \frac{1}{1+e^x}$$

At last we have that the rate for the system tunneling events, $\Gamma^{\pm}_{s,n}$, includes the ones for the left and right terminals:

$$\Gamma^{\pm}_{s,n} = \Gamma^{\pm}_{1,n} + \Gamma^{\pm}_{2,n} \tag{8.27}$$

Now we get the stationary solutions, for the occupation probabilities of the allowed states, via master equation. It is important to underline that now we look at the system as it were classic. The master equation we are writing is classic, although we use the transition rates that have a quantum nature. For writing such master equation, we define:

$$\rho = \Big(p(0,0),\, p(1,0),\, p(0,1),\, p(1,1)\Big)^T \tag{8.28}$$

thus the master equation reads:

$$d_t\rho = \mathcal{M}\rho \tag{8.29}$$

where

$$\mathcal{M} = \begin{pmatrix} -\left(\Gamma^{-}_{s,0} + \Gamma^{-}_{g,0}\right) & \Gamma^{+}_{s,0} & \Gamma^{+}_{g,0} & 0 \\ \Gamma^{-}_{s,0} & -(\Gamma^{+}_{s,0} + \Gamma^{-}_{g,1}) & 0 & \Gamma^{+}_{g,1} \\ \Gamma^{-}_{g,0} & 0 & -\left(\Gamma^{-}_{s,1} + \Gamma^{+}_{g,0}\right) & \Gamma^{+}_{s,1} \\ 0 & \Gamma^{-}_{g,1} & \Gamma^{-}_{s,1} & -\left(\Gamma^{+}_{s,1} - \Gamma^{+}_{g,1}\right) \end{pmatrix} \tag{8.30}$$

The eqn. (8.29) allows for steady state solutions:

$$\begin{cases} \bar{p}(0,0) = \gamma^{-3} \sum_{\alpha=s,g} \sum_{i=\pm 1} \sum_{n=0,1} \Gamma^{+}_{\alpha,0} \Gamma^{i}_{\alpha,1} \Gamma^{+}_{\bar{l},n} \delta_{|1-i|,2n} \\ \bar{p}(0,1) = \gamma^{-3} \sum_{i=\pm 1} \sum_{n=0,1} \left(\Gamma^{-}_{s,0} \Gamma^{i}_{s,1} \Gamma^{+}_{g,n} + \Gamma^{i}_{g,0} \Gamma^{+}_{g,1} \Gamma^{-}_{s,n} \delta_{|1-i|,2n} \right) \\ \bar{p}(1,0) = \gamma^{-3} \sum_{i=\pm 1} \sum_{n=0,1} \left(\Gamma^{i}_{s,0} \Gamma^{+}_{s,1} \Gamma^{-}_{g,n} + \Gamma^{-}_{g,0} \Gamma^{i}_{g,1} \Gamma^{+}_{s,n} \delta_{|1-i|,2n} \right) \\ \bar{p}(1,1) = \gamma^{-3} \sum_{\alpha=s,g} \sum_{i=\pm 1} \sum_{n=0,1} \Gamma^{i}_{\alpha,0} \Gamma^{-}_{\alpha,1} \Gamma^{-}_{\bar{\alpha},n} \delta_{|1-i|,2n} \end{cases} \tag{8.31}$$

where $\gamma^3 = \sum_{\alpha,i,n} = \Gamma_{\alpha,n} \left(\Gamma^{\bar{i}}_{\alpha,\bar{n}} \Gamma^{\bar{i}}_{\bar{\alpha},n} + \Gamma^{i}_{\bar{\alpha},n} \sum_j \Gamma^{j}_{\bar{\alpha},n} \delta_{|1-j|,2n} \right)$ (the sign "bar", on the top of the indices in this latter writing, denotes the opposite value of the subscripts) and the normalization condition $\sum_{n_s,n_g} \bar{p}(n_g, n_s) = 1$ stands. Although eqn. 8.31 give the steady state solution we also give some information about the characteristic time needed to get such final state. An analytical form of this time scale is not reported here but a general discussion can be carried out. Since the master equation in (8.29) represents a system of four first order differential equations, its solution can be written as the following linear combination of four eigenvectors of $\mathcal{M}$: $\{p_1, p_2, p_3, p_4\}$:

$$p = \sum_i \alpha_i p_1 e^{r_i t} \tag{8.32}$$

. α_i are free parameters to be chosen according to some condition and r_i indicates the eigenvalue relative to the eigenvector p_i, then t is the time. For such master equation we have one null eigenvalue allowing for a final steady state represented by the relative eigenvector. This latter is given by the quadruple in (8.31). Then three different non null eigenvalues remain. Such eigenvalues are negative and give an exponential dumping for the relative eigenvector as $e^{-|r_i|t}$. The characteristic times of these dumping are $\tau_i = 1/|r_i|$ and they can be very different one respect to each other. The steady state form for the charge current and heat currents in the system and in the gate are written using the steady state probabilities in eqns. (8.31) as given in [82].
For the charge current we have:

$$I = q \sum_n \left(\Gamma^{+}_{l,n} \bar{p}(1,n) - \Gamma^{-}_{l,n} \bar{p}(0,n) \right) \tag{8.33}$$

On the other hand, for the heat currents into the first and second terminal of the SET, we have:

$$J_l = \sum_n (E_{sn} - qV_l) \left(\Gamma^{+}_{l,n} \bar{p}(1,n) - \Gamma^{-}_{l,n} \bar{p}(0,n) \right) \quad \text{with } l = 1,2 \tag{8.34}$$

and finally for the heat current into the gate terminal we have:

$$J_g = \sum_n (E_{g,n} - qV_g) \left(\Gamma^+_{g,n} \bar{p}(n,1) - \Gamma^{-0}_{g,n} \bar{p}(n,0) \right) \tag{8.35}$$

Then we can define the energy currents as $W_l = J_l + V_l I_l$.
It is important to note that charge and energy currents are conserved:

$$\sum_l W_l = \sum_l I_l = 0 \tag{8.36}$$

while for the heat currents the Joul law stands:

$$\sum_l J_l = \sum_l (V_i - V_l) I_l \tag{8.37}$$

where V_i is a reference voltage of one of the circuit's terminals.

Now we want to get an important result which links together the gate heat current J_g and the charge current I. At first we need to note that the heat current J_g, through the steady state condition, can be expressed (for calculations see appendix B.1) as:

$$J_g = E_c \gamma^{-3} \left(\Gamma^-_{g,0} \Gamma^-_{s,1} \Gamma^+_{s,0} \Gamma^+_{g,1} - \Gamma^-_{s,0} \Gamma^+_{g,1} \Gamma^+_{s,1} \Gamma^+_{g,0} \right) \tag{8.38}$$

In eqn. (8.38) the two contributions included in the braket are proportional to the probability that the system performs two different cycles over the four states of the system. Furthermore E_c takes now the role of the quanta of energy transferred during these cycles. The first cycle is:

$$(0,0) \xrightarrow{\Gamma^-_{g,0}} (0,1) \xrightarrow{\Gamma^-_{s,1}} (1,1) \xrightarrow{\Gamma^+_{g,1}} (1,0) \xrightarrow{\Gamma^-_{s,0}} (0,0) \tag{8.39}$$

Now this cycle the gate gives an amount of heat E_c to the system. Otherwise the second cycle

$$(0,0) \xrightarrow{\Gamma^-_{s,0}} (1,0) \xrightarrow{\Gamma^-_{g,1}} (1,1) \xrightarrow{\Gamma^+_{s,1}} (0,1) \xrightarrow{\Gamma^+_{g,0}} (0,0) \tag{8.40}$$

is performed. Now the gate takes an amount of heat E_c from the system.

However from the expression (8.38) we can get the wanted link with the current I (the calculations are reported in the appendix B.4):

$$I = q \frac{\Gamma_{1,1}\Gamma_{2,0} - \Gamma_{1,0}\Gamma_{2,1}}{(\Gamma_{1,0} + \Gamma_{2,0}) + (\Gamma_{1,1} + \Gamma_{2,1})} \frac{J_g}{E_c} \tag{8.41}$$

The charge current is proportional to the heat current through the gate. When bias voltage is zero we can get some current I, given a certain temperature difference

between gate and system as shown in Figure 8.3. It is important to note that it is possible only if we have some asymmetry in the circuit in terms of parameters Γ which count, for instance, the tunneling resistances of the tunnel junctions. In this scenario also the heat currents in eqn. (B.4) are conserved. According to different temperature gradients we can have positive or negative J_g. It means that heat flows from the gate toward the SET or viceversa and thus also the sign of I into the SET changes. We can define the efficiency of such heat engine "heat-to-current".

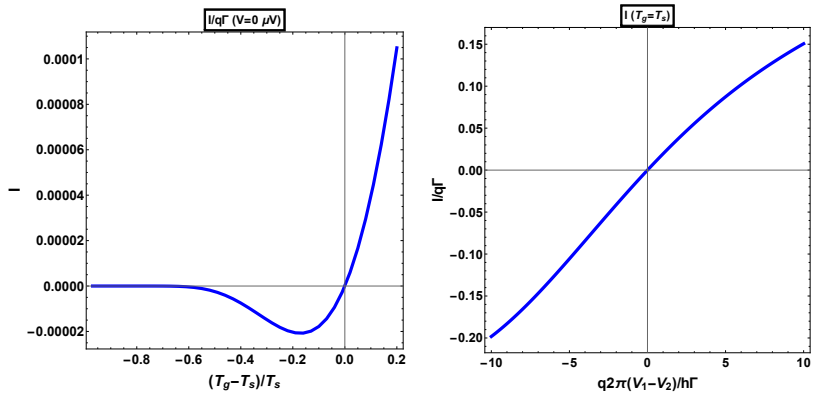

(a) I-ΔT at $\Delta V = 0$ (b) I-ΔV at $\Delta T = 0$

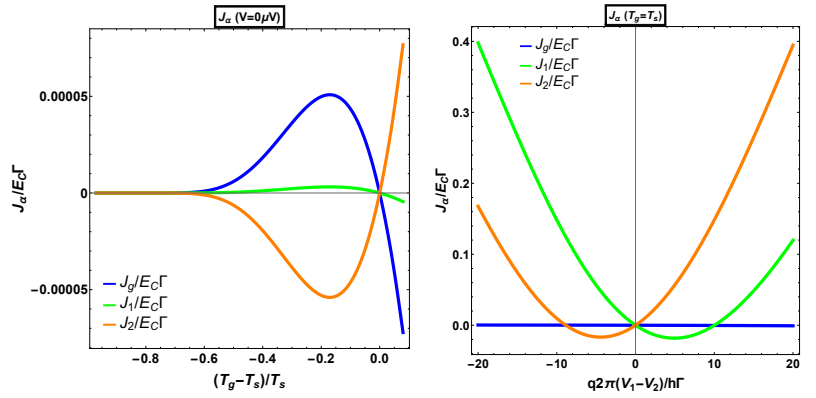

(c) J_l-ΔT at $\Delta V = 0$ (d) J_l-ΔV at $\Delta T = 0$

Figure 8.3: Charge and heat currents for different values of temperatures difference at zero bias voltage across the system and as function of various bias voltage at null temperature difference. We can see that the temperature gradient allows for non null charge current into the system also at zero bias as showed in Figure 8.3(a). At equilibrium no current (charge or heat) is present into the circuit.

When we apply a voltage ΔV it acts as a load for the engine (hereafter we will

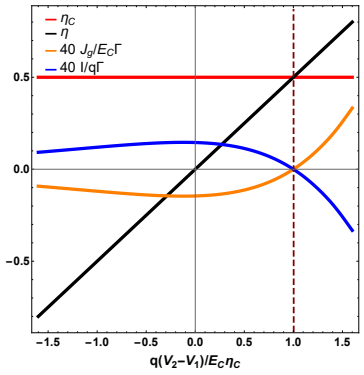

Figure 8.4: Given the temperature difference $(T_g - T_s)T_g = 0.25$ we vary the scaled bias voltage and at the value $\Delta V = E_c\eta_C/q$ the equilibrium is reached (no current is present in the circuit) while the efficiency of the heat-to-current engine equals the Carnot engine.

assume $T_g \geq T_s$). For instance when the circuit uses the heat from a hot reservoir and transforms it into useful work at power $P = I\Delta V$. The efficiency of such conversion is:

$$\eta = \frac{I\Delta V}{J_g} = \frac{q\Delta V}{E_c} \tag{8.42}$$

Such efficiency cannot grow at infinity since the second principle of the thermodynamics that limits it to the Carnot efficiency $\eta_C = 1 - T_c/T_h$. When η reaches such value then the contribution given in eqn. (8.38) about the two possible cycles are equal. There is the same probability that the electron in the system island tunnels toward right or left implying a whole null charge current into the SET. In such scenario the current are zero, as well as the entropy production and the power (the engine does not produces work) and $\eta = \eta_C$. The voltage for such conditions is $\Delta V = E_c\eta_C/q$.

8.3.1 Impossibility of Seebeck Effect Using Metallic Dots

Here we address the same circuit of the preceding section but we assume to use metallic dots instead of quantum dots. Such a small change implies that we cannot get any I into the SET for non null heat current J_g flowing between gate and system. We give an analytical demonstration of such impossibility as well as a plot of the current I vs. J_g that shows only fluctuation of I at magnitude which is not appreciable for all J_g.

Assuming the same temperature T_s inside the system as well as in the gate, T_g, the transition rates are given by eqn. (8.19). Also for this case we want to find a

relation between the charge current I and the heat current J_g.It is useful to reduce the expression for the transition rate for a metallic dot, to the same form of the one of a quantum dot.

As first step we give the charging Hamiltonian for the system that, as said in [88], reads:

$$H_{ch} = E_c^{(s)}(n_s - n_G)^2 + E_c^{(g)}(N_g - N_G)^{(G)} + j(n_s - n_G)(N_g - N_G) \quad (8.43)$$

Parameters n_G and N_G respectively characterize the system (s) and the gate (g) islands, j gives the coupling between such two components. Then n_s and N_g are the number of excesses of charge (electrons) for the system and the gate dots.
When an electron tunnels into or out a metallic dot it experiences an energy cost:

$$\Delta E_{\alpha,n} = H_{ch}(n_s', N_g') - H_{ch}(n_s, N_g) \pm V/2 \quad (8.44)$$

The last term, $\pm V/2$, depends on the fact that the tunneling has been done against or toward the bias. Such bias across the SET is V and it is 0 for the gate component. The subscript n again expresses the fact that, during the tunneling event in the island α, the other island hosts $n = n_s$ or $n = N_g$ electrons.

Finally, as for the preceding case, where quantum dots have been considered, we riexpress the expression for the transition rates for the metallic dots, eqn. (8.19), in the form of eqn. (B.4): $\Gamma_{\alpha,n}^{\pm} = \Gamma_{\alpha,n} f_{\alpha,n}^{\pm}$. We note that tunneling outside or inside the dot toward or from the same lead, $\Gamma_{\alpha,n}^{\pm}$, are processes where the energy cost for the electron has the same modulus, $|\Delta E_{\alpha,n}|$. Thus the rates are such that:

$$\Gamma_{\alpha,n}^{\pm} = \Gamma(\pm \Delta E_{\alpha,n}) \quad (8.45)$$

where, in this case, we have indicated with $\Delta E_{\alpha,n}$ the energy cost for the tunneling outside the dot. Thus, considering a generic energy cost $\Delta E_{\alpha,n}$ for the tunneling (inside or outside tunneling), the equation form (8.19), written in terms of energy cost for the metallic dot case, can be rewritten as:

$$\Gamma(\Delta E_{\alpha,n}) = \Gamma'(\Delta E_{\alpha,n}) f(\Delta E_{\alpha,n}) \quad (8.46)$$

where $\Gamma'(\Delta E_{\alpha,n}) = \Gamma(\Delta E_{\alpha,n}) + \Gamma(-\Delta E_{\alpha,n})$. Such form can be achieved, as shown in appendix B.3, by defining:

$$\Gamma'(\Delta E_{\alpha,n}) = \left(\frac{1}{e^2 R_T}\right)\left(\frac{(-\Delta E_{\alpha,n})\sinh(\Delta E_{\alpha,n}/kT)}{1 - \cosh(\Delta E_{\alpha,n}/kT)}\right) \quad (8.47)$$

and

$$f(\Delta E_{\alpha,n}) = e^{-\Delta E_{\alpha,n}/(2kT)} \frac{\sinh((\Delta E_{\alpha,n}/2kT))}{(\Delta E_{\alpha,n}/kT)} \quad (8.48)$$

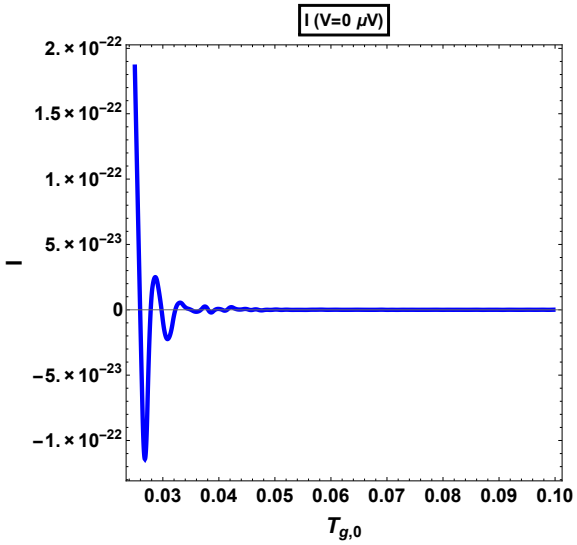

Figure 8.5: Irrelevant charge current fluctuations in the regime $n_g = N_g = 0.5$ for $V = 0$ and $T_s = 0.067$ as function of T_g. The metallic nature of the islands does not allow for heat-to-current harvesting.

Recovering the steps of appendix B.2, in which the functions f as well as $\Gamma_{\alpha,n}$ are not explicated, we can get the same result linking I an J_g for this case, where now the coupling constant j is present:

$$I = q\frac{\Gamma_{1,1}\Gamma_{2,0} - \Gamma_{1,0}\Gamma_{2,1}}{(\Gamma_{1,0} + \Gamma_{2,0})(\Gamma_{1,1} + \Gamma_{2,1})}\frac{J_g}{2j} \tag{8.49}$$

The term $\Gamma_{1,1}\Gamma_{2,0} - \Gamma_{1,0}\Gamma_{2,1}$ is exactly zero for $V = 0$. Such term does not depends on the gate. There is not charge current in the SET for whatever value of heat current across gate and system. This is the main difference about the metallic dot circuit respect to the quantum dot one.

Chapter 9

Conclusions

In this thesis we addressed several topical items of great importance in the development of recent quantum physics and in their prospective technological applications.

The first subject is related to designing heat engines. We considered a quantum Otto cycle with irreversible isochoric and adiabatic processes. We first described the production of entropy for a closed quantum system, where the irreversibility of the branch is described in terms of the relative entropy between the state ρ_τ at the end of the transformation, and the reference state ρ_A which one would obtain if the transformation were reversible (for instance in the case of a quasi-static driving). In the Otto cycle we considered, the working substance is characterized by some disorder consisting of an ensemble of misaligned spins interacting with a magnetic field. Net work, power, efficiency and efficiency at maximum power have been calculated. We found that such quantities are affected by finite-time processes in the cycle or by the degree of disorder. We finally propose an experimental optical implementation of the Otto cycle.

The possibility of getting quantum states which, instead, survive under dissipative phenomena, such as disorder or other perturbations motivated us to study topological order. We briefly described the difference between standard quantum order and topological order. The latter is characterized by topological invariants, useful for building up topological classes defined by discrete symmetries such as time reversal or particle-hole symmetries. In particular, we studied the Kitaev model, generalizing it in the case of many-neighbors interactions. We considered longer ranges in the hopping and pairing terms, in the presence or in the absence of time reversal symmetry. Several phase diagrams have been derived, showing the presence of Majorana zero modes (MZM) as well as massive edge modes (MEM). These modes were found by analysing the case of infinitely long superconducting coupling terms, but we showed that it is possible to get MZMs also for finite

length wires Finally, we derive the entire set of Bogoliubov equations for a generic case (with more than first neighbors interactions, with and without time reversal symmetry) providing the solution for the time-reversal case.

The last issue we addressed is related to single electron tunneling devices. In such systems it is possible to perform "heat-to-current" harvesting using a quantum dot circuit as in Figure 8.2, however we found that this is not the case if we substitute such dots with metallic islands. In contrast to the single energy level dot, in the presence of a heat flow the energy band in a metallic dot prevents the formation of a charge current. The final aim we postpone for future investigations is studying those (thermo)dynamical properties when topological components, like the Kitaev chains, are inserted in such circuits.

Appendices

Appendix A

Quantum Thermodynamics

A.1 Change of Energies in a Reversible Quantum Adiabatic Transformation

A reversible quantum adiabatic transformation is characterized by the condition:

$$E_n^{\lambda_f} - E_m^{\lambda_f} = \xi \left(E_n^{\lambda_0} - E_m^{\lambda_0} \right) \tag{A.1}$$

with:

$$\beta_{eff} = \frac{\beta_i}{\xi} \tag{A.2}$$

This condition is generally different from the condition standing for the eigenvalues of $H(\lambda_t)$ in a isothermal transformation:

$$, E_n^{\lambda_f} = \xi E_n^{\lambda_0} \tag{A.3}$$

where ξ is the ratio of energy levels and $0 < \xi < 1$ holds for expansions and $\xi > 1$ for compressions. Let us assume to have chosen the offset of the energy at $t = 0$ such that the lowest energy level has a non null value, $E_1^{\lambda_0} \neq 0$. Let us define χ the raport of $E_1^{\lambda_f}$ on $E_1^{\lambda_0}$:

$$\chi = \frac{E_1^{\lambda_f}}{E_1^{\lambda_0}} \tag{A.4}$$

In the contest of a reversible quantum adiabatic transformation, by eqn. (A.4), we can get:

$$\begin{aligned} E_n^{\lambda_f} - E_1^{\lambda_f} &= E_n^{\lambda_f} - \chi E_1^{\lambda_0} \\ &= \xi E_n^{\lambda_0} + (\chi - \xi) E_1^{\lambda_0} \end{aligned} \tag{A.5}$$

The above result will be very useful later. Another important result is got by considering the partition functions of the initial canonical equilibrium state and the final state of the reversible quantum adiabatic branch at the effective temperature T_{eff}. We write the initial partition function as:

$$\begin{aligned} Z_i &= \sum_n e^{-\beta_i E_n^{\lambda_0}} \\ &= e^{-\beta_i E_1^{\lambda_0}} \sum_n \exp\{E_n^{\lambda_0} - E_1^{\lambda_0}\} \end{aligned} \tag{A.6}$$

On the other hand, about the final state we have:

$$\begin{aligned} Z_f &= \sum_n e^{-\beta_{eff} E_n^{\lambda_f}} \\ &= e^{-\beta_{eff} E_1^{\lambda_f}} \sum_n \exp\{-\beta_{eff}(E_n^{\lambda_f} - E_1^{\lambda_f})\} \\ &= e^{-\beta_{eff} E_1^{\lambda_f}} \sum_n \exp\{-\beta_i(E_n^{\lambda_i} - E_1^{\lambda_i})\} \end{aligned} \tag{A.7}$$

Where, in the last passage above, we have used eqns. (A.1) and (A.2). Thus we focus on the raport:

$$\begin{aligned} \frac{Z_f}{Z_i} &= \exp\left\{-\beta_{eff} E_1^{\lambda_f} + \beta_i E_1^{\lambda_0}\right\} \\ &= \exp\left\{-\beta_1 \left(\frac{\chi}{\xi}\right) E_1^{\lambda_0} + \beta_i E_1^{\lambda_0}\right\} \\ &= \exp\left\{\beta_i E_1^{\lambda_0} \left(1 - \frac{\chi}{\xi}\right)\right\} \end{aligned} \tag{A.8}$$

where we have used eqn. (A.2) togheter with eqn. (A.5).

A.2 Identity of first order momentum between average $\hat{W}_t$ and the Average Work Via pdf

Here we show that the work obtained by averaging on the work pdf is equal to the difference of average energies $\Delta U = U_\tau - \mathcal{U}_i$. At first we develop $\langle w \rangle$ according to the work pdf definition:

$$\begin{aligned} \langle w \rangle &= \int dw \sum_{n,m} w\, P_n^{(0)} P_{m|n}^{(\tau)} \delta\left[w - (E_n^{\lambda_\tau} - E_n^{\lambda_0})\right] \\ &= \sum_{n,m} (E_n^{\lambda_\tau} - E_n^{\lambda_0}) P_n^{(0)} P_{m|n}^{(\tau)} \end{aligned} \tag{A.9}$$

now we approach the variable ΔU:

$$\begin{aligned}
\Delta U &= U_\tau - \mathcal{U}_i \\
&= Tr\left(\rho_\tau H(\lambda_\tau)\right) - Tr\left(\rho_i H(\lambda_0)\right) \\
&= \sum_n \left(E_n^{\lambda_\tau} P_n^{(\lambda_\tau)} - E_n^{\lambda_0} P_n^{(\lambda_0)} \right) \\
&= \sum_m E_m^{(\lambda_\tau)} \left(\sum_n P_{m|n}^{(\tau)} P_n^{(0)} \right) - \sum_n E_n^{\lambda_0} P_n^0 \\
&= \sum_m E_m^{(\lambda_\tau)} \left(\sum_n P_{m|n}^{(\tau)} P_n^{(0)} \right) - \sum_n E_n^{\lambda_0} P_n^0 \sum_m P_{m|n}^{(\tau)} \\
&= \sum_{n,m} P_n^{(0)} P_{m|n}^{(\tau)} \left(E_m^{\lambda_\tau} - E_n^{\lambda_0} \right)
\end{aligned} \tag{A.10}$$

That is just the expression eqn. (A.9) for $\langle w \rangle$

A.3 Inner Friction Work and Quantum Relative Entropy

Here we approach separately both terms in eqn. (3.56) and show that they coincide. The left side of that equation can be developed as:

$$\begin{aligned}
\langle w_{fric} \rangle &= \langle w \rangle - \langle w_{i\to A} \rangle \\
&= Tr(\rho_f H_f) - \mathcal{U}_A \\
&= \sum_m \epsilon_m^{(f)} \left[\left\langle \epsilon_m^{(f)} \middle| \rho_\tau \middle| \epsilon_m^{(f)} \right\rangle - P_m^{(A)} \right]
\end{aligned} \tag{A.11}$$

where $P_m^{(A)}$ represents the population of the m-th level in the state ρ_A, gained at the and of the reversible adiabatic transformation. On the other hand the relative entropy can be expressed as:

$$\begin{aligned}
D(\rho_\tau || \rho_A) &= Tr\left(\rho_\tau \ln\left(\rho_\tau\right)\right) - Tr\left(\rho_\tau \ln \rho_A\right) \\
&= \sum_m P_m^{(i)} \ln P_m^{(i)} - \left\langle \epsilon_m^{(f)} \middle| \rho_\tau \middle| \epsilon_m^{(f)} \right\rangle \ln P_m^{(A)} \\
&= \sum_m \ln P_m^{(A)} \left[P_m^{(i)} - \left\langle \epsilon_m^{(f)} \middle| \rho_\tau \middle| \epsilon_m^{(f)} \right\rangle \right] \\
&= \sum_m \beta_A \epsilon_m^{(f)} \left[\left\langle \epsilon_m^{(f)} \middle| \rho_\tau \middle| \epsilon_m^{(f)} \right\rangle - P_m^{(A)} \right]
\end{aligned} \tag{A.12}$$

For the above passages remember that $P_m^{(i)} = P_m^{(A)}$. The latter result is just the first one, eqn. (A.11), time a factor $1/\beta_A$ as written in eqn. (3.56).

A.4 Entropy Production and Quantum Relative Entropy

Here we show that the average entropy $\langle s \rangle$, expressed in eqn. (3.65a), can be given in terms of average energy functionals multiplied by appropriate inverse temperatures, as in eqn. (3.65b), and then we will show the equivalence between the entropy production $\langle \Sigma \rangle$ and the quantum relative entropy $D(\rho_\tau || \rho_A)$. Let us begin by explicating the form of $\langle s \rangle$:

$$\begin{aligned}
\langle s \rangle &= \sum_s \sum_{n,m} P_n^{(0)} P_{m|n}^{(\tau)} \delta \left[s - \left(\beta_A E_m^{\lambda_\tau} - \beta_i E_n^{\lambda_0} \right) \right] ss \\
&= \beta_A \underbrace{\sum_m P_n^{(0)} P_{m|n}^{(\tau)}}_{=P_m^{(\tau)}} - \beta_i \sum E_n^{\lambda_0} P_n^{(0)} \underbrace{\sum_m P_{m|n}^{(\tau)}}_{=1} \\
&= \beta_A \sum_n \left[\left(\xi E_n^{\lambda_0} + (\chi - \xi) E_1^{\lambda_0} \right) P_n^{(\tau)} - \xi \beta_A E_n^{(n)} P_n^{(0)} \right] \\
&= \beta_A \sum_n \left[\xi E_n^{(0)} \left(P_n^{(\tau)} - P_n^{(0)} \right) \right] + \beta_A (\chi - \xi) E_1^{(0)} \underbrace{\sum_n P_n^{(\tau)}}_{=1}
\end{aligned} \tag{A.13}$$

Where, for going to the second to the third step, we used eqns. (A.2) and (A.5). The same result is got by considering:

$$\begin{aligned}
&\beta_A Tr\left(\rho_\tau H(\lambda_\tau)\right) - \beta_i Tr\left(\rho_i H(\lambda_0)\right) \\
&\qquad = \beta_A \sum_n \left[P_n^{(\tau)} \left(\xi E_n^{\lambda_0} + (\chi - \xi) E_1^{\lambda_0} \right) - \xi P_n^{(0)} E_n^{\lambda_0} \right] \\
&\qquad = \beta_A \left[\sum_n \xi E_n^{\lambda_0} \left(P_n^{(\tau)} - P_n^{(0)} \right) \right] + \beta_A (\chi - \xi) E_n^{\lambda_0} \underbrace{\sum_n P_n^{(\tau)}}_{=1}
\end{aligned} \tag{A.14}$$

that is equal to the preceding thus we got the preceding result.
Now we develop the entropies difference:

$$\begin{aligned}
\beta_A F_A - \beta_i F_i &= \beta_A \left(-\frac{1}{\beta_A} \right) \ln(Z_A) - \beta_A \left(-\frac{1}{\beta_i} \right) \ln(Z_i) \\
&= \ln\left(\frac{Z_i}{Z_A} \right) \\
&= \beta_i E_1^{(0)} \left(\frac{\chi}{\xi} - 1 \right) \\
&= \beta_A E_1^{(0)} (\chi - \xi)
\end{aligned} \tag{A.15}$$

Thus:

$$\begin{aligned}\langle\Sigma\rangle &= \langle s\rangle - \beta_A F_A + \beta_i F_i \\ &= \beta_A \sum_n \xi E_n^{(0)} \left(P_n^{(\tau)} - P_n^{(0)}\right)\end{aligned} \tag{A.16}$$

At last we can show that the form of $D(\rho_\tau||\rho_A)$ can be brought into the one of the preceding eqn. (A.16):

$$\begin{aligned}D(\rho_\tau||\rho_A) &= \beta_A \sum_n E_n^{(\tau)} \left(P_n^{(tau)} - P_n^{()}\right) \\ &= \beta_A \sum_n \left(\xi E_n^{(0)} + (\chi - \xi) E_1^{(0)}\right) \left(P_n^{(\tau)} - P_n^{(0)}\right) \\ &= \langle\Sigma\rangle + \beta_A(\chi - \xi) E_1^{(0)} \left(\underbrace{\sum_n P_n^{(\tau)}}_{=1} - \underbrace{\sum_n P_n^{(0)}}_{=1}\right) \\ &= \langle\Sigma\rangle\end{aligned} \tag{A.17}$$

A.5 Cumulants Series for Limit Entropy

Here we show haw the expression $\beta_A F_A - \beta_i F_i$ can be expressed in series of cumulants. At first let

$$g(x) = \ln\left(\left\langle e^{-xs}\right\rangle\right) \tag{A.18}$$

be the generating function for the cumulants with:

$$C_n = (-1)^n \frac{d^n g}{dx^n}\bigg|_{x=0} \tag{A.19}$$

It follow that:

$$g(x) = \sum_{n=1} \frac{(-1)^n}{n!} C_n x^n \tag{A.20}$$

By eqn. (A.20) and taking $s = 1$ we get:

$$g(1) = \ln\left(\left\langle e^{-s}\right\rangle\right) = \sum_{n=1} \frac{(-1)^n}{n!} C_n \tag{A.21}$$

Which concludes our demonstration.

Appendix B

Single Electron Devices

B.1 Dependence of J_g from the cycles of the engine

Here we show the expression (8.38).
We start considering that since we are in a steady state regime, $d_t\rho = 0$, the following relation about the currents holds:

$$\underbrace{\Gamma^{+}_{g,0}\bar{p}(0,1) - \Gamma_{g,0}\bar{p}(0,0)}_{\mathcal{J}^{0,0}_{1,0}} = -\underbrace{\left(\Gamma^{+}_{g,1}\bar{p}(1,1) - \Gamma^{-}_{g,1}\bar{p}(1,0)\right)}_{\mathcal{J}^{1,1}_{1,0}} \tag{B.1}$$

We remember that $\mathcal{J}^{n'_s,n_s}_{n'_g,n_g}$ is the probability current for the transition $(n_s, n_g) \to (n'_s, n'_g)$. Then inserting eqn. (B.1) into the expression for J_g (eqn. (8.35)) we get:

$$\begin{aligned} J_g &= \sum_n (E_{g,n} - qV_g)\left(\Gamma^{+}_{g,n}\bar{p}(n,1) - \Gamma^{-0}_{g,n}\bar{p}(n,0)\right) \\ &= -(E_{g,0} - qV_g)\mathcal{J}^{0,0}_{1,0} - (E_{g,1} - qV_g)\mathcal{J}^{1,1}_{1,0} \\ &= \mathcal{J}^{0,0}_{1,0}(E_{g,1} - E_{g,0}) \\ &= E_c\mathcal{J}^{0,0}_{1,0} \end{aligned} \tag{B.2}$$

Then by developing $\mathcal{J}^{0,0}_{1,0}$ in the above expression according to eqns. (8.31) we finally get eqn. (8.38).

B.2 Dependence of I form J_g

Here we show the expression eqn. (8.41). For this aim it is useful to define:

$$f^{-}_{\alpha,0} = f\left[(E_{\alpha,n} - qV_\alpha)/(kT_\alpha)\right] \tag{B.3a}$$

$$f^{+}_{\alpha,0} = 1 - f^{-}_{\alpha,0} \tag{B.3b}$$

So that the expression for the rates can be written as:

$$\Gamma^{\pm}_{\alpha,n} = \Gamma_{\alpha,n} f^{\pm}_{\alpha,n} \tag{B.4}$$

From eqn. (8.38), using eqns. (8.31), we can get:

$$\begin{aligned} J_g &= \frac{E_c}{\gamma^3}\Big(f^{-}_{g,0} f^{-}_{s,1} f^{+}_{s,0} f^{+}_{g,1} \Gamma_{g,0}\Gamma_{s,1}\Gamma_{s,0}\Gamma_{g,1} \\ &\quad - f^{-}_{s,0} f^{-}_{g,1} f^{+}_{s,1} f^{+}_{g,0} \Gamma_{g,0}\Gamma_{s,1}\Gamma_{s,0}\Gamma_{g,1}\Big) \\ &= \frac{E_c}{\gamma^3}\Gamma_{g,0}\Gamma_{s,1}\Gamma_{s,0}\Gamma_{g,1}\left(f^{-}_{g,0} f^{-}_{s,1} f^{+}_{s,0} f^{+}_{g,1} - f^{-}_{s,0} f^{-}_{g,1} f^{+}_{s,1} f^{+}_{g,0}\right) \end{aligned} \tag{B.5}$$

On the other hand, about the charge current, we have:

$$I = q\left(\underbrace{\Gamma_{2,0}\Gamma_{s,1} - \Gamma_{2,1}\Gamma_{s,0}}_{*} \right) (\Gamma_{g,0}\Gamma_{g,1}) \left(f^{-}_{g,0} f^{-}_{s,1} f^{+}_{s,0} f^{+}_{g,1} - f^{-}_{s,0} f^{-}_{g,1} f^{+}_{s,1} f^{+}_{g,0}\right) \tag{B.6}$$

The above term $*$ can be developed as:

$$\begin{aligned} \Gamma_{2,0}\Gamma_{s,1} - \Gamma_{2,1}\Gamma_{s,0} &= \Gamma_{2,0}\Gamma_{1,1} + \Gamma_{2,0}\Gamma_{2,1} - \Gamma_{2,1}\Gamma_{1,0} - \Gamma_{2,1}\Gamma_{2,0} \\ &= \Gamma_{2,0}\Gamma_{1,1} - \Gamma_{2,1}\Gamma_{1,0} \end{aligned} \tag{B.7}$$

thus:

$$\frac{I}{J_g} = \frac{q}{E_c}\left(\frac{\Gamma_{2,0}\Gamma_{1,1} - \Gamma_{2,1}\Gamma_{1,0}}{\Gamma_{s,0}\Gamma_{s,1}} \right) \tag{B.8}$$

that immediately proves eqn. (8.37).

B.3 Rewriting metallic dot transition rates

The function $\Gamma'(\Delta E_{\alpha,n})$ is directly obtained by its definition:

$$\begin{aligned} \Gamma'(\Delta E_{\alpha,n}) &= \Gamma'(\Delta E_{\alpha,n}) + \Gamma(\Delta E_{\alpha,n}) + \Gamma(-\Delta E_{\alpha,n}) \\ &= \left(\frac{1}{e^2 R_T}\right)\left(\frac{\Delta E_{\alpha,n}}{\exp\{\Delta E_{\alpha,n}/(kT)\} - 1} + \frac{-\Delta E_{\alpha,n}}{\exp\{-\Delta E_{\alpha,n}/(kT)\} - 1} \right) \\ &= \left(\frac{1}{e^2 R_T}\right)\left(\frac{-\Delta E_{\alpha,n}\sinh(\Delta E_{\alpha,n}/(kT))}{1 - \cosh(\Delta E_{\alpha,n}/(kT))} \right) \end{aligned} \tag{B.9}$$

Now we address the function $f(\Delta E_{\alpha,n})$ that is not the Fermi-Dirac distribution, although we have used the same symbol f to address both of them. Such function is obtained putting the above result, eqn. (8.47), into the expression for the transition rate:

$$\left(\frac{\Delta E_{\alpha,n}}{\exp\{\Delta E_{\alpha,n}/(kT)\}-1}\right) = \left(\frac{-\Delta E_{\alpha,n}\sinh(\Delta E_{\alpha,n}/(kT))}{1-\cosh(\Delta E_{\alpha,n}/(kT)))}\right) f(\Delta E_{\alpha,n})$$

$$\frac{1}{2}\frac{-\exp(-\Delta E_{\alpha,n}/(kT))+1}{\cosh(\Delta E_{\alpha,n}/(kT))-1} = \frac{\sinh(\Delta E_{\alpha,n}/(kT))}{1-\cosh(\Delta E_{\alpha,n}/(kT))}$$

$$\frac{1}{2}\frac{\left(e^{\Delta E_{\alpha,n}/(2kT)}-e^{-\Delta E_{\alpha,n}/(2kT)}\right)}{e^{-\Delta E_{\alpha,n}/(2kT)}} = \sinh(\Delta E_{\alpha,n}/(kT))f(\Delta E_{\alpha,n})$$

and from the last passage we get:

$$f(\Delta E_{\alpha,n}) = e^{-\Delta E_{\alpha,n}/(2kT)}\left(\frac{\sinh(\Delta E_{\alpha,n}/(2kT))}{\sinh(\Delta E_{\alpha,n}/(kT))}\right) \tag{B.10}$$

that is what we wanted to show.

B.4 zero I at zero bias voltage

Here we give the explicit form of the coefficient $\Gamma_{s,1}$ and $\Gamma_{s,0}$ respect to the energy cost of the processes that they describe. By this way we directly prove that the amount $\Gamma_{1,1}\Gamma_{2,0} - \Gamma_{1,0}\Gamma_{2,1}$ is exactly zero for $V = 0$.

The addressed transition rates are given by:

$$\Gamma_{1,1} = \left(\frac{\Delta E^{(+)}_{1,1}}{\exp\{\Delta E^{(+)}_{1,1}/(kT)\}-1} + \frac{-\Delta E^{(+)}_{1,1}}{\exp\{-\Delta E^{(+)}_{1,1}/(kT)\}-1}\right) \tag{B.11a}$$

$$\Gamma_{2,0} = \left(\frac{\Delta E^{(+)}_{2,0}}{\exp\{\Delta E^{(+)}_{2,0}/(kT)\}-1} + \frac{-\Delta E^{(+)}_{2,0}}{\exp\{-\Delta E^{(+)}_{2,0}/(kT)\}-1}\right) \tag{B.11b}$$

$$\Gamma_{1,0} = \left(\frac{\Delta E^{(+)}_{1,0}}{\exp\{\Delta E^{(+)}_{1,0}/(kT)\}-1} + \frac{-\Delta E^{(+)}_{1,0}}{\exp\{-\Delta E^{(+)}_{1,0}/(kT)\}-1}\right) \tag{B.11c}$$

$$\Gamma_{2,1} = \left(\frac{\Delta E^{(+)}_{2,1}}{\exp\{\Delta E^{(+)}_{2,1}/(kT)\}-1} + \frac{-\Delta E^{(+)}_{2,1}}{\exp\{-\Delta E^{(+)}_{2,1}/(kT)\}-1}\right) \tag{B.11d}$$

where the energy costs are given by:

$$\Delta E^{(+)}_{1,1} = 2j(N_g-1) + E^{(s)}_c(2n_g-1) + \frac{qV}{2} \tag{B.12a}$$

$$\Delta E_{2,1}^{(+)} = 2j(N_g - 1) + E_c^{(s)}(2n_g - 1) - \frac{qV}{2} \tag{B.12b}$$

$$\Delta E_{2,0}^{(+)} = 2jN_g + E_c^{(s)}(2n_g - 1) - \frac{qV}{2} \tag{B.12c}$$

$$\Delta E_{1,0}^{(+)} = 2jN_g + E_c^{(s)}(2n_g - 1) + \frac{qV}{2} \tag{B.12d}$$

It can be seen that for $V = 0$ then $\Delta E_{2,0}^{(+)} = \Delta E_{1,0}^{(+)}$ and $\Delta E_{1,1}^{(+)} = \Delta E_{2,1}^{(+)}$ so that we also have $\Gamma_{2,0}^{(+)} = \Gamma_{1,0}^{(+)}$ and $\Gamma_{1,1}^{(+)} = \Gamma_{2,1}^{(+)}$. From this latter result it follows that $\Gamma_{1,1}^{(+)}\Gamma_{2,0}^{(+)} = \Gamma_{2,1}^{(+)}\Gamma_{1,0}^{(+)}$ so that the charge current is identically null for such zero bias regime.

Bibliography

[1] Xiao-Gang Wen, *Quantum Field Theory and Many Body Systems*, OUP Oxford, September 06 2007

[2] C. Jarzynski, *Equalities and Inequalities: Irreversibility and the Second Law of Thermodynamics at the Nanoscale* , Annual Review of Condensed Matter Physics Vol. **2**: 329-351

[3] M. Campisi, P. Hänggi and P. Talkner, *Quantum Fluctuation Relations: Foundations and Applications*, Rev. Mod. Phys. **83**, 1653

[4] C. Nayak, S. H. Simon, A. Stern, M.l Freedman and S. Das Sarma, *Non-Abelian anyons and topological quantum computation*, Rev. Mod. Phys. **80**, 1083 (2008)

[5] A. Yu Kitaev, *Unpaired Majorana fermions in quantum wires*, Uspekhi Fizicheskikh Nauk, Russian Academy of Sciences **44**, 121 (2000)

[6] R. H́utzen, A. Zazunov, B. Braunecker, A. Levy Yeyati, and R. Egger, *Majorana Single-Charge Transistor*, Phys. Rev. Lett. **109**, 166403 (2012)

[7] H.-P. Breuer, F. Petruccione, *The Theory of Open Quantum System*, OUP Oxford (2007)

[8] P. Meystre, Murray Sargent III, *Elements of Quantum Optics*, Springer-Verlag; 4th edizions (2007)

[9] Messiah Albert, *"XVII". Quantum Mechanics. Dover Publications.* ISBN 0-486-40924-4 (1999).

[10] T. D. Kieu, Phys. Rev. Lett. **93**, 140403 (2004); T. D. Kieu, Eur. Phys. J. D 39, 115 (2006); H. T. Quan, P. Zhang, and C. P. Sun, Phys. Rev. E **72**, 056110 (2005).

[11] T. L. Hill, *Statistical Mechanics: Principles and Selected Applications*, MC Graw Hill, New York 1956

[12] C. Jarzynski, *Micriscopic Analysis of Clausius-Duhem Processes*, J. Stat. Physics, **96**, 415 (1999)

[13] H. T. Quan, Yu-xi Liu, C. P. Sun, and Franco Nori, *Quantum thermodynamic cycles and quantum heat engines*, Phys. Rev. E 76, 031105 (2007)

[14] G. Thomas and R. S. Joha, Phys. Rev. E **83**, 031135 (2011); X. L. Huang, Y. Liu, Z. W. and X. Y. Niu, Eur. Phys. J. Plus (2014) **129**: 4

[15] J. E. Geusic, E. O. Schulz-DuBios, and H. E. D. Scovil, Phys. Rev. **156**, 343 (1967); Carl M Bender, D. C Brody, and B.d K Meister, Journal of Physics A: Mathematical and General, Volume **33**, Number 24; M. O. Scully, Phys. Rev. Lett. **104**, 207701 (2010); E. Latifah, A. Purwanto, Journal of Modern Physics **2**, 1366-1372 (2011); M. Polettini, G. Verley and M. Esposito Phys. Rev. Lett. 114 050601 (2015)

[16] Huang X-L, Niu X-Y, XiuX-M and Yi X-X 2014 Eur. Phys. J.D **68**:32 (2014)

[17] S. W. Kim, T. Sagawa, S. de Liberato and M. Ueda, Phys. Rev. Lett. **106**, 070401 (2011); M. Plesch, O. Dahlsten, J. Goold, and V. Vedral, Phys. Rev. Lett. **111**, 188901 (2013)

[18] M. O. Scully, M. S. Zubairy, G. S. Agarwal, Herbert Walther, Science, **299**, 5608 862-864 (2003); M. Esposito, R. Kawai, K. Lindenberg, and C. Van den Broeck, Phys. Rev. E **81**, 041106 (2010); O. Abah, J. Ronagel, G. Jacob, S. Deffner, F. Schmidt-Kaler, K. Singer, and E. Lutz, Phys. Rev. Lett. **109**, 203006 (2012); Ronagel, O. Abah, F. Schmidt-Kaler, K. Singer, and E. Lutz, Phys. Rev. Lett. **112**, 030602 (2014)

[19] J. Ronagel1, Samuel T. Dawkins, K. N. Tolazzi, O. Abah, E. Lutz, F. Schmidt-Kaler, K. Singer, Science **352**, 6283 325-329 (2016)

[20] A. E. Allahverdyan, *Nonequilibrium quantum fluctuations of work*, Phys. Rev. E **90**, 032137 (2014)

[21] P. Talkner, E. Lutz and P. Hänggi, *Fluctuation theorems: Work is not an observable*, Phys. Rev. E **75**, 050102(R) (2007)

[22] R. L. Stratonovich, *Nonlinear Nonequilibrium Thermodynamics I, Linear and Nonlinear Fluctuation-Dissipation Theorems*, ISBN: 978-3-642-77345-7 (1992)

[23] C. Jarzynski, *Comparison of far-from-equilibrium work relations* Comptes Rendus Physique, Volume 8, Issue 5, Pages 495-506

[24] C. Jarzynski, *Nonequilibrium equality for free energy differences*, PRL **78**, 2690-2693 (1997)

[25] G.E.Crooks, *Entropy production fluctuation theorem and the nonequilibrium work relation for free energy difference*, PRE **60**, 2721-2726

[26] G.N. Bochkov, Y.E. Kuzovlev, *General theory of thermal fluctuations in nonlinear systems*, Sov. Phys. JETP **45**, 125-130 (1997)

[27] S. Yukawa, *A quantum analogue of the Jarzynsky equality for free energy calculations*, J. Chem. Phys. **130**, 171102

[28] T. Feldmann, R. Kosloff, *Performance of discrete heat engines and heat pumps in finite time*, Phys. Rev. E, **61**, 4774 (2000)

[29] Sakuray, *modern quantum mechanics*

[30] P. Talkner, P. Hänggi, and M. Morillo, *Microcanonical quantum fluctuation theorems*, Phys. Rev. E **77** 051131 (2008)

[31] B. P. Venkatesh, G. Watanabe and P. Talkner, *Quantum fluctuation theorems and power measurements*, New J. Phys. **17**, 075018 (2015)

[32] S. Defner and E. Lutz,*cerca il titolo*, Phys. Rev. Lett. **105**, 170402 (2010)

[33] F. Galve and E. Lutz, *Energy cost and optimal entanglement production in harmonic chains* Phys. Rev. A **79**, 032327 (2009); F. Galve and E. Lutz, *Nonequilibrium thermodynamic analysis of squeezing*, Phys. Rev. A **79**, 055804 (2009)

[34] A. Silva, Phys. Rev. Lett. **101**, 120603 (2008); F.N.C. Paraan and A. Silva, Phys. Rev. E **80**, 061130 (2009); R. Dorner, J. Goold, C. Cormick, M. Paternostro, V. Vedral, Phys. Rev. Lett. **109**, 160601 (2012);

[35] J. Yi, Y. W. Kim, P. Talkner, Phys. Rev. E **85**, 051107 (2012); A. Sindona, J. Goold, N. Lo Gullo, F. Plastina, New J. Phys. **16**, 045013 (2014)

[36] T J G Apollaro, G. Francica, M. Paternostro and M. Campisi, *Work statistics, irreversible heat and correlations build-up in joining two spin chains*, Phisica Scripta Vol. **2015** Number T165 (2014)

[37] F. Plastina, A. Alecce, T. J. G. Apollaro, G. Falcone, G. Francica, F. Galve, N. Lo Gullo, and R. Zambrini, *Irreversible work and inner friction in quantum thermodynamic processes*, Phys. Rev. Lett. **113**, 260601 (2014)

[38] H. Tasaki, *Jarzynski Relations for Quantum Systems and Some Applications*, arXiv::cond-mat/0009244v2 (2000)

[39] R. Wang, J. Wang, J. He and Y. Ma, *Efficiency at maximum power of a heat engine working with a two-level atomic system*, Phys. Rev. E **87**, 042119 (2013)

[40] R. Kosloff and T. Feldmann, *Optimal performance of reciprocating demagnetization quantum refrigerators*, Phys. REv. E, **83**, 011134 (2010)

[41] A Alecce, F Galve, N Lo Gullo, L Dell'Anna, F Plastina and R Zambrini, *Quantum Otto cycle with inner friction: finite-time and disorder effects*, NJP **17**, 075007 (2015)

[42] R. Kosloff and T. Feldmann, Phys. Rev. E **65**, 055102 (2002); R. Kosloff and T. Feldmann, Phys. Rev. E **68**, 016101 (2003); R. Kosloff and T. Feldmann 2004 Phys. Rev. E **70** 046110; R. Kosloff and T. Feldmann 2010 Phys. Rev. E **82** 011134; R. Kosloff and T. Feldmann 2012 Phys. Rev. E **85** 051114.

[43] M. V. Berry, J. Phys. A: Math. Theor. **42**, 365303 (2009); X. Chen et al., Phys. Rev. Lett. **104**, 063002 (2010); J.-F. Scha, X.-L. Song, P. Capuzzi, P. Vignolo, G. Labeyrie, Europhys. Lett. **93**, 23001 (2011); M. G. Bason, M. Viteau, N. Malossi, P. Huillery, E. Arimondo, D. Ciampini, R. Fazio, V. Giovannetti, R. Mannella and O. Morsch, Nat. Phys. **8**, 145 (2012); N. Malossi, M. G. Bason, M. Viteau, E. Arimondo, R. Mannella, O. Morsch and D. Ciampini, Phys. Rev. A **87**, 012116 (2013); A. Del Campo, J. Goold, M. Paternostro, arXiv:1305.3223 (2013); J. Deng, Q.-h. Wang, Z. Liu, P. Hänggi, J. Gong, Phys. Rev. E **88**, 062122 (2013).

[44] T. Feldmann and R. Kosloff, *ciao*, Phys. Rev. E **73**, 025107(R) (2006).

[45] B. H. Liu, L. Li, Y. F. Huang, C. F. Li, G. C. Guo, E. M. Laine, H P.r Breuer and J. Piilo, *Experimental control of the transition from Markovian to non-Markovian dynamics of open quantum systems*, Nature Phys., **7** 931-934 (2011)

[46] X. G. Wen, *An Introduction of Topological Orders*, http://dao.mit.edu/wen

[47] D.C. Tsui, H.L. Stormer, and A.C. Gossard, *Two-Dimensional Magnetotransport in the Extreme Quantum Limit*, Phys. Rev. Lett. **48** 1559 (1982).

[48] K. v. Klitzing, G. Dorda, and M. Pepper, *New Method for High-Accuracy Determination of the Fine-Structure Constant Based on Quantized Hall Resistance*, Phys. Rev. Lett. **45** 494 (1980).

[49] R. Laughlin, *Quantized Hall conductivity in two dimensions*, Phys. Rev. B **23** 5632 (1981).

[50] C. Kittel, *Introduction to Solid State Physics, 8th Edition*, Wiley (2004); ISBN : 978-0-471-41526-8

[51] X.-G. Wen, Phys. Rev. B **40**, 7387 (1989) ; X. G. Wen, Int. J. Mod. Phys. B **4**, 239 (1990) . X. G. Wen and Q. Niu, Phys. Rev. B **41**, 9377 (1990).

[52] F.D.M. Haldane, Phys. Rev. Lett. **51**, 605 (1983).

[53] F.D.M. Haldane and E.H. Rezayi, Phys. Rev. B **31**, 2529 (1985); D.P. Li, Int. J. Mod. Phys. B **7**, 2655 (1993); E. Keski-Vakkuri, and X.G. Wen, Int. J. Mod. Phys. B **7**, 4227 (1993)

[54] H.K. Onnes, Leiden Comm. 122b, 124c (1911).

[55] L. J. Lang and S. Chen, *Majorana fermions in density modulated p-wave superconducting wires*, Phys. Rev. B **86**, 205135 (2012)

[56] W. De Gottardi, D. Sen and S. Vishveshwara, New Journal of Physics **13** 065028 (2011); W. DeGotterdi, M. Thakurathi, S. Vishveshvara and D. Sen, *Majorana Fermions in superconducting wires: effects of long-range hopping, broken time-reversal symmetry, and potential landscapes*, Phys. Rev. B **88**, 165111 (2013)

[57] A. R. Akhmerov, *topological quantum computation away from the ground state using Majorana fermions*, Phys. Rev. B **82**, 020509 (R) (2010)

[58] J. Alicea, Y. Oreg, G. Refael, F. von Oppen and M. P. A. Fisher, *Non-Abelian statistics and topological quantum information processing in 1D wire networks*, Nature Physics **7**, 412-417 (2011)

[59] P. Pfeuty, Ann. of Phys. **57**, 79-90 (1970); E. Lieb, T. Schultz and D. Mattis, Ann. of Phys. **16** 407-466 (1961)

[60] J. Alicea Rep. Prog. Phys. **75** 076501 (2012); C. W. J. Beenakker, Annu. Rev. Condens. Matter Phys **4**, 113 (2013)

[61] F. Pientka, Y. Peng, L. Glazman and F. von Oppen, *Topological superconducting phase and Majorana bound states in Shiba chains*, Phys. Scr. **T164** (2015) 014008 (9pp)

[62] R. M. Lutchyn, J. D. Sau and S. D. Sarma Phys. Rev. Lett. **105** 077001 (2010); Y. Oreg, G. Refael and F. von Oppen, Phys. Rev. Lett. **105**, 177002 (2010)

[63] V. Mourik, K. Zou, S. M. Frolov, S. R. Plissard, E. P. Bakkers, L. PL Kouwenhoven, Science, **336** 6084 1003-1007 (2012); A. Das, Y. Ronen, Y. Most, Y. Oreg, M. Heiblum and Hadas Shtrikman, Nature Physics **8**, 887-895 (2012); S. Nadj-Perge, I. K. Drozdov, J. Li, H. Chen, S. Jeon, J. Seo, A. H. MacDonald, B. A. Bernevig, A. Yazdani, Science **346** 6209 602-607 (2014)

[64] A. A. Zvyagin, Phys. Rev. B **90**, 014507 (2014)

[65] Berg, *note for GGI in Arcetri* (2015)

[66] S Das Sarma, M. Freedman and C. Nayak, *Majorana zero mopdes and topological quantum computation*, npj Quantum Information **1**, 15001 (2015)

[67] S. Duplij, W. Siegel and J. Bagger, *Concise Enciclopedia of Supersymmetry and noncommutative structures in mathematics and physics*, Kluwer Academic Publisher

[68] M. Leijnse and K. Flensberg, *Introduction to topological superconductivity and majorana fermions*, ArXiv:1206.1736v2, (2012)

[69] M. Nakahara, *Geometry, Topology and Physics - Second Edition*, Institute of physics Publishing, 2003

[70] J. C. Budich and B. Trauzettel, *From the adiabatic theorem toof quantum mechanics to topologica states of matter*, Physica Status Solidi Rapid Res. Lett. **7**, 109 (2013).

[71] S. Ryu, A. P. Schnyder, A. Furusaki and A.W.W. Ludwig, *Topological insulatirs and superconductors: tenfold way and dimensional hierarchy*, N.J. Phys. **12**, 065010 (2010)

[72] A. Altland and M. Zirnbauer, Phys. REv. B **55**, 1142 -1161 (1997) , A. Kitaev, AIP Conf. Proc. **11340**, 22 (2009); S. Tewari1 and J. D. Sau2, Phys. Rev. Lett. **109**, 150408 (2012); L. Fidkowski and A. Kitaev, Phys. Rev. B **83**, 075103 (2011)

[73] Y. Niu, S. B. Chung, C.H. Hsu, I. Mandal, S. Raghu, and S. Chakravarty, Phys. Rev. B **85**, 035110 (2012); Q.-J. Tong, J.-H. An, J. Gong, H.-G. Luo, and C. H. Oh, arXiv:1211.2498 (2012).

[74] Yuezhen Niu, Suk Bum Chung, Chen-Hsuan Hsu, Ipsita Mandal, S. Raghu, and Sudip Chakravarty,*Majorana zero modes in a quantum Ising chain with longer-ranged interactions*, Phys. Rev. B **85**, 035110 (2012)

[75] N. Read and D. Green,*Paired states of fermions in two dimensions with breaking of parity and time-reversal symmetries and the fractional quantum Hall effect*, Phys. Rev. B **61**, number 15 (2000)

[76] J. C. Budich and E. Ardonne, *Equivalent topological invariants for one-dimensional Majorana wires in symmetry class D*, Phys. Rev. B **88**, 075419 (2013)

[77] D. vodola, L Lepori, E. Ercolessi,A. V. Gorshkov, G. Pupillo,*Kitaev Chain with Long-Range Pairing*, Phys. Rev. Lett. **113**, 156402, 9 October 2014

[78] A. Ghazaryan and T. Chakraborty, *Long-range Coulomb interaction and Majorana fermions*, Phys. Rev. B **92**, 115138

[79] Davide Vodola, Luca Lepori, Elisa Ercolessi, and Guido Pupillo, *Long-range Ising and Kitaev Models: Phases, Correlations and Edge Modes*, New J. Phys. **18** (2016) 015001

[80] O. Viyuela, D. Vodola, G. Pupillo, M. A. Delgado, *Topological Massive Dirac Edge Modeds and Long-Range superconducting Hamiltonians*, ArXiv: 1511.05018v1 November 16 2015

[81] Z. C. Shi, X. Q. Shao and X. X. Yi2, ArcXiv:1507,03657v2 (2015)

[82] R. Sánchez and Müttiker, *Optimal energy quanta to current conversion*, Phys. Rev. B **83**, 085428 (2011)

[83] B. Sothmann, R. Sánchez and A. N. Jordan, Nanotechnology **26** (2015) 032001 (23 pp); H. Thierschmann, R. Sánchez, B. Sothmann, F. Arnold, C. Heyn, W. Hansen and L. W. Molenkamp, Nature Nanotechnology **10**, 854-858 (2015)

[84] Averin, D.V. and Likharev, K.K. J Low Temp Phys (1986) 62: 345.

[85] L. S. Kutzmin and K. K. Likharev, *Direct observation of discrete correlated single-electron tunneling*, Pisma Zh. Eksp. Teor. Fiz. **45**, 8 389-390 (1987)

[86] M. H. Devoret, *Quantum fluctuation in electrical circuits*, Course Notes (1995); H. Gabert and M. H. Devoret, *Single Charge Tunneling*, Plenum Press, New York, 1992

[87] J. M. Horowitz and M. Esposito, *Thermodynamic with Continous Information Flow*, Phys. Rev. X **4**, 031015 (2014)

[88] J. V. Koski, A. Kutvonen, I. M. Khaymovich, T. Ala-Nissila and J. P. Pekola, *On-Chip Maxwell's Demon and an Information-Powered Refrigerator*

Abstract

The work presented in this thesis meanly addresses two topics in theoretical physics which are *quantum thermodynamics* and *topological order*. In the first case, physicists are trying to build up a theory able to describe quite in general phenomena involving heat and energy exchanges in quantum systems. The second topic, instead, is related to exotic phenomena and states of matter like the quantum Hall effect (QHE) or topological insulators and topological superconductors.

In the first part od the thesis we define the quantum dynamics for closed and open systems. This is a key ingredient to address the field of quantum thermodynamics. Then, after an introductory part about the quantum thermodynamic transformations, we move toward the field of nonequilibrium fluctuation relations. We address the problem of irreversibility in classical as well as quantum mechanics. Here we present one of our main result. We characterize the "thermodynamic" irreversible adiabatic evolution of a quantum system starting such branch in a thermal equilibrium state at inverse temperature β_i. We give the amount of thermodynamic entropy growth for the process. As direct application of the preceding result we then address a quantum Otto cycle (QOC) working at finite power. We saw that the increasing of irreversible character of the evolution affects the main figures of merit of the cycle.

The second part of the thesis addresses the field of topological order. At first we introduce the concept of topological orders, classes and invariants. Then we introduce the well known Kitaev model for 1 D superconductors. This model predicts Majorana zero mode at the ends of the wire (the 1 D system). MZM are topological states showing great resistance against disorder, local perturbations and any dissipative element. Then we consider a generalized Kitaev model where long range interactions are accounted. We get rich topological phase diagrams showing the presence of several MZM per edge. We study the appearing/disappearing dynamics of the modes according to the time reversal symmetry, that is fundamental in the study of topological phase. The phase diagrams we obtained also show the presence of massive edge modes. In this last case the topological invariants do not well describe any transition. At last we focused on a very limit cases where MZM are obtained at finite length of the wire. Such cases are really interesting since the great advance we can get from the finiteness of the wire in an experimental setup.

The last part is about single electron tunneling devices. Here we got a different ability to work as "heat-to-current harvester" for a device using quantum dots respect to an analogue one using metallic dots.

These different arguments find their unity by considering recent scientific works in which heat transport is addressed in single electron transistor devices where some element of the circuit shows a topological behaviour.

Riassunto

Il lavoro presentato in questa tesi tratta principalmente due argomenti quali le termodinamica quantistica e l'ordine topologico. Nel primo caso fisici stanno provando a costruire una teoria capace to descrivere abbastanza in generale gli scambi di calore ed energia in sistemi quantistici. Il secondo argomento, invece, si relaziona a fenomini e stati della meteria esotici come l'effetto fractional quantum hall o gli isolanti e superconduttori topologici.

Nella prima parte della tesi definiamo la dinamica quantistica per un sistema chiuso ed aperto. Questo é fondamentale per trattare il campo della termodinamica quantistica. Poi, dopo una parte introduttiva sulle trasformazioni termodinamiche quantistiche, ci si sposta verso il campo delle relazioni di fluttuazione non all'equilibrio. Viene trattato il problema dell'irreversibilità tanto nella meccanica classica quanto in quella quantistica. Qui presentiamo uno dei nostri maggiori risultati. Caratterizziamo un'evoluzione adiabatica termodinamica irreversibile di un sistema quantistico il cui stato iniziale é uno di equilibrio alla temperatura inversa iniziale β_i. Viene ricavato l'incremento di entropia termodinamica del processo. Come applicazione diretta del risultato precedente si é considerato un ciclo Otto quantistico (QOC). Abbiamo notato che l'aumentare del carattere irreversibile dell'evoluzione inficia le principali figure di merito del ciclo.

La seconda parte della tisi, invece, guarda al campo dell'ordine topologico. All'inizio introduciamo i concetti di ordine, classi ed invarianti topologici. Poi introduciamo il ben noto modello di Kitaev per superconduttori 1 D. Questo modello prevede Majorana zero mode (MZM) ai capi del filo (il sistema 1 D). I Majorana zero modes sono stati topologici che mostrano una grande resistenza contro il disordine, perurbazioni locali e ogni genere di elemento dissipativo. In viene considerata una generalizzazione del modello di Kitaev con interazioni a molti vicini. Vengono ricavati diagrammi di fase topologica molto ricchi che mostrano la presenza di molti MZM per lato. Inoltre si studia l'apparire e scomparire di tali modi a seconda della simmetria di inversione temporale, che é fondamentale per lo studio della fase topologica. I diagrammi di fase mostrano anche la presenza di massive edge modes. In questo ultimo caso gli invarianti topologici non descrivono bene tutte le transizioni. In fine ci siamo focalizzati sul caso limite dove gli MZM sono ottenuti quando il sistema ha una lunghezza finita. Tali casi sono molto interressanti visto il grande vantaggio che possiamo ricavarne in un setup sperimentale dato che il sistema può grandezza ridotta.

L'ultima parte é sui dispositivi single electron tunneling. Qui abbiamo descritto la differente capacità a lavorare come heat-to-current harvester per un dispositivo che usa quantum dots rispetto ad uno analogo che usa metallic dots.

Questi argomenti differenti trovano un punto di unione considerando lavori scientifici recenti in cui si considera trasporto di calore su dispositivi

single electron tuunneling in cui alcune delle componenti circuitali dei dispositivi mostrano una natura topologica. Sono sistemi perfetti dai quali possiamo ottenere nuovi fenomeni di trasporto.